Monitoring ground settlement to guide sewer asset management

Jojanneke Dirksen

Monitoring ground settlement to guide sewer asset management

Dit proefschrift is goedgekeurd door de promotor:
Prof.dr.ir. F.H.L.R. Clemens
Copromotor: Dr.ir. J.G. Langeveld

Samenstelling van de promotiecommissie:

'A wise man would build his house upon a rock.'

From: The 'Wise and Foolish Builders', Matthew 7:24-27

Contents

Chapter 1

Introduction

1.1   Broad context of the thesis

A sewer system is described as a network of pipelines and ancillary works which conveys waste water from drains to a treatment plant or other place of disposal [EN 752:2008, 2008]. The primary function is to protect society by preventing human contact with waste water and the prevention of flooding by collecting and transporting sewage. Important requirements are the protection of the surface water and groundwater system.

To safeguard proper functioning over time, the system needs to be managed. According to the EN 752 [EN 752:2008, 2008], integrated sewer system management is the process of achieving an understanding of existing and proposed drain and sewer systems, and using this information to develop strategies to ensure that the hydraulic, environmental, structural and operational performance meets the specified performance requirements taking into account future conditions and economic efficiency. The integrated sewer system management process is illustrated in figure 1.1. Following the flow chart of figure 1.1, management starts with investigating the current condition. Next step is to analyse the data and compare the gathered information with imposed performance requirements. If the functioning of the system does not meet the requirements, intervention is needed.

When implementing the management process, difficulties arise when trying to define requirements that are measurable and relate to the performance of the system. Information about the currently used performance requirements in the Netherlands can be found in the municipal sewer plans that are obliged by law (article 4.22, Wet mileubeheer). In line with NEN-EN 752 [EN 752:2008, 2008], the requirements are clearly defined, verifiable and easy to use. Examples are:

- *'obstruction removal in two hours after identification'*

- *'critical states for ... must be prevented'* Using threshold values (warning and intervention criteria) the results of visual inspection are aggregated

into three different scores: good state, alarm state and critical state on three different themes: leaktightness, stability and flow. The currently used performance requirement is a condition of maximum alarm state for all sewer pipes [details can be found in NEN 3398:2004, 2004].

- *'Based on hydraulic model calculations, design storm no.8 should be properly discharged'*

Despite the fact that the basic idea behind most performance indicators is good (e.g. limiting nuisance, maintaining good condition pipes, proper discharge of rainwater), the necessary data is generally not available (e.g. number of persons affected, flooding events) or unreliable (visual sewer inspection data). It is concluded that the currently used data sources, like the ones mentioned, are mainly chosen based on availability not on their relation with the actual performance of the system.

To get a better understanding of the actual management process, van Riel [van Riel et al., in preparation] assessed the availability and use of information in decision-making for sewer system renewal in the Netherlands by interviews. Among other things it was found that for decision making for sewer system renewal also other, not sewer related motives play an important role in the planning: integration of sewer works with other public works (road renewal) to limit costs and nuisance for the citizen. Van Riel concluded that, as the current and future condition of the sewer system is generally not known or fully understood, decisions regarding sewer replacement are to a large extent intuitive and not fully justified or evaluated.

Difficulties with the definition of useful performance indicators are not limited to the Netherlands. As described in Ashley and Hopkinson [2002], setting performance indicators in the United Kingdom faces similar challenges. Ashley and
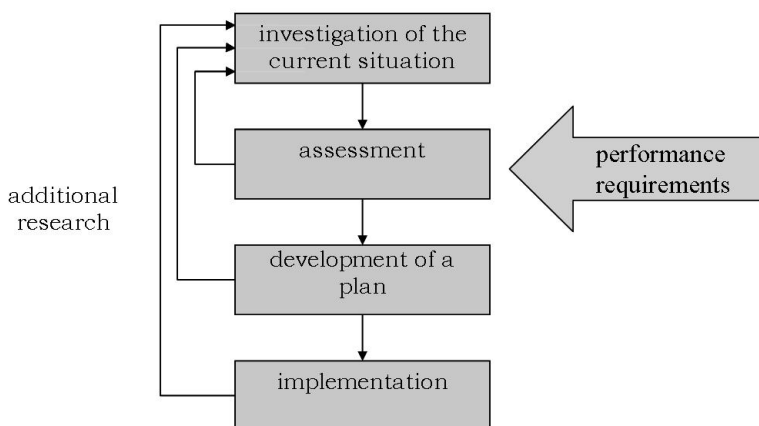
Figure 1.1: Sewer system management process [EN 752:2008, 2008].

Hopkinson [2002] conclude that new research is required if the correct balance in devising appropriate performance indicators is to be attained. In Le Gauffre et al. [2007], a methodology is presented for the development of decision criteria for sewer asset management. Among other things, six principles to define indicators and criteria are proposed. One of these principles stresses the need for an understanding of the relationships between defects, dysfunctions and impacts. The qualitative models used to describe these relationships, however, still need to be parametrized, validated and tested on sensitivity towards unreliable and/or incomplete data.

It can be concluded that given the current situation, it is impossible to judge effectiveness and efficiency of measures. As stressed by Le Gauffre et al. [2007], a better understanding of the relevant failure mechanisms is necessary to improve the decision making process. An comprehensive overview of failure mechanisms can be found in Stanic et al. [accepted]. When relevant failure mechanisms are known, one can decide which (indicator) parameters need to be monitored in order to attain information about the need for intervention or additional information. Besides, understanding of the underlying causes of dysfunctioning gives the opportunity to evaluate the costs and benefits of different types of measures.

1.2 Sewer asset management in the city of Amsterdam

The sewers of the city of Amsterdam are managed by Waternet, the joint executive service of the Amstel, Gooi and Vecht Regional Water Management Board and the City of Amsterdam. In Amsterdam decisions on sewer rehabilitation and replacement are often based on visual inspection reports according to the EN 13508-2 [EN13508-2, 2003]. Despite Waternet's considerable effort into the inspection of sewers (visual inspection of all sewers at least every 10 years), sewer managers do not think that sewer inspection provide sufficient information to base their decisions on. Lacking information includes the prediction of future condition states, the relation between local defects and system performance and the causes of the development of the observed defects. Additionally, the quality of visual inspection data is poor [Dirksen et al., 2013]. Consequently, because the system needs to be managed, there is an immediate need for an alternative source of reliable information to guide asset management.

Like many megacities (e.g. Jakarta, Bangkok, Tokyo, Shanghai), Amsterdam is situated in a delta area. As delta areas are characterized by soft soil conditions, it is likely that (differential) settlement is the most important cause for dysfunctioning. That the structural condition of the sewer is not the determining factor also became clear from a questionnaire among Amsterdam sewer managers. This questionnaire learned that the incidence of sewer collapses (a dysfunction caused by structural deterioration) is virtually non-existing [more information about this questionnaire can be found in van Riel et al., in preparation]. Therefore, studying

the influence of settlement on sewer system functioning will probably give insight in the most relevant deterioration processes of sewer systems in these areas. Ultimately, knowledge of the ground settlement and the relation between settlement (differences) and sewer system dysfunctioning can help the sewer manager to predict and act upon these negative influences in an effective way.

1.3   This thesis

It is evident that knowledge about the sewer deterioration processes is a prerequisite for effective and efficient sewer asset management. As the variables influencing the deterioration process are numerous, the predominant failure mechanisms are different for each system or even within a system. As this study is funded by Waternet, it was intended to study failure mechanisms relevant for the sewer system of Amsterdam. Because the city of Amsterdam is located in an area with significant settlement, the objective of this thesis is to assess methods to monitor (differential) settlement and to apply these methods to study the influence of settlement on the performance of the sewer system in the Amsterdam area.

To the author's knowledge, the influence of settlement on sewer system functioning have not yet been studied using empirical data. Therefore a large part of this thesis focusses on the assessment of the potential and accuracy of methods to study (differential) settlement. Research questions associated with the measurement techniques are:

- How to measure settlement rates?

- How to measure the (relative) position of sewer pipes?

- What is the data uncertainty?

- Is it possible to estimate settlement rates in the Amsterdam area based on the available data?

Fortunately the answer to the last question is 'yes' giving the opportunity to study the influence of settlement on the functioning of the sewer system. Main objective is to assess and describe the failure mechanisms related to settlement (differences) for the sanitary sewers of combined and separate sewer systems. Main research questions are:

- What kind of dysfunctioning is caused by (differential) settlement?

- Can the occurrence of dysfunctioning be predicted when settlement rates are known?

1.4   Thesis outline

In chapter 2 the reproducibility of visual sewer inspection data is studied. The conclusions of this study are the main motivation to study the potential of an alter-

native data source to guide asset management, namely settlement data. Therefore this chapter serves as an introduction.

In chapter 3 two methods to measure (differential) settlement: sewer invert measurements and sewer invert profile measurements are described. Both methods are described including a data quality assessment.

The focus of chapter 4 is the calculation of the settlement rates in the Amsterdam area using historical sewer invert level measurements. To provide an understanding of the calculated settlement rates, the chapter starts with an introduction about the geological history of the Amsterdam area.

Chapter 5 assess settlement on a smaller scale by the analysis of the differential settlement of sewer pipes by sewer invert measurements. The chapter concludes with the analysis of the settlement process of the sewers subjected to the largest settlement differences: hinge sewers.

Chapter 6 concludes with an analysis of the relation between (differential) settlement and failure. For a combined sewer system the influence of settlement on the storage capacity and the pollution potential is analysed. For sanitary sewers of separate sewer systems the relation between sags and the occurrence of blockages is studied.

Finally chapter 7 summarizes the main conclusions and gives suggestions for further research.

The measurement data used for the analyses described in this thesis is available at the author and at the Delft University of Technology.

Bibliography

Ashley, R., Hopkinson, P., 2002. Sewer system and performance indicators - into the 21st century. Urban Water 4, 123–135.

Dirksen, J., Clemens, F., Korving, H., Cherqui, F., Le Gauffre, P., Ertl, T., Plihal, H., Müller, K., Snaterse, C., 2013. The consistency of visual sewer inspection data. Structure and Infrastructure Engineering 9 (3), 214–228, first published on: 07 February 2011 (iFirst).

EN 752:2008, 2008. Drain and sewer systems outside buildings.

EN13508-2, 2003. Conditions of drain and sewer systems outside buildings - part 2: Visual inspection coding system.

Le Gauffre, P., Joannis, C., Vasconcelos, E., Breysse, D., Gibello, C., Desmulliez, J.-J., 2007. Performance indicators and multicriteria decision support for sewer asset management. Journal of Infrastructure Systems 13, 105–114.

NEN 3398:2004, 2004. Buitenriolering, onderzoek en toestandsbeoordeling van objecten.

Stanic, N., Langeveld, J., Clemens, F., accepted. HAZard and OPerability (HAZOP) analysis for identification of information needs for sewer asset management. Structure and Infrastructure Engineering.

van Riel, W., Langeveld, J., Herder, P., Clemens, F., in preparation. Intuition and information in decision making for sewer asset management.

Chapter 2

Visual inspection of sewers

This chapter is extracted from a paper entitled 'The consistency of visual sewer inspection data.' published in Structure and Infrastructure Engineering [Dirksen et al., 2013].

Visual sewer inspection is the primary investigation technique used in sewer system management. Often in practice, and even in some research studies reported in the literature [e.g. Baur and Herz, 2002], the quality (accuracy and completeness) of the data is not questioned. Some papers on deterioration modelling stress the importance of data quality [e.g. Wirahadikusumah et al., 2001, Ariaratnam et al., 2001]. However, a comprehensive evaluation of the quality of visual sewer inspection data has not yet been published.

In this chapter several European case studies are analysed to study the accuracy of data obtained from visual sewer inspection. The chapter starts with three paragraphs introducing the topic. In the first paragraph a short introduction into the responses of observers to visual information from a psychological point of view is given. The second paragraph describes the current practice followed by a description of the history of visual inspection coding systems in paragraph 2.3. After the introductory paragraphs, the European case studies used for analysis of the accuracy of visual inspection data are described in paragraph 2.4, followed by the methods and results in paragraph 2.5. The chapter ends with conclusions and recommendations.

2.1 Background

In psychology the capability of a person to process visual information is a commonly studied subject. In general, the aim of these studies is to describe and understand the process in which visual information (stimuli) is transformed into the response of an observer. Some studies focus explicitly on the reliability of the responses. Macmillan and Creelman [1991] assume that errors arise due to the inevitable variability, either in the stimulus input or within the observer. Miller

7

[1956] describes the observer as a communication system. Using examples he argues that, when the amount of input information (stimuli) is increased, the information transmitted by the observer will first increase, but this will eventually level off at some asymptotic value which is the channel capacity of the individual observer. These studies showed that responses of observers to visual information are variable.

Insight in the occurrence of errors can be gained from studies regarding the accuracy of the subjective assessment of visual information in professions other than sewer management. In the field of medical science Norman [1992] reviewed the influence of expertise in visual diagnoses. It was found that for the visual assessment of x-rays, CT scans, and MRIs the diagnosis of the observer is incorrect in typically 20% to 40% of all cases. It was further found that experienced observers make fewer errors in the assessment of visual records. Another example can be found in bridge management where bridges are, like sewers, generally inspected by means of visual inspection techniques. Phares et al. [2004] studied the accuracy of the inspection techniques commonly used to inspect bridges. It was observed that, when inspecting a bridge on 3 different elements (deck, superstructure and substructure) on a 10- point rating scale, 95% of the collected data varied within two rating points of the average. In addition, only 68% of these ratings varied within one rating point. Phares concluded that the data obtained from the visual inspection technique showed significant variability. Regarding sewer inspection data these two distinct examples make clear that a considerable amount of variability can be expected if persons are to be used to assess images to quantify the condition of a sewer.

2.2 General practice

The visual inspection process of sewers can be systematized by three sequential steps (figure 2.1). In each step of the process errors can be made resulting in an incomplete or incorrect sewer inspection report.

Generally, for the collection of images from within sewer pipes a remotely controlled CCTV camera is used. The movement of the camera is controlled by the inspector. Errors in the first step of the process occur when not all features can be observed on the images. This can occur when conditions such as a fouled
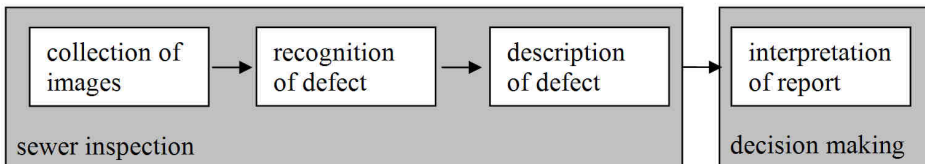
Figure 2.1: Flow diagram describing the sewer inspection process.

lens, insufficient lighting, and too fast camera movement results in defects not appearing on the collected images.

When a defect can be observed in the images, the second step in the analysis is the recognition of the defects. In general, the inspector simultaneously controls the camera and evaluates the footage. The number and type of defects to be examined is governed by prescribed coding systems. In November 2002 the European Committee for Standardization approved the 'EN 13508-2, Conditions of drain and sewer systems outside buildings Part 2: Visual inspection coding system' [EN 13508-2, 2003]. Before this standard was enacted, several similar national standards were used. Two types of errors can occur: either a defect is present but not reported (false negative) or a defect is reported although not present (false positive). Errors in the recognition of defects can occur when for example the inspector is focused on one particular defect and as a consequence ignores other types of defects. Also the incidence of defects may influence the ability to recognize defects, i.e. an inspector may therefore miss a rarer defect. The ability of an inspector to identify particular defects may also change over time.

The third step concerns the description of the recognized defect in more detail by means of a characterization, a quantification of its magnitude and identifying its location. In general the coding system provides a method to describe recognized defects in more detail. As an example the prescribed description method concerning the defect 'fissure' according to EN 13508-2 is given in figure 2.2. To characterize the features of a defect in more detail, the EN 13508-2 imposes for each defect up to two supplementary lists of descriptions. In addition, up to two

Fissure			
BAB			
	Characterisation 1	The nature of the fissure : — surface crack (A) – a crack only in the surface; — crack (B) – crack lines visible on the pipe wall, pieces still in place; — fracture (C) – crack visibly open in a pipe wall, pieces still in place.	
	Characterisation 2	The orientation of the fissure: — longitudinal (A) – A crack or fracture which is mainly parallel to the axis of the pipe; — circumferential (B) – A crack or fracture which is mainly around the circumference of the pipe; — complex (C) - A group of cracks or fractures which cannot be described as longitudinal or circumferential; — helical (D).	
	Quantification	The width of the fissure in millimetres.	
	Circumferential location	The position should be recorded.	

Figure 2.2: Coding system for the defect 'fissure', EN 13508-2.

methods to quantify the defect and a method to describe the location can be specified. Errors in the description of the defects occur when the reported characterization, quantification and the location of a defect does not correspond with the actual situation. Uncertainties can arise when the descriptions of the defect categories or methods in the coding system are ambiguous. Another example of a probable cause of error is the incorrect application of the coding system. The availability of the coding system when assessing the images and the use of specific computer generated forms to fill in the results also probably influences the occurrence of this type of error.

When the inspection report of a sewer is complete, the next step in the analysis is the interpretation of the results (see figure 2.1). Because all possible defects are described in detail, the interpretation of these comprehensive reports is demanding. Therefore, for each individual sewer the inspection report is generally summarized using a rating system. The calculated score can apply to each type of defect individually or to the overall condition of the sewer. It is important to realize that the applied rating system will affect the influence of errors in the inspection report on the decision making process. Hitherto no international standard concerning an agreed rating system to assist with the decision making process has been issued yet.

An example of such a rating system can be found in the annex of the Dutch standard [NEN 3398:2004, 2004]. The described rating system is however informative, not normative. According to this rating system, for each defect threshold values (warning and intervention criteria) are used to aggregate the inspection result into three different scores: good state, alarm state and critical state. The defects are further grouped into three themes: leaktightness, stability and flow. The highest score of a defect in the group determines the rating for that theme: good, alarm of critical state. As the applied rating system differs for each study, details will be provided when necessary.

Since decisions regarding sewer rehabilitation/ replacement involve large investments, the opinion of an expert is considered highly advisable. As a result, expert judgement is an integral part of the interpretation of sewer inspection data. By using expert opinion, however, an additional source of uncertainty is introduced because expert opinion is, like visual inspection, subjective and can be influenced by human perception.

It is concluded that in the sewer condition assessment process using visual sewer inspection data two steps can be distinguished: first the initial assessment (defect recognition and description) and secondly the synthesis of the inspection results into a rating or decision regarding sewer rehabilitation. Because the number and type of inconsistencies introduced in the second step is highly influenced by the used method and the way in which expert judgement is utilized, this study mainly focusses on the errors made in the first part of the assessment (i.e. defect recognition and description).

2.3 History of visual inspection coding systems

Visual inspection of sewers came into general use in the 1980s. In order to be able to uniformly document and to allow for automatically processing the observations, coding and classifications systems were developed in various European countries (e.g. UK Department of the Environment/NWC 1980; Germany, ATV 1988; the Netherlands, DHV/Rioned 1988). The only system applied in Europe that had the status of a national standard, was the Dutch system [NEN 3399:1992, 1992]. This system described 18 different features, in three main functional groups: water tightness, structural stability and operational performance. Each feature was rated in 5 classes distinguished by mostly qualitative descriptions ('characterizations'), resulting in a maximum of 90 different observations. No features or feature descriptions which can only be assessed subjectively (e.g. classifications like good, moderate or bad) were included. The starting point was to only include features that are relevant for the condition assessment of sewers. Further details on the development of the Dutch standard can be found in Snaterse [1989].

In 1994, the Dutch classification system was translated and submitted as a candidate for European standardization within the European Committee for Standardization (CEN). In order to encourage cross-border competition and data exchange within Europe, CEN approved this initiative. The standard, EN 13508-2, was developed as part 2 of the range of standards on investigation and assessment of drains and sewers outside buildings. EN 13508-2 was approved by CEN on November 4th of 2002.

The European coding system had to contain all features that were within all the existing national coding systems. This meant that the aim was changed from 'what do you want to know' (Dutch approach) to 'what are you able to know' (which followed practice in other EU countries). The result was a coding system containing more than 25 features with one or two characterizations for each feature. Every characterization also contained 3 to 10 possible descriptions which could be measured, or could be measured using future techniques. As a consequence this standard results in the coding of a much larger number of different observations (> 1000). Another premise for the European coding system was the independence between observation and assessment which had significant consequences for the practice in some European countries. Each country was allowed to make its own national annex to the standard and select the codes they want to apply. The use of the codes relating the observed features, their descriptions and a specific electronic data exchange format was mandatory.

In 2010, EN 13508-2 has been amended based on comments from general practice, this has led to an increased level of detail. The standard has only recently been implemented in most European countries. It must be stressed however, that the manner of application of the standard differs as described in the national annexes.

2.4 Description of European case studies

Uncertainties are introduced in the sewer system management process due to the use of uncertain data that is then given a subjective assessment, followed by expert based decision support systems. In this management process, three types of human (subjective) assessment of data can be distinguished:

- the recognition of defects

- the description of defects

- the interpretation of inspection reports

Using data from several European case studies, the errors introduced by the use of each type of subjective assessment described above, has been analysed in this study.

For the analysis three types of datasets are used: (1) the examination results from sewer inspector training courses, (2) data from the deliberate, repetitive inspection of the same sewer and (3) data gathered in day-to-day practice. In total the results of six different case studies performed in Austria, France, Germany and the Netherlands are available. As can be seen in table 2.1, the European coding system, EN 13508-2, has been used in some cases but in others the national coding systems have been applied. The last column refers to the type of analysis carried out on the data source.

Table 2.1: Information on the available data sources from:
the Netherlands (NL), Austria (AU), France (FR) and Germany (D).

type of data	data source	coding system	analyses
inspector examination results	NL	NEN 3399	defect recognition defect recognition+description
	AU	ATV M143-2	defect recognition defect recognition+description
	AU	EN 13508-2	defect recognition defect recognition+description
gathered in day-to-day practice	D	ATV M143-2	defect recognition defect recognition+description+ interpretation
	NL	NEN/EN	defect recognition
repetitive interpretation of the same sewer inspection report	FR	EN 13508-2	interpretation

2.4.1 Inspector examination results

Two case studies of the analysis of inspector examination results are available. Korving [2004] and Korving and Clemens [2004] analysed the examination results from 1993 until 2002 of the training course 'Visual inspection of sewers', which is the entrance exam for inspection personnel in the Netherlands. Plihal [2009] analysed the examination results of the training course 'Kanalinspektion' from the Österreichischen Wasser- und Abfallwirtschaftverband (ÖWAV) from 1999 until 2008. Plihal split the data into two groups according to the coding systems that were used: a national norm and from 2006 onwards the European norm. For the analyses only the examination results from candidates that passed the examination were used.

During the examinations, the candidates were given photographs of sewers and asked to describe the condition of the sewer according to the coding system. Figure 2.3 shows an example of a photograph which was typically one of those that could have been used for the examination. For each photograph a correct answer was formulated by the examiners; most photographs showed sewers with more than one defect.

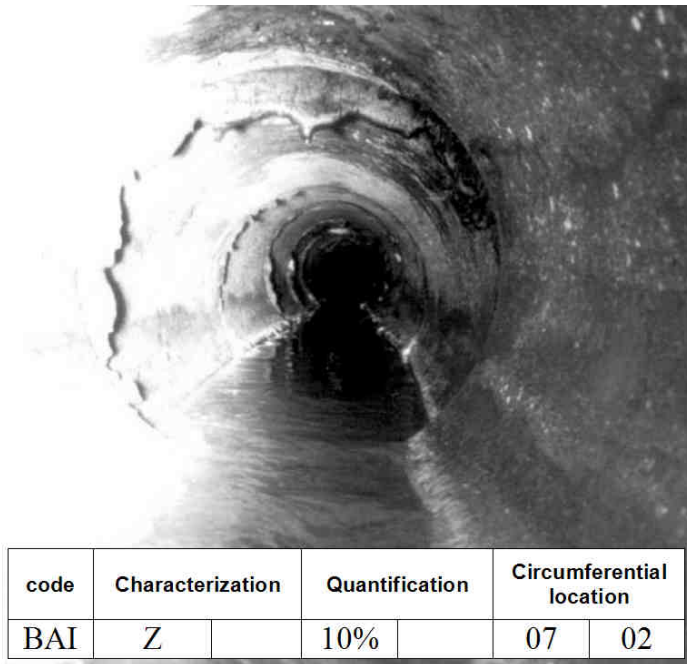| code	Characterization		Quantification		Circumferential location	
BAI	Z		10%		07	02

Figure 2.3: Example of a photograph used for examination. Among others, the defect 'intruding sealing material' can be observed; the correct description of this defect according the EN 13508-2 is shown.

Table 2.2 summarizes the number of photographs and candidates that were used in the two courses. For the Dutch course and the Austrian course using the ATV M 143-2 [ATV M 143-2: 1999, 1999] coding system only a small number (14 and 23) of different photographs were available. Most of these photographs showed more than one defect, some defects were not included in the examination; other defects were only present on one or two photographs. Therefore, when analysing the ability of the candidates to recognize and describe these defects, the results will probably be influenced by the characteristics of these photographs. The Austrian course using the EN 13508-2 classification uses 211 different photographs. But, because only the examinations of 113 candidates are available, some defects although present on multiple photographs, are examined only by a few candidates.

The candidates for the Dutch course 'Visual inspection of sewers' were asked to evaluate 10 different photographs using the coding system as described in NEN 3399 [NEN 3399:1992, 1992]. This coding system assigns 18 different defects using a 5-point rating system; rate 1: the aspect is hardly observable, rate 5: the defect is present in its maximum appearance. By the definition of the rating system it was aimed to use measurable boundaries (e.g. reduction of cross sectional area), nevertheless, for some photographs an appropriate rating could not be defined unambiguously by the examiners. For the defect 'settled deposits', for example, of the 14 different photographs used, 2 photographs were assigned an appropriate answer consisting of 2 different ratings; for one photograph even 3 different ratings were obtained. This indicates that even when using measurable boundaries, for some situations a single correct rating cannot be defined unambiguously.

Until 2006, the ATV M143-2 standard was applied in Austria. This standard prescribes a four letter code. The first letter is obligatory and describes the type of defect; in total 14 different defects are possible. The following letters allow for the description of the defect: characterization (25 possibilities), indication of leaks (9) and position (11). The use of these additional fields is optional, if none of the prescribed characterizations match the actual situation than this designation can be left empty. If required, the defect can be described using an open text field. The candidates of the ATV course were asked to evaluate six different photographs. All candidates chose to answer using a text field instead

Table 2.2: Some figures of the data sources regarding inspector examination results.

country	coding system	number of different photographs	number of candidates	number of photographs/candidate
NL	NEN 3399	14	325	10
AUa	ATV M143-2	23	190	6
AUb	EN 13508-2	211	113	7

of a code. In order to analyse the data, the observations were transcribed using the ATV M143-2 coding system.

From 2006 onwards EN 13508-2 was applied in Austria. This coding system was described earlier in paragraph 2.2. The coding system prescribes 27 different defects. During the examination the candidates were obliged to answer using a code instead of a text field. In order to assist the candidate, a copy of the EN 13508-2 was provided during the examination.

2.4.2 Data gathered in day-to-day practice

The performance of the candidates on a sewer inspector examination, as described in the previous section, can differ from the performance of an experienced inspector on a day-to-day basis for a number of reasons. Firstly, the candidates analysed photographs instead of a video, secondly, the candidates are inexperienced and recently educated and finally, the candidates were probably concentrated on the task and not subject to time pressure or distracted by external influences. Therefore, the results of the two case studies using data gathered in day-to-day practice will be analysed and compared to the results from the sewer inspection courses.

In Germany the inspection results of the city of Braunschweig were analysed by Hüben [2002], additionally Dirksen [2009] analysed inspection data of four municipalities in the Netherlands. Sewer practice in Germany and the Netherlands is quite similar: before an inspection the sewer is cleaned thoroughly and the inspector simultaneously controls the camera and evaluates the footage. Both studies only include the results of sewers for which the full length of the sewer could be inspected. The variability in the results obtained by two different inspectors is assessed by analysing results for sewer pipes that are inspected twice.

Hüben analysed inspection data of the city of Braunschweig collected from 1998 until 2001, a total of 307 sewers with two inspections carried out at two different times were available. During this period the coding system ATV M143-2 was used. The applied coding system was slightly changed when the equipment of the inspection vehicle was renewed in April 1999. Only adjustments in the method to describe defects were made; the number and type of defects remained unchanged.

After completion of the sewer inspection, ATV M149 [ATV M 149: 1999, 1999] provides a method to summarize results into one condition score for each sewer. In general, this score is determined by the highest classification given to a single defect. After the application of the standard rating system minor adjustments can be made by experts. Conditions which allow for adjustment are also described in ATV M149, for example when a defect has a high incidence the score may be adjusted. Sewer pipes which improved by two or more points between inspections were excluded from the database in order to sort out sewers which are likely to be replaced or rehabilitated between two inspections. As the improvement in condition state might also be caused by errors in the inspection, the exclusion of these sewers also influences the results of this study.

In the Netherlands, inspection data of four municipalities were analysed, details can be found in Dirksen [2006], Dirksen and Clemens [2008], Dirksen [2009]. Because only the ability to recognize defects was studied, inspection data analysed using the NEN 3399 (contents explained in paragraph 2.4.1) and the EN 13508-2 (paragraph 2.2 and 2.4.1) could be combined without major modifications. Information on sewer material, diameter and length was used to identify sewers which were likely to be replaced or rehabilitated; these data were removed from the database. Nevertheless, because this type of information is generally neither complete nor up-to-date, it is very likely that not all replaced or rehabilitated sewers could be removed.

2.4.3 Repetitive interpretation of the same sewer inspection report

In France a research project was initiated to develop an objective tool for the conversion of sewer inspection results into reliable performance indicators. For this research experts were asked to interpret sewer inspection results. The variation in the interpretation was studied in order to calibrate the confidence intervals of the outcome of the conversion tool. Details on this study can be found in Werey et al. [2007] and Le Gauffre and Cherqui [2009].

To calibrate the tool, the data from 60 sewers were interpreted by 4 to 6 experts each. The experts were invited to describe the condition of the sewer for ten performance indicators: infiltration, exfiltration, decrease of hydraulic capacity, silting by sand, blockage, destabilization, ongoing corrosion, ongoing degradation from root intrusion, ongoing degradation from abrasion and evidence of collapse. For each indicator a four point rating system was used to define the level of severity for each defect:

1. no or few observed defects,

2. situation with low levels of defects, sewer to be kept under surveillance,

3. situation with a reasonable number and scope of defects, needing intervention but timing is to be prioritised,

4. unacceptable situation in any context; rapid intervention is required.

The inspection reports which were given to the experts described the condition of the sewer using the EN 13508-2, the previous French coding system AGHTM [AGHTM, 1999] and the EN 13508-2 after transcription from the French system. The inspection reports did not include any additional information on the characteristics of the inspected sewer.

2.5 Methods and results

Although the set-up and the coding systems differ in the case studies, the results of each case study can be combined and compared by analysing data reproducibility

in order to determine the reliability of the data. In the following section, the examined errors introduced by subjective assessment are:

- recognize defects (paragraph 2.5.1),

- recognize and describe defects (paragraph 2.5.2),

- interpret sewer inspection results (paragraph 2.5.3) and

- recognize and describe defects and interpret sewer inspection results (paragraph 2.5.4).

2.5.1 Defect recognition

The ability to recognize defects can be assessed using the inspector examination results of the sewer inspection courses and the data gathered in day-to-day practice as can be seen in table 2.1.

Inspector examination results

Inspector examination results from three data sources are available each using a different coding system. Two Austrian data sets of examination results are available: one using the ATV coding system and the other one using the EN coding system. Data from Dutch inspection examinations using the NEN coding system are also available.

The observations of the candidates were compared against the 'correct' answer as formulated by the examiners. Two types of errors are identified:

- false negative (FN): a defect is not observed although it is present,

- false positive (FP): a defect is observed although no defect is present.

As indicated in table 2.3, for most defects a single code could be used to verify if the defect was recognized. For the NEN 3399 coding system two defects (displaced joint and attached deposits) are specified by multiple codes. For the ATV coding system the second letter of the code, describing the characteristic of a defect, was also checked to verify the appropriate recognition of a defect. Because the candidates described the condition of the sewer using text rather than a code the results only express the ability to recognize defects.

In order to calculate the probability of each type of error, for each defect two subsets are made. The first subset only contains the responses of candidates to photographs in which a defect is present according to the examiners. This subset will be used to calculate the probability of a false negative. The probability is calculated by the weighted mean, a weighting factor is required to account for the number of candidates who examined a photograph. The second subset only contains photographs in which a defect was not present according to the examiners. This subset will be used to calculate the probability of a false positive using the same method. Subsets that contain less than 30 responses are not included. The results of this analysis are shown in figure 2.4.

From the results it is concluded that the probability of a false negative is significantly larger than the probability of a false positive. This implies that when a defect is included in a sewer inspection report one can be quite sure that the defect was actually present in the sewer. The other situation: a defect that is not mentioned in an inspection report is however less reliable. Sewer inspection reports therefore provide a too optimistic view about the condition of a sewer.

Table 2.3: Information about the identified defects. For each defect the corresponding code(s) are indicated for each applied coding system. In addition the number of photographs in which a specific defect, identified by the examiners, was present.

defect description	NEN 3399	number of photos	ATV M143-2	number of photos	EN 13508-2	number of photos
fissure	B3	1	R-	7	BAB	31
break/collapse	B1	2	B-	5	BAC	14
surface damage	B2	5			BAF	25
intruding connection	C1	1	SE-	1	BAG	10
defective connection			SO-	2	BAH	15
intruding sealing mat. ring other	A7	3	HG-	1		
displaced joint	A3,A4,A5	3			BAJ	22
soil visible trough defect					BAO	25
roots	C2	2	HP-	5	BBA	6
attached deposits	C3,C4	1			BBB	14
settled deposits	C5	3			BBC	10
ingress of soil	A2	1				
other obstacles	C6	3	HE-	1	BBE	13
infiltration	A1	6	U-	4	BBF	15
connection			A-	1		
water level	C7	9				
closed connection			AU-	1		
badly build connection			SN-	3		
crossing cable			HZ-	1		

The results corresponds with the theory of Miller [1956] who argues that a person is only able to process a certain amount of information; the channel capacity of the observer. Because the probability of a false negative is large, indicating that information is not transmitted, it very likely that for sewer inspection the amount of information available to an inspector often exceeds the channel capacity of the inspector.

When comparing the results of the three inspection courses for individual defects it appears that the probability of a false positive and a false negative seems to vary depending on the defect and used standard. These variations are probably caused by the use of only a small amount of different photographs for the NEN and ATV courses as can be seen in table 2.3. For the EN inspection course more photographs were used, therefore the results of the EN inspection course are believed to more closely represent the actual probability of a false positive or false negative. From the results of the EN course it can be concluded that only one defect, 'roots', has a significantly lower probability of a false negative in comparison to the other defects. Apparently defects with distinct features (such as roots) are easier to recognize. For the other defects the probability of a false negative is of the order of 0.25 whilst the probability of a false positive is around 0.04.
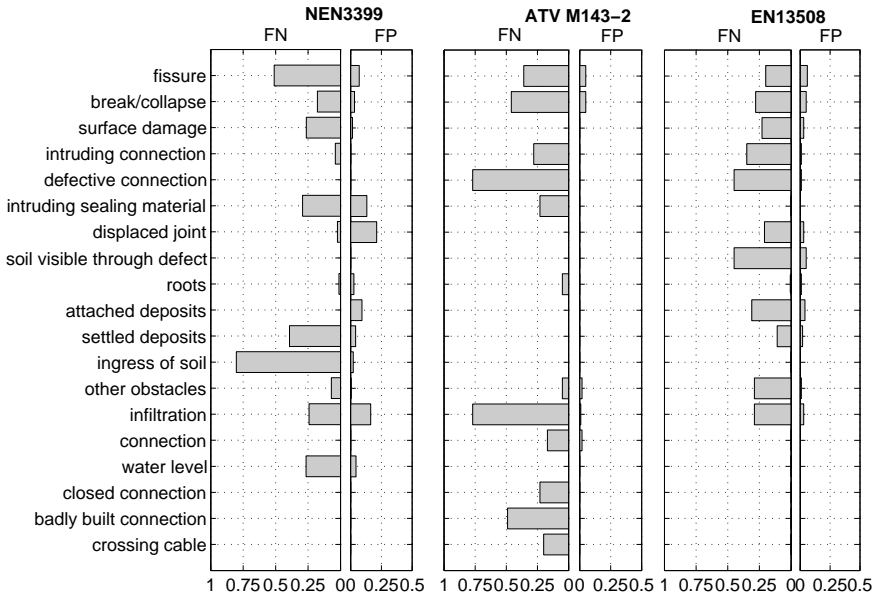

Figure 2.4: Probability of a false positive (FP) and false negative (FN) derived from the inspector examination results of the course 'Visual inspection of sewers' in the Netherlands using the NEN3399 and the sewer inspection course from the ÖWAV using ATV M143-2 and NEN 13508-2 in Austria.

Data gathered in day-to-day practice

The ability to recognize defects can also be investigated using the two case studies of data gathered in practice. Details of the two case studies, one in Germany and one in the Netherlands are described earlier in this chapter.

To investigate the ability to recognize defects, the number of defects which 'disappear' between two inspections was analysed. Only defects that are very unlikely to disappear without any active rehabilitation or replacement are examined. These defects are: leak tightness, different types of joint displacements, damage, corrosion, fissures, missing wall and the presence of connections.

For the data gathered from four municipalities in the Netherlands the number of sewers for which a certain defect is identified at the first inspection, but not at the second inspection is quantified. The data gathered in Germany (one municipality) is analysed more precisely by including the location where a defect was encountered. Therefore, for the German data, the number of locations where a certain defect is identified at the first inspection, but not at the second inspection is quantified.

Table 2.4: Investigated defects. For each of the three different coding systems used, the code which is used to verify the presence of a defect is indicated.

	Germany		the Netherlands			
	ATV M143-2		NEN 3399		EN 13508-2	
defect	code	description	code	description	code	description
leak tightness	U	observable leaks	A1	infiltration of groundwater	BBF	infiltration
displ. joint	L	displ. joint				
longitudinal displ.			A3	longitudinal displ.	BAJA	displ. joint, longitudinal
radial displ.			A4	radial displ.	BAJB	displ. joint, radial
angular displ.			A5	angular displ.	BAJC	displ. joint, angular
damage			B1	damage by mechanical action	BAFA	surface damage, mechanical damage
corrosion	C	corrosion	B2	surface damage by corrosion	BAFB/ BAFC/ BAFD	surface damage, chemical corrosion
					BAFE	surface damage, cause unknown
fissure	R	fissure	B3	fissures	BAB	fissure
connection	A	connection				

Table 2.4 lists the codes for each of the different coding systems which were used to identify the sewers/locations where a defect was present. For the analysis of the German data only the first letter of the code referring to 'type of defect' is examined. For the Dutch data using the EN 13508-2 the characterization of the defect needs to be checked to confirm the presence of a defect. Hence the results therefore do not exclusively describe the ability of an inspector to recognize a defect. For each case study, defects that were present in less than 10 sewers according to the first inspection have been excluded from the analysis, since the calculated percentages in that case may not be statistically representative.

The results of this analysis for both the German and the Dutch inspection data are presented in figure 2.5. As can be seen in the figure the calculated percentages vary greatly for the different defects and municipalities. The percentages for the defect 'infiltration' range from 6 to 79 percent. Nevertheless, although varying between municipalities, the number of 'disappearing defects' is significant. The percentages for the municipality of Braunschweig are a bit higher; this is probably caused by the inclusion of the defect location in the analyses.

Comparison of the ability to recognize defects from both data sources

In order to verify if the results from the data gathered in practice are consistent with the results from the sewer inspection courses, the probability of a 'disappearing defect' is examined in more detail. The probability of this event will be estimated using the probabilities of a false positive and a false negative based on the results of the inspector examination course. The estimated probability of a
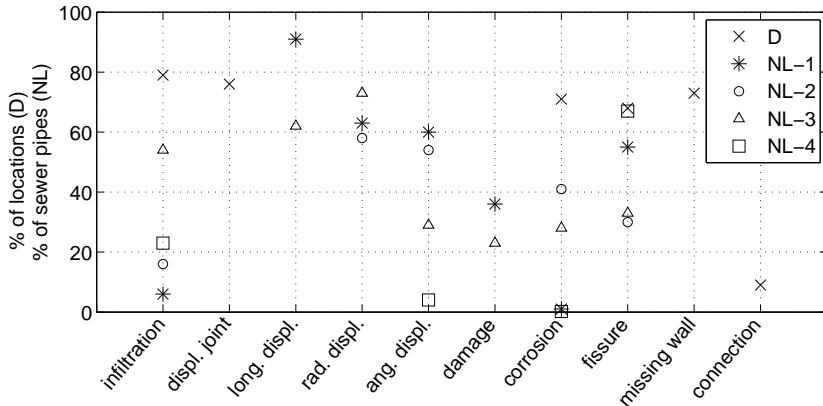

Figure 2.5: Sewers inspected more than once for four municipalities in the Netherlands (NL 1 to 4) and one municipality in Germany (D). The graphs indicate per defect type the percentage of sewers/locations for which the defect was registered at the first inspection but not at the second inspection.

'disappearing defect' will be compared to the observed probability as found in day-to-day practice. Strictly the event of the estimated probability is related to the observation of a photograph whereas the observed probabilities are related to a single location in a sewer (German case study) or to a whole sewer (Dutch case study).

To estimate the probability of the event 'disappearing defect', the actual occurrence of a defect is indicated using the letter 'α' and the observation is indicated using the letter 'β'. Furthermore it is assumed that for each defect a sewer can be in two states: state 1: defect not present; and state 2: defect present. The event tree for the event 'disappearing defect' (or $\beta_2 = 1|\beta_1 = 2$) results in:
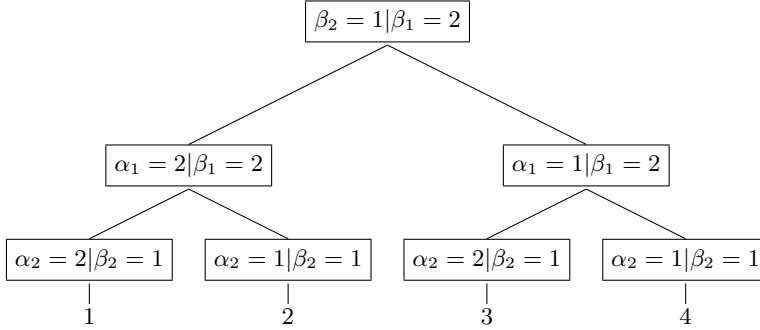
From the event tree it is concluded that four sequences of events are possible. Sequence 2 describes the situation where a defect is present during the first inspection ($\alpha_1 = 2$) but not during the second inspection ($\alpha_2 = 1$). Because only defects are examined that are very unlikely to disappear without any rehabilitation or replacement, the occurrence of this sequence is unlikely.

For the other three sequences first the unconditional probabilities are calculated ($P(\beta_1 = 2, \beta_2 = 1)$). For the probability of a false negative and a false positive the estimated probabilities based on the inspector examinations as described in this paragraph are used such that $P(FN) = 0.25$ and $P(FP) = 0.04$.

$$
\begin{aligned}
1 : P(&\alpha_1 = 2, \beta_1 = 2, \alpha_2 = 2, \beta_2 = 1) \\
&= P(\alpha_1 = 2) \cdot P(\beta_1 = 2|\alpha_1 = 2) \cdot P(\alpha_2 = 2|\alpha_1 = 2) \cdot P(\beta_2 = 1|\alpha_2 = 2) \\
&= P(\alpha_1 = 2) \cdot (1 - P(FN)) \cdot 1 \cdot P(FN) \\
&= 0.1875 \cdot P(\alpha_1 = 2)
\end{aligned} \tag{2.1}
$$

$$
\begin{aligned}
3 : P(&\alpha_1 = 1, \beta_1 = 2, \alpha_2 = 2, \beta_2 = 1) \\
&= P(\alpha_1 = 1) \cdot P(\beta_1 = 2|\alpha_1 = 1) \cdot P(\alpha_2 = 2|\alpha_1 = 1) \cdot P(\beta_2 = 1|\alpha_2 = 2) \\
&= P(\alpha_1 = 1) \cdot P(FP) \cdot P(\alpha_2 = 2|\alpha_1 = 1) \cdot P(FN) \\
&= 0.01 \cdot (1 - P(\alpha_1 = 2)) \cdot (1 - P(\alpha_2 = 1|\alpha_1 = 1))
\end{aligned} \tag{2.2}
$$

$$4 : P(\alpha_1 = 1, \beta_1 = 2, \alpha_2 = 1, \beta_2 = 1)$$
$$= P(\alpha_1 = 1) \cdot P(\beta_1 = 2|\alpha_1 = 1) \cdot P(\alpha_2 = 1|\alpha_1 = 1) \cdot P(\beta_2 = 1|\alpha_2 = 1)$$
$$= P(\alpha_1 = 1) \cdot P(FP) \cdot P(\alpha_2 = 1|\alpha_1 = 1) \cdot (1 - P(FP)) \qquad (2.3)$$
$$= 0.0384 \cdot (1 - P(\alpha_1 = 2)) \cdot P(\alpha_2 = 1|\alpha_1 = 1)$$

As can be seen all probabilities are dependent on the probability that the defect is present when the first inspection is carried out: $P(\alpha_1 = 2)$. For the probability of sequence 3 and 4 another probability is of the influence: the probability that a defect which was not present during the first inspection is also not present during the second inspection ($P(\alpha_2 = 1|\alpha_1 = 1)$). When the probabilities on sequences 3 and 4 are summed it can be seen that the frequency of occurrence of this event is of marginal influence on the total probability of a 'disappearing defect'. For further analysis the event that a defect develops between inspections ($1 - P(\alpha_2 = 1|\alpha_1 = 1)$) is assumed not to occur because the interval between inspections is small in comparison to the rate at which defects are likely to develop. Consequently the probability ($P(\alpha_2 = 1|\alpha_1 = 1)$ is one, and therefore sequence 3 can be excluded from further analysis.

In order to calculate the probability of a 'disappearing defect' under the condition that the defect was present according to the first inspection (or $P(\beta_2 = 1|\beta_1 = 2)$), the unconditional probabilities need to be divided by the probability that a defect was present according to the first inspection ($P(\beta_1 = 2)$). This probability can be calculated by:

$$P(\beta_1 = 2) = P(\beta_1 = 2|\alpha_1 = 2) + P(\beta_1 = 2|\alpha_1 = 1)$$
$$= P(\alpha_1 = 2) \cdot (1 - P(FN)) + (1 - P(\alpha_1 = 2) \cdot P(FP) \qquad (2.4)$$
$$= 0.04 + 0.71 P(\alpha_1 = 2)$$

resulting in the following conditional probabilities:

$$1 : P(\alpha_1 = 2, \alpha_2 = 2, \beta_2 = 1|\beta_1 = 2)$$
$$= \frac{P(\alpha_1 = 2, \beta_1 = 2, \alpha_2 = 2, \beta_2 = 1)}{P(\beta_1 = 2)} \qquad (2.5)$$
$$= \frac{0.1875 \cdot P(\alpha_1 = 2)}{0.04 + 0.71 P(\alpha_1 = 2)}$$

$$4 : P(\alpha_1 = 1, \alpha_2 = 1, \beta_2 = 1|\beta_1 = 2)$$
$$= \frac{P(\alpha_1 = 1, \beta_1 = 2, \alpha_2 = 1, \beta_2 = 1)}{P(\beta_1 = 2)} \qquad (2.6)$$
$$= \frac{0.0384 \cdot (1 - P(\alpha_1 = 2))}{0.04 + 0.71 P(\alpha_1 = 2)}$$

The probabilities on sequences 1 and 4 as well as the total probability of a 'disappearing defect' as a function of the probability that a defect was present during the first inspection are shown in figure 2.6. In order to verify if the results from the data gathered in practice are consistent with the results from the sewer inspection

courses, the probability of a 'disappearing defect' using the false positive and a false negative as found from the sewer inspection course will be used to estimate the probability of a 'disappearing defect' as found in practice. In order to do so, the last step is to estimate the probability that a defect was present during the first inspection ($P(\alpha_1 = 2)$) for the data gathered in practice. This probability can be approximated using the probability that a defect was recognized during any inspection ($P(\beta = 2)$) following:

$$
\begin{aligned}
P(\beta = 2) =& P(\alpha = 2) \cdot P(\beta = 2 | \alpha = 2) + P(\alpha = 1) \cdot P(\beta = 2 | \alpha = 1) \\
=& P(\alpha = 2) \cdot (1 - P(FN)) + (1 - P(\alpha = 2)) \cdot P(FP) \\
=& P(\alpha = 2) \cdot (1 - P(FN) - P(FP)) + P(FP)
\end{aligned} \tag{2.7}
$$

therefore $P(\alpha = 2)$ equals

$$
\begin{aligned}
P(\alpha = 2) =& \frac{P(\beta = 2) - P(FP)}{1 - P(FN) - P(FP)} \\
=& \frac{P(\beta = 2) - 0.04}{0.71}
\end{aligned} \tag{2.8}
$$

This probability can be used to estimate $P(\alpha_1 = 2)$ if the sewers that are inspected twice are a random subset of all inspections performed in a municipality.

To finalize the analysis, for each defect listed in table 2.4 the probability that a defect was present during the first inspection ($P(\alpha = 2)$) is calculated by equation 2.8. Using the graph of figure 2.6, this probability is used to estimate the probability of a 'disappearing defect'. The results are presented in figure 2.7; the observed probabilities in figure 2.7 are the same probabilities as presented in figure 2.5.

As can be seen in figure 2.7, the estimated and observed probabilities are in the same order of magnitude. As no structural deviation between the observed
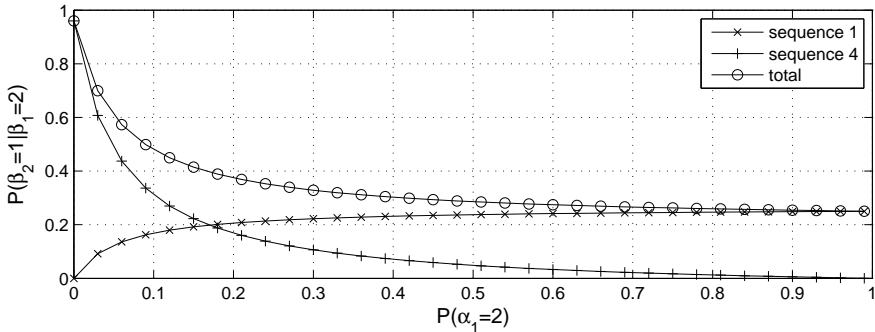
Figure 2.6: Probability of a 'disappearing defect' given that the first inspection indicated that the defect was present as a function of the probability that the defect was actually present during the first inspection.

and estimated probability for individual defects or municipalities can be found, the difference between the observed and estimated probability can not be further reduced by adjusting the probability of a false positive or a false negative. Therefore, despite the fact that different events were analysed, the order of magnitude of the probability of a false positive and a false negative of respectively 0.04 and 0.25, are consistent with the results of the analysis of the data gathered in practice. Results indicate however that probabilities do vary between individual defects and municipalities. These differences will be examined in the following.

For most defects of which the observed probability is high (> 0.3), the estimated probability is too low and visa versa. This observation can be explained by the hypothesis that inspectors in practice are more alert towards defects that are present frequently (e.g. lower probability on a false negative). It may be interesting to elaborate the relation between the incidence of a defect and the probability on a false negative further. Additionally, the influence of the appearance or severity of a defect on defect recognition might be an interesting research topic.

2.5.2 Combined error, defect recognition and defect description

To analyse the ability of an inspector to recognize and describe defects concurrently, the results of the two inspection courses are used. Details of these data sources can be found in paragraph 2.4.1. The errors caused by the use of these two abilities was analysed by calculating the probability that a candidate was unable to respond according to the correct answer. For the calculation only the responses of candidates to photographs were used where, in line with the correct answer, a defect was present. Subsets that contain less than 30 responses are not
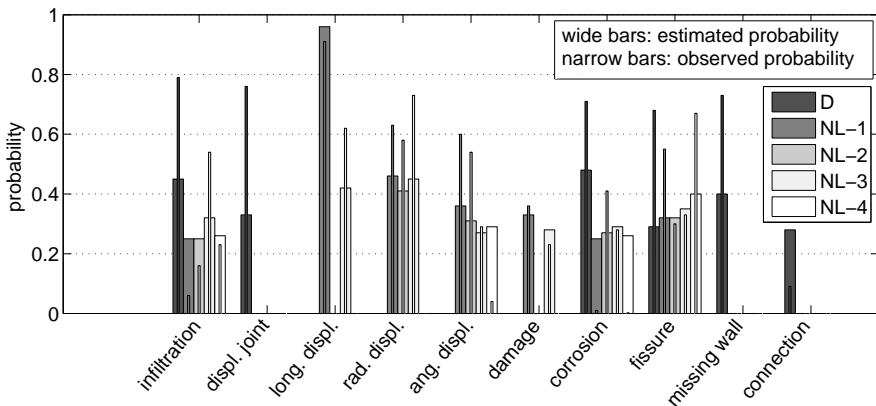
Figure 2.7: Estimated and observed probability of a 'disappearing defect'.

included. Incorrect responses to photographs where a defect was not present are previously studied as false positives (paragraph 2.5.1). It should be noted that, because all responses to photographs where a defect was present are analysed, false negatives are not excluded from the analysis.

For the Dutch inspection course the NEN 3399 was used, according to this standard a rating system is used to assign a level of severity to each defect as described in paragraph 2.2. This implies that the candidate must choose from, depending on the type of defect, at maximum 5 ratings for each defect. As pointed out previously in paragraph 2.4.1, some photographs are assigned with multiple correct ratings and some defects are only present on one or two photographs (table 2.3).

Because only a limited amount of different photographs are used for the examination, a detailed analysis of the deviation from the accepted answer is not possible. Nevertheless, the results as presented in figure 2.8 clearly indicate that the probability of an incorrect coding is significant. This is quite surprising since the number of possible ratings is limited and the coding system explicitly aims at providing unambiguous measurable boundaries. Further research on the distribution of answers around the accepted answer may give an indication of the accuracy of this type of defect description.

Comparing figure 2.8 with figure 2.4 learns that a large part of the incorrect coding is caused by the failure of recognition. The small number of candidates that recognized the defect but assigned the wrong rating is probably the result of the assignment of multiple correct ratings by the examiners for the majority of photographs as previously indicated in paragraph 2.4.1. More information about the type of answers given by the candidates can be found in van der Steen et al. [accepted, 9 May 2013] (included in appendix A).

Using the examination data from Austria, two analyses have been made of the
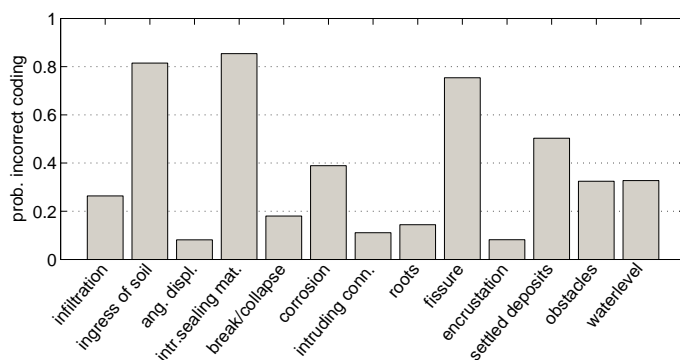
Figure 2.8: Probability of incorrect coding derived from the inspector examination results of the course 'Visual inspection of sewers' in the Netherlands (based on the results of Korving [2004]).

responses of candidates to photographs in which a defect was present (figure 2.9 and figure 2.10). For the first analysis, denoted check B, it was verified whether the candidate was able to respond in line with the accepted answer. The second analysis (check A) was less strict; for the examinations using the ATV coding system only the first 3 letters of the code were verified; for the EN coding system also incomplete characterizations and/or quantifications were accepted providing the three letter main code was correct. Subsets that contain less than 30 responses are not included. It is noted that the Dutch examination data are based on a numerical classification system whereas the data from Australia are based on a descriptive system.

As can in figure 2.9 and figure 2.10, the probability of an incorrect coding (check B) is for all defects (except 'connection' in the ATV coding system) larger
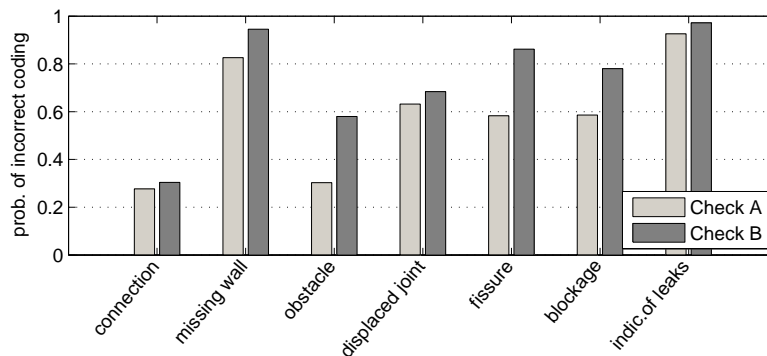
Figure 2.9: Probability of incorrect coding derived from the inspector examination results of the ÖWAV using the ATV coding system.
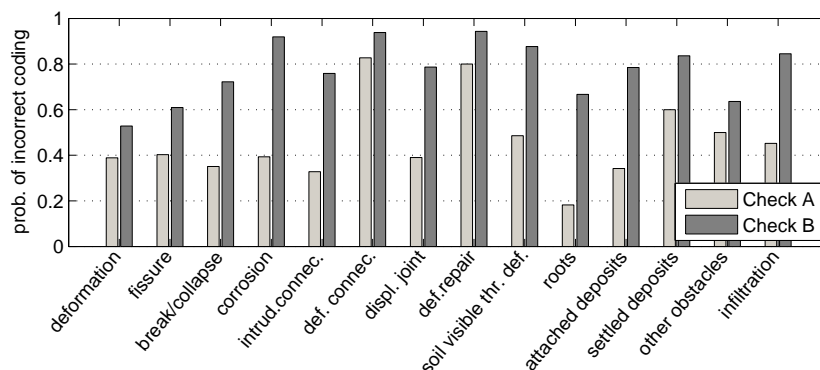
Figure 2.10: Probability of incorrect coding derived from the inspector examination results of the ÖWAV using the EN coding system.

than the probability of a correct coding. For some defects even probabilities over 80% of an incorrect coding are found. In order to correctly identify the defect 'fissure' in a photograph depicting a fissure for example, first the fissure needs to be recognized (probability ±0.75), secondly the characterization 1 (3 options), and than characterization 2 (4 options) needs to be correctly noted. An error in each one of these steps results in an incorrect coding. This implies that a large probability of an incorrect coding is easily possible as shown from the analysis of the examination data.

These results clearly indicate that, by using this type of coding systems, reproducible results can not be expected. Therefore inspection results using this type of coding systems mistakenly suggest a level of detail which in fact is unlikely to be obtained. A disadvantage of the use of a descriptive coding system is that this type of defect description does not allow for a quantitative analysis of the accuracy of the data (e.g. on a 10-point rating scale the condition is 7 ± 2, at a level of confidence of 95%).

2.5.3 Interpretation of sewer inspection data

Variations in the interpretation of inspection reports were analysed using the results of the study from France. In this study inspection data of 60 sewers were interpreted by a group of experts. Each photograph was examined by 4 to 6 different experts. The experts were asked to give an indication of the severity of 10 performance indicators using a 4-point rating scale. For each performance indicator the percentage of inspection reports where the difference in interpretation of the different experts varied at least 2 points was calculated. The results are shown in figure 2.11.

On average the experts did not agree on the interpretation of approximately 40% of the inspection reports. For the performance indicators 'infiltration' and
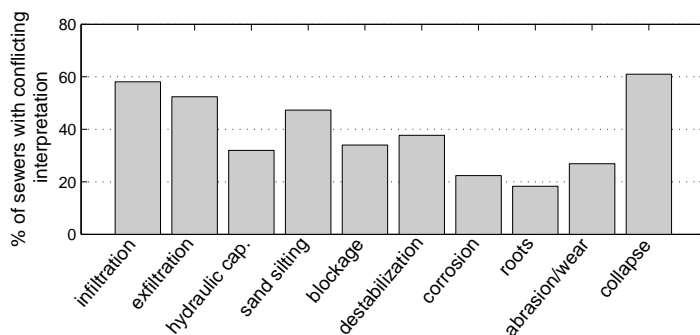
Figure 2.11: Percentage of sewers for which the interpretation of the inspection report by 4 to 6 different experts showed a difference of at least 2 points.

'collapse' the percentage is even higher at around 60%. For the performance indicators 'corrosion' and 'roots' agreement appears to have been achieved in most cases. This is probably caused by the fact very few defects related to 'corrosion' or 'roots' were found in the 60 sewers (consequently most sewers are rated as class 1).

Detailed analysis of the data showed that some experts consistently rate specific performance indicators higher than other experts. For the performance indicator 'infiltration' the percentages of sewer inspection reports where an expert assigned the lowest, the highest or a ranking which was neither the lowest nor the highest are calculated. The results are shown in table 2.5. As can be seen experts X6 and X7 assigned in most cases the highest grade in contrast to experts X4 and X8; experts X3 and X9 have more moderate opinions. Experts that gave high rankings for 'infiltration' did not necessarily gave the relatively high rankings for other performance indicators.

Based on these results it is concluded that when using subjective assessment to interpret sewer inspection reports personal errors (i.e. a systematic error in observations peculiar to the observer) are introduced. These errors should be added to the errors already introduced during the initial analysis of the images. Therefore, it is very likely that any final decision is only tentatively linked to the actual condition of the inspected sewer pipe.

It may be interesting to investigate how the uncertainties in the sewer condition assessment process (inspection and interpretation) are affected when defects are described by a photograph instead of a text formulated according to a prescribed coding system. In that way two sources of errors may be reduced. Firstly, the errors introduced when describing a defect are eliminated. And secondly, the variation in interpretation of sewer inspection reports may also be reduced because humans are able to interpret very complex pictorial patterns and obtain much more information than can be conveyed in a piece of text.

Table 2.5: Results of a detailed analysis of the interpretation of inspection reports for the performance indicator 'infiltration'.

expert id.	number of interpreted inspection reports	% of interpretations where the expert assigned:		
		the lowest grade	the highest grade	nor the highest nor the lowest
X3	17	12	6	82
X4	34	18	3	79
X6	43	0	23	77
X7	42	2	29	69
X8	30	23	7	70
X9	32	9	0	91

2.5.4 Analysis of the combined uncertainty caused by the use of multiple capabilities

One data source, the data gathered in Germany, allows for the analysis of the combined uncertainty caused by the use of multiple capabilities. The reason is that this data source not only consists of the inspection data but also includes information on the interpretation of the data by means of a rating system. As already discussed an inspection report of a single sewer is in general summarized using a rating system. The calculated score can apply to each type of defect individually or to the overall condition of the sewer as in the data gathered in Germany.

Data gathered in day-to-day practice

In Germany the ATV-M 149 is used to summarize inspection results into one condition score referring to the condition state of the whole sewer. Hüben [2002] analysed the differences in the condition score between two inspections. The dataset was split into two to account for a slight modification in inspection protocol in April 1999. The result of the analysis is presented in figure 2.12.

The results indicate that over 50% of the sewers changed in condition score between two inspections. The number of sewers improving in condition (increased condition score) and deteriorating in condition (decreased condition score) are almost equal according to the observations. In order to investigate the influence of the duration between inspections on the results the number of months between inspections was determined. For each change in condition score the average num-

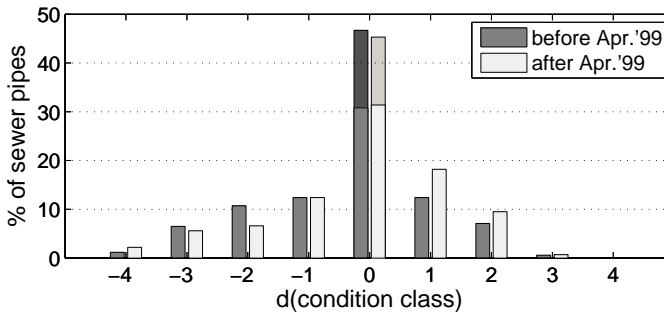Figure 2.12: Sewer pipes inspected more than once for the municipality of Braunschweig in Germany. The graph indicates the difference in overall condition score between two inspections. For pipes in which the overall condition score did not change, the upper part of the bar indicates the percentage where the defects and their classification in the two consecutive reports were identical. [Hüben, 2002]

ber of months between inspections was calculated. No significant differences were found for sewers improving and deteriorating in condition. It can be concluded that even after application of a rating system which assigns an overall condition score for the condition of the whole sewer, inconsistencies caused by human (subjective) assessment during the sewer inspection process are still apparent and significantly influence the results.

2.6 Conclusion and recommendations

In the sewer condition assessment process, three types of subjective assessment of data can be identified:

- the recognition of defects,
- the description of defects,
- the interpretation of inspection reports.

Each type of subjective assessment introduces uncertainties in the overall condition assessment. The errors introduced by each type of subjective assessment is studied using three types of data: inspector examination results of sewer inspection courses in Austria and the Netherlands, field data from four municipalities in the Netherlands and one municipality in Germany, and the results of repetitive interpretation of the inspection results of the same sewer in France.

For the recognition of defects based on the analysis of examination results, it was found that the probability that an inspector fails to recognize the presence of a defect (false negative) is significantly larger than the probability that a defect is reported although it is not present (false positive). The probability of a false positive is in the order of a few percent, the probability of a false negative is in the order of 25%. From the analysis presented in this chapter it became clear that the performance of experienced inspectors does not differ significantly from that of recently trained inspectors. Furthermore it was found that it is very likely that the probability of a false negative is inversely related to the incidence of a defect.

Regarding the description of defects, currently applied coding systems are too complex to give consistent, reproducible results because the level of detail to describe the condition of the sewer cannot be accomplished by visual means only. The analysis of the sewer inspector examination data using the EN 13508-2 showed that the probability of an incorrect observation (defect recognition and/or description) for all defects was over 50%. Analysis of the data gathered in practice in Germany proved that, even after application of a rating system which assigns an overall condition score for the whole sewer, inconsistencies caused by subjective identification of defects during the sewer inspection process are still apparent and significantly influence the results.

The errors introduced by the use of subjective assessment to interpret sewer inspection results was studied by analysing the variation in interpretation by

different experts of the inspection report of the same sewer. It was concluded that on a four point rating scale the variation in interpretation is significant.

Finally it is concluded that the suspected variability in observations, as described in paragraph 2.1, is confirmed.

Recommendations:

1. In order to improve the reproducibility of sewer inspection reports, the inspection coding systems should be significantly simplified. It is recommended to assess the ability of a person to subjectively evaluate visual data consistently and used the results as a starting point for a new coding system. A classification system using a discrete numerical classification system such as used when inspecting bridges [Phares et al., 2004] allows for a numerical definition of the variability and therefore improves the understanding of the impact of this variation on the decision making process.

2. It may be useful to investigate the variation in interpretation for pipes in which defects are described using a photograph instead of text. In this way defects only need to be recognized and photographed by the inspector; uncertainties caused by the description of defect using a prescribed coding system are eliminated.

3. To improve the reproducibility of the data, it is recommended to supply sewer inspectors with feed-back on the reliability of their inspection results. When no feedback is given it is very likely that the perception of inspectors towards defects changes over time resulting in personal errors. This assumption is supported by experience in medical practice where it was found that frequent feed-back from colleagues as well as patients enhances the reduction of mistakes [Norman, 1992].

4. Because accuracy of visual inspection data is low, the additional use of other types of information to investigate sewer system functioning is recommended. A comprehensive overview of other sources of information can be found in Le Gauffre et al. [2007].

After publishing and presenting the results of the study described in this chapter, a frequently heard comment was that the appearance of the defect was not taken into account whereas it is likely that the severity of the defect influences the ability to recognize a defect. A defect in its maximum appearance, for example, might be easier to recognize compared to the same, but less severe defect. As the Dutch training course for sewer inspectors was revised, the 10 photographs that were used for the examination from 1992 until 2012 became available. Studying these photographs along with the answers of passed candidates (in total 492) revealed that also severe, clearly visible defects are overlooked. As the coding system was changed in 2004, it was also possible to study the influence of the used coding system on the answers given by the candidates. It was found that the applied coding system had a significant influence on the probability of a false negative.

The results of this study are published in van der Steen et al. [accepted, 9 May 2013] and sent in for presentation at the 5th Leading Edge conference on Strategic Asset Management in 2013. The paper of van der Steen et al. [accepted, 9 May 2013] can be found in appendix A.

Bibliography

AGHTM, 1999. Les ouvrages dassainissement non-visitables: fiches pathognomiques. TSM - Techniques Sciences Méthodes.

Ariaratnam, S., El-Assaly, A., Yang, Y., 2001. Assessment of infrastructure inspection needs logistic models. Journal of Infrastructure Systems 7 (4), 160–165.

ATV M 143-2: 1999, 1999. Inspektion, Instandsetzung, Sanierung und Erneuerung von Entwässerungskanälen und - leitungen, Teil 2: Optische Inspektion.

ATV M 149: 1999, 1999. Zustandserfassung, -klasssifizierung und - bewertung von Entwässerungssystemen auerhalb von Gebäuden.

Baur, R., Herz, R., 2002. Selective inspection planning with ageing forecast for sewer types. Water Science and Technology 46 (6-7), 389–396.

Dirksen, J., 2006. Probabilistic modelling of sewer deterioration. Master's thesis, Delft University of Technology.

Dirksen, J., 2009. Strategic asset management of water supply and wastewater infrastructures; The role of uncertainty in urban drainage decisions: uncertainty in inspection data and their impact on rehabilitation decisions. IWA Publishing, Ch. 6, pp. 273–287.

Dirksen, J., Clemens, F., 2008. Probabilistic modeling of sewer deterioration using inspection data. Water Science and Technology 57 (10), 1635–1641.

Dirksen, J., Clemens, F., Korving, H., Cherqui, F., Le Gauffre, P., Ertl, T., Plihal, H., Müller, K., Snaterse, C., 2013. The consistency of visual sewer inspection data. Structure and Infrastructure Engineering 9 (3), 214–228, first published on: 07 February 2011 (iFirst).

EN 13508-2, 2003. Conditions of drain and sewer systems outside buildings - part 2: Visual inspection coding system.

Hüben, S., 2002. Einflüsse auf die Qualität der Zustandsklassifizierung von Kanalhaltungen. Master's thesis, Rheinisch - Westfälisch Technische Hochschule Aachen.

Korving, H., 2004. Probabilistic assessment of the performance of combined sewer systems. Ph.D. thesis, Delft University of Technology.

Korving, H., Clemens, F., 2004. Reliability of coding of visual inspections of sewers. In: Proceedings of the 4th international conference on Sewer Processes and Networks, Funchal, Madeira, Portugal.

Le Gauffre, P., Cherqui, F., 2009. Sewer rehabilitation criteria evaluated by fusion of fuzzy indicators. In: Proceedings of Leading Edge Sewer Asset Management conference, Miami, USA.

Le Gauffre, P., Joannis, C., Vasconcelos, E., Breysse, D., Gibello, C., Desmulliez, J.-J., 2007. Performance indicators and multicriteria decision support for sewer asset management. Journal of Infrastructure Systems 13 (2), 105–114.

Macmillan, N., Creelman, C., 1991. Detection theory: a users guide. New York: Cambridge University Press.

Miller, G., 1956. The magical number seven, plus or minus two: some limits on our capacity for information processing. Psychological Review 63 (2), 81–97.

NEN 3398:2004, 2004. Buitenriolering, onderzoek en toestandsbeoordeling van objecten.

NEN 3399:1992, 1992. Buitenriolering, classificatie systeem bij visuele inspectie van riolen.

Norman, G., 1992. Expertise in visual diagnosis: a review of the literature. Academic Medicine 67 (10 suppl.), S78–S83.

Phares, B., Washer, G., Rolander, D., Graybeal, B., Moore, M., 2004. Routine highway bridge inspection condition documentation accuracy and reliability. Journal of Bridge Engineering 9 (4), 403–413.

Plihal, H., 2009. Evaluierung von Manahmen zur Qualitätssicherung bei der Kamerabasierten Kanalinspection. Master's thesis, Universität für Bodenkultur Wien, Department Wasser-Atmosphäre-Umwelt.

Snaterse, C., 1989. Feststellung, Klassifizierung und Erhebung von Schäden an Kanälen in den Niederlanden. In: In proceedings of the 2nd international conference on pipeline construction, Hamburg, Gemany. pp. 385–399.

van der Steen, A., Dirksen, J., Clemens, F., accepted, 9 May 2013. Visual sewer inspection: detail of coding system versus data quality? Structure and Infrastructure Engineering.

Werey, C., Cherqui, F., Ibrahim, M., Le Gauffre, P., 2007. Performance assessment of urban infrastructure services; Sewer asset management tool: dealing with experts opinions. IWA Publishing, Ch. 2, pp. 125–134.

Wirahadikusumah, R., Abraham, D., Iseley, T., 2001. Challenging issues in modeling deterioration of combined sewers. Journal of Infrastructure Systems 7 (2), 77–84.

Chapter 3

Monitoring Settlement

The first paragraph of this chapter is based on a paper entitled 'Quality and use of sewer invert measurements.' published Structure and Infrastructure Engineering [Dirksen et al., 2013]. The second paragraph is based on a paper entitled 'Slope profile measurement of sewer inverts.' submitted to Automation in Construction.

Currently, decisions on sewer rehabilitation are often based on visual inspection. The use of visual sewer inspection as the primary investigation technique, however, has major drawbacks. As shown in the previous chapter, visual sewer inspection data is poorly reproducible. Therefore, it is very likely that any final decision or result of a deterioration model based on this data source is only tentatively linked to the actual (or future) condition of the inspected sewer pipe. Consequently, sewer management based on visual inspection data will likely result in ineffective management. In other words, there is an immediate need for an alternative source of reliable information to guide sewer rehabilitation.

In many deltas settlement significantly influences the vertical position of sewer system elements. Consequently, it is likely that sewers might fail before the end of the usually assumed lifetime of 60 years. Monitoring and assessing sewer settlement in areas prone to settlement might be an alternative to the unreliable visual inspection data. As illustrated by figure 3.1, problems are not likely caused by settlement itself, but rather by a difference in settlement rates. Settlement differences can occur at different spatial scales. Figure 3.1 illustrates two scales: differential settlement on network level (figure 3.1B) and differential settlement of sewer pipes (figure 3.1B). At pipe level, differential settlement is most likely to cause the development of local defects such as fractures, open joints and infiltration. Examples of dysfunctioning caused by settlement differences on network level are a decrease in storage capacity and fouling of the system. As a result, the sewer system may not comply with the original design standards in terms of flooding and/or environmental demands.

The analysis of differential settlement on both scales (pipe and network level)

requires different methods. For the analysis of settlement on network level, measurements of the sewer invert level at the location of the connection of a manhole are used. Measurements of the profile of sewer invert by the camera tractor are used to assess settlement of sewer pipes. The quality of both types of measurements will be described in this chapter.

3.1 Monitoring settlement on network level

In general, settlement is monitored by repetitive measurements of the vertical position of the same object. The accuracy with which the settlement process can be observed depends on the number, frequency and accuracy of the measurements, duration of measurement period and the dynamics of the settlement process. Table 3.1 [Raad voor aarde en klimaat, 2007] compares different devices or methods to measure the vertical position of an object regarding costs, resolution in space and time, measurement accuracy and applicability. The methods are discussed in more detail in the following.

Traditionally a levelling instrument is used to determine the vertical position of an object. Because this device can only measure height differences, the measurement starts from a benchmark with a known elevation. In the Netherlands around 13000 of these benchmarks (or NAP bolts) are available. With this measurement an accuracy in the order of millimetres can be attained. The main drawback of the method is that it is quite costly, because the measurement is time consuming and requires qualified personnel.

GPS was developed at the end of the 20th century. Nowadays real-time kinematic GPS positioning provides centimetre-level precision and is commonly used in surveying and navigation. However, reliable GPS tracking requires good sky visibility which is not always the case in urban areas. As a result, the quality reduces to a systematic error of $5 - 10\,m$ (GPS without ground stations) see e.g. MacGougan et al. [2009]. Another difficulty of the method is that GPS position
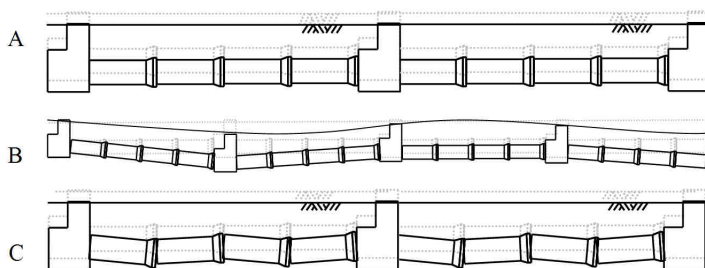
Figure 3.1: Differential settlement: a) no settlement difference, b) network level: settlement differences between manholes, c) pipe level: differential settlement of pipes.

measurements are relative to the geoide. In order to attain a position relative to NAP, the position of the geoide relative to NAP (Normaal Amsterdams Peil or Amsterdam Ordnance Datum) should be known. In the Netherlands this relative position is know up to a level of $\pm 7\,mm$ [de Bruijne et al., 2005].

Aircraft based lidar is particularly successful in detecting subtle topographic features such as river terraces, river channel banks and dikes. At the instigation of surface water managers, the area of the Netherlands has been measured twice using lidar. The first measurement (Actueel Hoogtebestand Nederland-1 or AHN-1) was measured between 1996-2003 with a systematic error of $\pm 0.05m$ and a random error with $\sigma = 0.15\,m$; the second measurement (AHN-2, 2007-2012) has a smaller random error with $\sigma = 0.05\,m$ [van der Zon, 2011]. Despite this improvement, the method is still not accurate enough to monitor settlement rates in the order of a few $mm\,year^{-1}$. Another drawback of the method is that in urban areas, the 'shadows' of high buildings hamper the measurement of the whole surface area.

Space-borne radar interferometry is a cost-effective and powerful technique capable of observing the earth's topography and surface movement for any given area with a high resolution on a wide spatial scale with regular repeat intervals. In the late 1990s, the Persistent Scatterer Interferometry (PSI) technique [Ferretti et al., 2000] was introduced to process a stack of images and to extract deformation by exploiting coherent pixels. This technique provides relatively high density of such coherent pixels in urban regions and high precision in surface movement estimation. Further Dheenathayalan and Hanssen [2011] and Dheenathayalan et al. [2011] demonstrate how radar images can be used to monitor and interpret surface movement in urban areas. Another practical example of the application of radar images to analyse deformation history of a dike can be found in Hanssen and Leijen [2009]. The main limitation is that it is an opportunity based technique and therefore the settlement measurement at a given desired location or object

Table 3.1: Comparison between different methods to monitor settlement.

device or method	cost	spatial resolution	resolution in time	accuracy	applicability
levelling instrument	high	point measurement	low	high	unlimited
GPS	average	point measurement	high/ average	average	unlimited
lidar	low	semi-continuous	high/ average	low	limited
radar	low	point measurement	average	high/ average	limited

cannot be guaranteed.

Although large parts of the Netherlands are settlement prone, currently no national monitoring network has been installed. As a consequence, figures on local settlement rates cannot be given for most cities in the Netherlands, including Amsterdam. For the city of Amsterdam, however, an alternative data source is available: historical data on the vertical position of the sewer invert. Although this parameter was not measured with the specific aim to monitor settlement, the nature of the data, i.e. repeated measurements of the vertical position of the same object, allows estimating historical settlement rates. An additional advantage of this data source is that it is directly related to the studied infrastructure: the sewer system.

3.1.1 Sewer invert measurements

To determine the vertical position of the sewer invert, two properties are measured: the vertical position of the manhole cover and the distance between manhole cover and sewer invert (figure 3.2). In theory, the level of the manhole cover only can also be used to estimate settlement rates, but, because all objects on ground level are influenced by road maintenance, these time series are often discontinuous.

The level of each manhole cover is measured relative to NAP using a levelling instrument (figure 3.3). The measurement starts from a bench mark (NAP bolt). These bench marks are usually stainless steel pins attached to objects with a piled foundation such as buildings and bridges. In the Netherlands, bench marks are usually within reach of $1\,km$.

Figure 3.4 gives an example of the layout of a survey. As can be seen, the survey consists of several runs. The first observation of each run is made to a bench mark or to a known point from a previous run and is termed backside. Each run also ends with the measurement of a known point. In paragraph 3.1.2 the difference in both readings is used to estimate the measurement uncertainty.

Since sewer systems are constructed in built-up areas, not all manholes are within direct sight of a benchmark. To facilitate measurement of all manhole
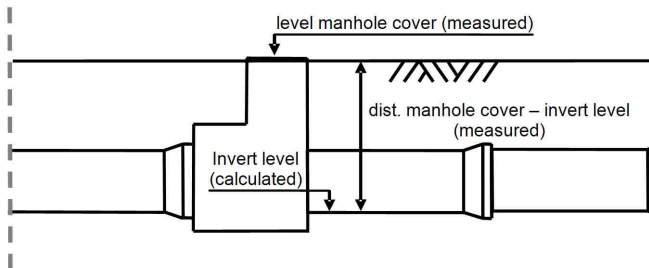
Figure 3.2: Measured and calculated properties.

covers, the instrument needs to be relocated several times. Each location of the instrument is called a change point. As can be seen in figure 3.4, manholes are frequently used as change points.

After the measurement of the level of the manhole cover, the distance between manhole cover and invert level is measured using a rod. An extra bar is welded perpendicular to the rod; this bar is positioned on the invert of the sewer and a foot is placed on the manhole close to the rod (figure 3.3). The distance to be measured is indicated by the underside of the shoe and can be read on the rod. As can be seen in figure 3.3, the rod is marked in $0.01\,m$ increments.

All measured values are processed by a computer; doubtful values (level manhole cover is increasing, large deviation from previous measurement) are identified and measured for a second time. Based on the level of the manhole cover and the distance between manhole and invert level, the level of the sewer invert is calculated.

Figure 3.3: Left: measurement of a manhole cover using a levelling instrument. Middle: measurement of the distance between invert level and manhole cover using a rod. Right: graduation on the rod.
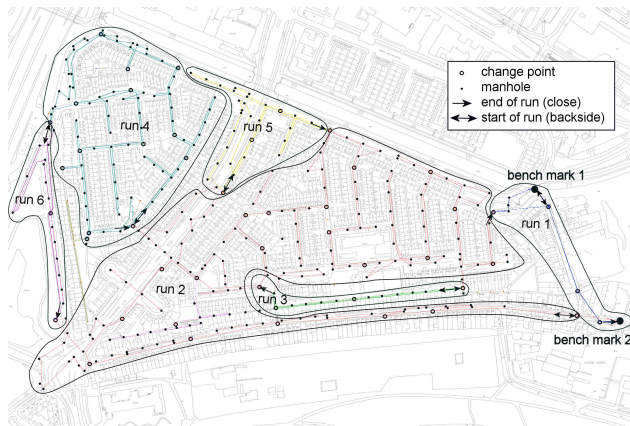
Figure 3.4: Survey layout in the Waddendijk area.

3.1.2 Sewer invert measurements - measurement error

Since no repetitive measurements within a short time interval are available, historical data is used to estimate the measurement error. This data allows estimating the error in the measurement of the level of the manhole cover and the error in the combined measurement (level manhole cover and distance between manhole cover and sewer invert). Based on these two errors, the error in the measurement of the distance between manhole and sewer invert is estimated.

Error in the measurement of the level of the manhole cover

As described previously, each run of the levelling survey is concluded with a measurement of a point with a known or previously measured level. The difference in both readings (closure error) is used to estimate the error in the measurement of the vertical position of the manhole cover. For this analysis, the data of levelling surveys contracted by the city of Amsterdam for the period of April 2009 until September 2011 is used. This database consists of 469 runs. All runs with a closure error larger than $0.05\,m$ were measured twice and are therefore excluded from this analysis. Figure 3.5 gives the histogram of the closure error in the remaining 439 runs. As expected (table 3.1) the method has a small error with a standard deviation ($s_{manhole}$) of $0.007\,m$; the average close is $0m$. From the probability plot it can be seen that the distribution is less peaked than a normal distribution. The relative heavy tails might be caused by processes that result in an error close to $0.05\,m$, for example when accidentally bumping against the levelling device.

Error in the determination of the sewer invert

For the analysis of the error in the determination of the sewer invert, time series of the vertical position of the sewer invert are used. The basis of the analysis

(a) distribution   (b) normal probability plot
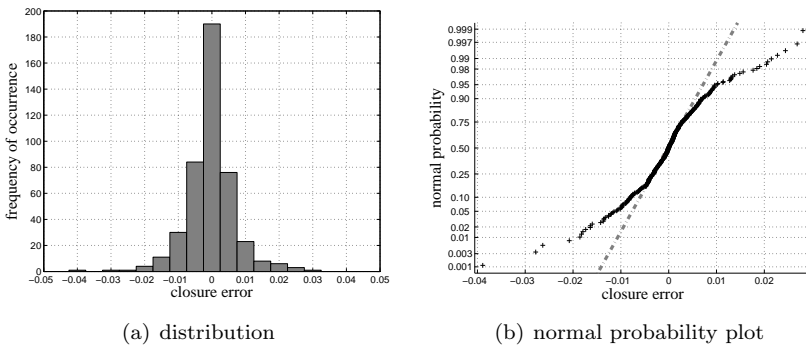
Figure 3.5: Distribution and probability plot of the closure error.

is the assumption that on a relatively short time span (in the order of several decades) and after initial settlement, the settlement process can be described by a linear model [e.g. Budhu, 2007]. The deviation of the individual measurements from the linear model is used to estimate the measurement error as explained in this paragraph. To describe the settlement process a linear model is used:

$$\hat{z} = a + bt \tag{3.1}$$

The parameters of the linear model are estimated by the measurement data according to

$$\left[\begin{array}{c} a \\ b \end{array} \right] = (T'T)^{-1} T'z \tag{3.2}$$

$$\text{with } z = \left[\begin{array}{c} z_1 \\ \vdots \\ z_n \end{array} \right] \text{ and } T = \left[\begin{array}{cc} 1 & t_1 \\ \vdots & \vdots \\ 1 & t_n \end{array} \right] \tag{3.3}$$

z_i refers to an observed value at moment t_i, $i = 1, 2, n$ and n represents the number of measurements.

The difference between the observed value, z_i, and the value estimated by the model, $\hat{z}_i$, can be used to estimate the measurement error (s_z) by [Otto, 2007].

$$MSS_R = \frac{\sum_{i=1}^{n} (z_i - \hat{z}_i)^2}{n - p} \cong s_z^2 \tag{3.4}$$

with MSS_R, the mean sum of squares due to the residuals and p refers to the number of independent parameters (for the linear model 2).

To illustrate the method, figure 3.6 shows the time series of one manhole. For this manhole, six measurements of the sewer invert level were available; the normal error is $\sqrt{MSS_R} \cong s_z = 0.014\,m$.
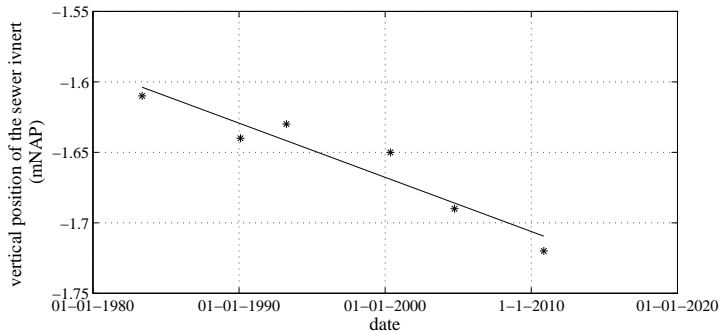
Figure 3.6: Measurement data and linear model for an invert level.

In theory, MSS_R is composed of the sum of squares of pure experimental error and the sum of squares due to a lack of fit. It is only possible to differentiate between these two if at least one replication is performed at an independent vector combination. Since this is not the case, the pure experimental error is slightly overestimated.

To test the adequacy of the linear model, the F test for goodness-of-fit was carried out. The F value is calculated by

$$F(p-1, n-p) = \frac{MSS_{fact}}{MSS_R} \tag{3.5}$$

with MSS_{fact} the mean sum of squares of the factors. MSS_{fact} is calculated by

$$MSS_{fact} = \frac{\sum\limits_{i=1}^{n}(\hat{z}_i - \bar{z})^2}{p-1} \tag{3.6}$$

If the F value is greater than the critical F value at significance level , it can be concluded that the linear model provides a good fit for the data. For the time series shown in figure 3.6, the F value was 39 which is larger than the critical F value at significance level $\alpha = 0.95$ of 8. Therefore, for this sewer invert, the linear model fits the data adequately.

To reliably estimate the measurement error, more time series of sewer invert levels are analysed. For this, historical data of the sewers in one area, Waddendijk, were gathered (historical maps of 1983, 1990 and 1993 and digital data from 1995 to 2009). Of in total 288 sewer inverts 6 historical measurements were available. For each of these sewer inverts the MSS_R was calculated and the goodness-of-fit test (for $\alpha = 0.95$) applied. In total 19 sewer inverts failed the goodness-of-fit test, the distribution of the MSS_R of the remaining 269 sewer inverts can be seen in figure 3.7. The distribution follows a log-normal distribution. The average MSS_R is $0.24 \cdot 10^{-3}$ resulting in a standard error of $\sqrt{MSS_R} \cong s_z = 0.016\,m$.
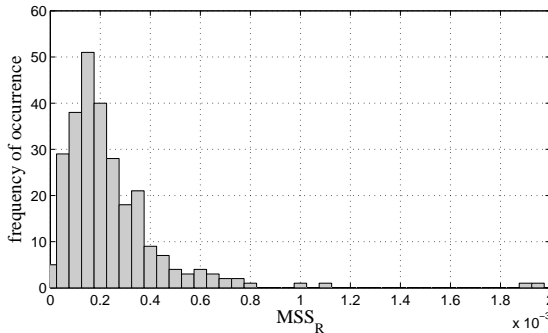
Figure 3.7: Distribution of MSS_R.

Error in the measurement of the distance between manhole and sewer

Combining both (uncorrelated) errors, the error of the measurement of the distance between manhole cover and sewer invert can be estimated by

$$s_z^2 = s_{manhole}^2 + s_{distance}^2 \tag{3.7}$$

or

$$s_{distance} = \sqrt{s_z^2 - s_{manhole}^2} \tag{3.8}$$

with $s_z = 0.016\,m$ and $s_{manhole} = 0.007\,m$ this results in $s_{distance} = 0.013\,m$. Since the measurement equipment is marked with a centimetre graduation (figure 3.3) an error of 1-2 centimetres was to be expected.

3.1.3 Calculation of the settlement rate

For settlement analysis and settlement predictions the settlement rate needs to be calculated. The settlement rate is equal to parameter b of the linear model (equation 3.1). To calculate the confidence interval (CI) for the parameter b in most situations the F-statistic for a given significance level (α) by [Otto, 2007] is used:

$$CI_b = \sqrt{F(\alpha; 1, n - p)s_b^2} \tag{3.9}$$

Where s_b^2 refers to the diagonal element in the variance-covariance matrix corresponding to parameter b which is calculated by:

$$C = MSS_R(T'T)^{-1} = \begin{bmatrix} s_a^2 & s_{ab}^2 \\ s_{ba}^2 & s_b^2 \end{bmatrix} \tag{3.10}$$

These equations however implicitly assume that the error in the measurements (MSS_R or s_z) is determined based on the same dataset whereas in our situation the error in the measurement is determined by an other, independent dataset. Applying these formulas would therefore result in a too large confidence interval. Because this situation (measurement error known) is uncommon, most books (e.g. Otto [2007] and Walpole and Myers [1993]) on linear regression do not include this scenario. In Rice [2007] the above formulas are derived in a more systematic way giving the opportunity to find the correct method to calculate the confidence interval. In Rice [2007] it can be found that the variation of the estimated b, $\hat{b}$ is equal to:

$$Var(\hat{b}) = \frac{\sigma^2}{\sum\limits_{i=1}^{n}(t_i - \bar{t})^2} \tag{3.11}$$

From which it follows that $\hat{b}$ has a normal distribution with mean b and standard deviation:

$$s_{\hat{b}} = \frac{s_z}{\sqrt{\sum\limits_{i=1}^{n}(t_i - \bar{t})^2}} \tag{3.12}$$

The width of the 95% confidence interval of a normal distributed parameter is equal to almost twice the standard deviation:

$$\hat{b} - 1.96 \frac{s_z}{\sqrt{\sum\limits_{i=1}^{n}(t_i - \bar{t})^2}} \leq b \leq \hat{b} + 1.96 \frac{s_z}{\sqrt{\sum\limits_{i=1}^{n}(t_i - \bar{t})^2}} \tag{3.13}$$

Because the width confidence interval depends only on the moment of measurement (by t_i and $\bar{t}$) and the error of an individual measurement (by s_z), the uncertainty in the settlement rate estimation of an intended measurement campaign can be estimated in advance using equation 3.13. For the example of figure 3.6 (measurement on: 16-5-1983, 7-2-1990, 30-3-1993, 12-5-2000, 29-9-2004 and 9-11-2010 and a s_z of $0.016\,m$), the estimation of b is $-3.8 \pm 1.4 \cdot 10^{-3}\,m\,year^{-1}$ at the 95% confidence limit.

In chapter 4 the settlement rate of individual manholes in the Waddendijk case study area will be presented and discussed.

3.2 Monitoring differential settlement of sewer pipes

In literature, settlement is often mentioned as one of the causes of sewer dysfunctioning. Examples of defects which are frequently related to settlement (differences) are displaced or open joints [DeSilva et al., 2005, Bishop et al., 1998] and fractures [Davies et al., 2001, Read and Vickridge, 1997].

To study these relations, the question arises how to measure the displacement of sewer pipes. In literature many information can be found concerning methods to locate underground assets from above the ground. These methods include ground penetrating radar, acoustic devices, induced current and radio frequency identification technology [Metje et al., 2007, Kumar and Sommerville, 2012]. The accurate and successful application of these methods however, depends highly on local conditions (soil properties, groundwater level) and the studied asset (depth, material). Therefore, to overcome these issues, a method that is able to measure the profile from within the sewer is preferred.

The most straightforward method to measure the slope profile from within the sewer is by using a camera tractor. These tractors are commonly used for the visual inspection [Wirahadikusumah et al., 1998]. Since this is the primary investigation technique in sewer system management, these systems have been continuously improved during the last decades. One of the more recent additions is the integration of a tilt meter. When driving through a sewer and measuring the location and slope simultaneously, a profile of the slope can be obtained.

The accuracy of the results of this measurement technique is determined by the specifications of the electronic tilt meter but also by the execution of the measurement and properties of the measured object. Examples of sources of errors are:

- roughness of surface of pipe (including joints)

- unequal size of the wheels

- path of the camera in the pipe not parallel to the axis of the sewer

- stretch of the cable

Because the minimal slope of a sewer is only 0.2% [Butler and Davies, 2004], the technique should be able to accurately measure slopes/slope differences of only a few tenths of a percentage. Although currently tractors are frequently equipped with an electronic tilt meter, information about the quality of the measurement is limited. In this paragraph the results of a study into the quality of the electronic tilt meter integrated in the IBAK KRA85 camera tractor are presented. Although the results of this study apply to one specific instrument, the method to assess the error (accuracy and precision) is generic.

3.2.1   Slope profile measurement

To measure the vertical profile of a sewer the electronic tilt meter integrated in the IBAK KRA85 camera tractor was used (figure 3.8). When driving through a sewer, this device can be used to obtain a profile of the slope of the sewer invert by measuring the tilt. In order to derive the vertical profile from the measurements, the position of the tractor has to be recorded as well. Because the wheels of the tractor might skid when driving through the sewer, the slope measurement is executed when reversing the tractor by pulling the cable. The camera is pulled mechanically by a winch of which the speed can be controlled by the inspector. The cable is guided by a pulley that rotates along with the cable; one rotation of the pulley corresponds to $0.1\,m$ cable.

Software programs deal with the collection and storage of the data. For this research the software of IBAK in conjunction with software provided by engineering firm Moons was used. By means of this software, the final result consists of a text file indicating a position and the corresponding slope.
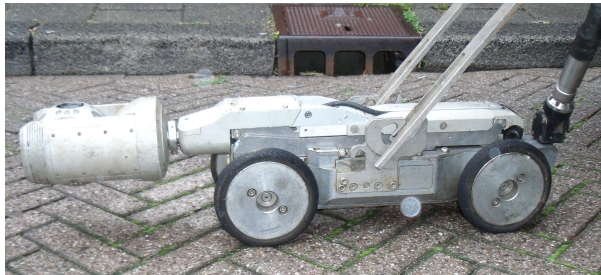
Figure 3.8: IBAK KRA85 camera tractor with camera.

To verify the relation between the actual situation, the measurement results and computer settings, the slope of a wooden board with a known inclination was measured. This simple test revealed that:

- The slope, defined as dz/dx (with dz, the rise and dx, the slope length) is measured in percentages.

- The slope is positive when the front wheel pair is located at a lower elevation than the back wheel pair (see figure 3.9).

- The position is measured in meters starting at the position where the slope measurement was begun (close to manhole B in figure 3.9).

- The first measurement value is recorded after pulling 0.1 meter cable; the registered position is 0.1. Therefore the positions recorded in the slope measurement file do not correspond to the locations shown on the video screen during the inspection.

- Normally the sewer is inspected before carrying out the slope measurement. Prior to the sewer inspection the starting location can be adjusted manually, for example to ensure that $x = 0$ is located at the beginning of the sewer. The adjustment of the starting location only influences the location shown on the video screen; it does not influence the result of the slope measurement.

Since the 'percentage' grade is the unit of the output of this device and the most commonly used unit when communicating slopes, this unit will also be used in this thesis.
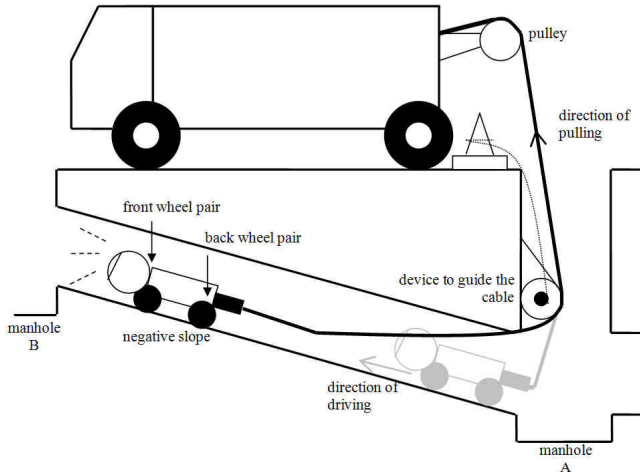
Figure 3.9: Measurement set-up.

As indicated in the manual provided by IBAK [IBAK software, 2009], frequent calibration is necessary to obtain accurate results. To calibrate the tilt meter, the tractor is placed on a plate of which the inclination in both horizontal directions (x and y) can be adjusted. A spirit level is used to assure that, after adjustments, the plate is horizontal in both directions. While being positioned on the horizontal plate, computer software resets the measured slope to zero. In order to include the uncertainty of the calibration in the analysis of the measurement error, all the measurements described in this paper are preceded by a calibration.

Some specifications of the tilt meter can be found in the manual provided by IBAK. According to this manual, all measurements acquired within one rotation of the pulley are averaged to derive one slope value. Since one rotation of the pulley corresponds to $0.1\,m$, the distance resolution is $0.1\,m$. The specified resolution of the slope measurement is 0.1%. The tiltmeter is able to measure values in the range of $\pm 12.5\%$.

The manual also gives an indication of the error of the measurement. According to the manual, the absolute measurement error is $\pm 0.2\%$. This implies that for a sewer of $30\,m$, the derived difference in vertical position of both sewer ends (ΔH) varies within $\pm \frac{30}{100} \cdot 0.2 = \pm 0.06\,m$.

To verify the accuracy and precision of the measurement, the slope of a concrete sewer was measured 10 times consecutively. The slope of the sewer was measured from both directions: 5 measurements starting from manhole A and 5 measurements starting from manhole B (figure 3.9). The results are shown in figure 3.10. For the interpretation of the results, both sets of slope measurements are converted such that $x = 0$ corresponds to the centre of manhole A: $x_{new} = 0$
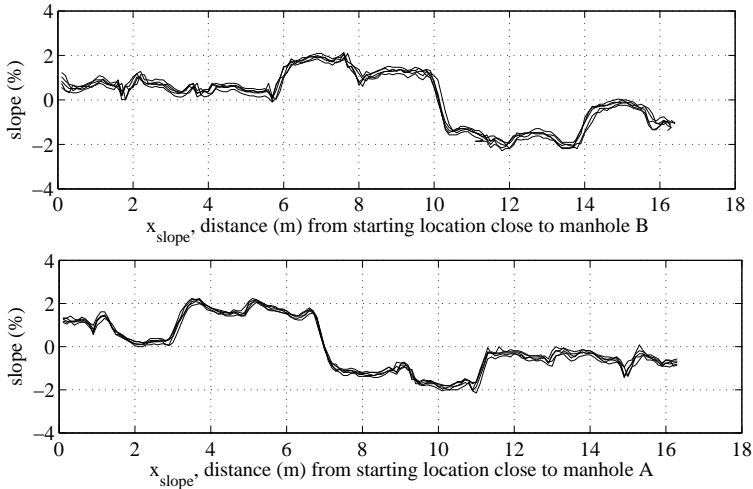
Figure 3.10: The result of 10 slope measurements: 5 for each direction (raw data).

(figure 3.11). By doing so the locations in the new slope measurement file will correspond with the locations as shown on the inspection video. The location of the first slope measurement in the new file (i.e. smallest x-value for which the slope could be measured) can be calculated when the following values are known:

- The starting position of the camera ($D_{initial}$, see figure 3.11). When installing the camera in the sewer, special care was taken to ensure that for each measurement the camera was positioned at the same distance from the connection of the sewer with the manhole. The distance between the beginning of the sewer and the centre of the camera lens when turned perpendicular to the direction of movement was estimated at $1.2\,m$. This distance is inserted in the computer which uses this value to adjust the location shown on the video screen.

- The distance between camera lens and centre of the axis of camera tractor (D_{lens}), $0.4\,m$.

- The radius of the manhole, this value is estimated at $0.4\,m$ ($D_{manhole}$).

- The distance covered by the camera when driving through the sewer ($D_{driving}$) and when pulling the camera ($D_{pulling}$).

The x-value in the new file where the last slope value in the original file was measured (i.e. smallest x-value for which the slope could be measured) can be calculated with:

$$x_{start} = D_{manhole} + D_{initial} + D_{driving} - D_{pulling} - D_{lens} + 0.05 \qquad (3.14)$$

The value $0.05\,m$, half of the distance resolution, is added to the equation in order to assign the tilt values to a location halfway the distance covered when collecting the data to calculate this value.
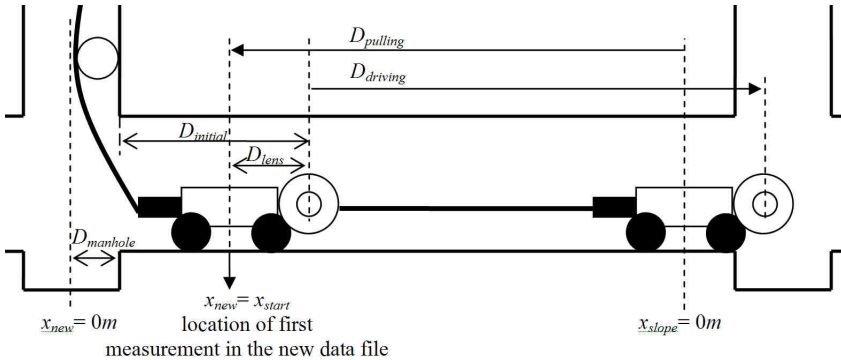
Figure 3.11: Distances required to alter the distance vector in such a way that it corresponds with the locations shown on the video screen during inspection.

By turning the camera head to a position perpendicular to the direction of movement, the location of pipe joints can be monitored. Using this method, also the location of the end of the sewer (i.e. connection with manhole) was recorded. Based on this information, the file is extended to cover all x-values from the center of both manholes. For the locations where no tilt value was obtained a NaN (Not any Number) is used instead.

Figure 3.12 shows the result of the described data transformations. To compare both sets of measurements, the sign of the slope of the second set is reversed and the x-vector is adjusted in order to represent the distance from manhole A instead of B (figure 3.9).

Additional to the 10 slope measurements of the same sewer, the slope measurements of in total 92 sewers were used to verify the accuracy of the measurement.

3.2.2 Slope profile measurement - measurement error

Analysis of the uncertainty in which the position is determined

Because the slope was measured from both directions, the accuracy in the position determination can be assessed. The accurateness of the position is of influence when extrapolating the slope measurements towards the ends of the sewer in order to derive the profile of a whole sewer. Especially the estimation of the starting position of the camera ($D_{initial}$) needs to be verified because an incorrect
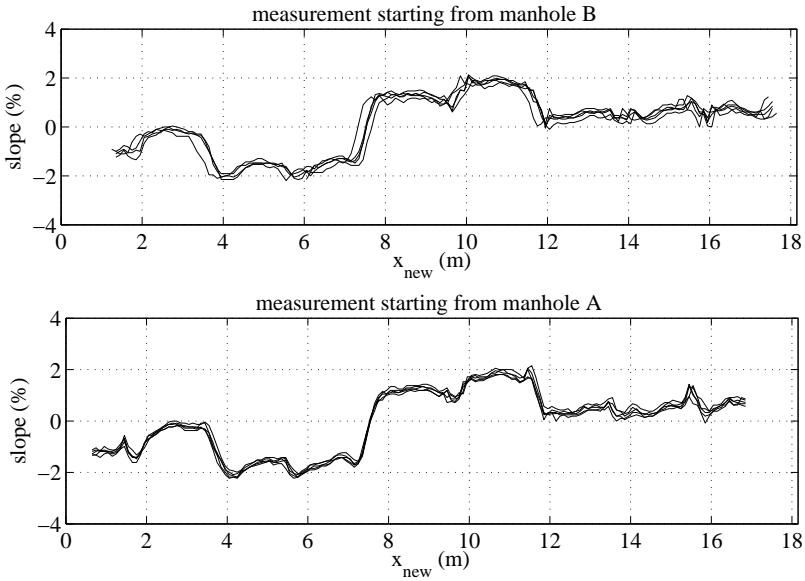
Figure 3.12: Measurement results after transformation of the distance vector.

estimation can cause a horizontal translation of the measurement data.

The accuracy in the position was analysed by calculating the mean slope profile, and comparing this to each individual dataset. By applying a horizontal translation to each dataset for different lags, the cross-correlation can be used to find the lag for which the greatest correspondence between both series was examined. A horizontal translation at the most optimal lag was applied to each dataset resulting in the graphs shown in figure 3.13.

As can be seen in the figure, from $x = 0$ until $x = 6$ one dataset does not match the others. During this measurement, measurement 4, the tractor blocked for unknown reasons. A firm tug at the cable resolved the problem but clearly influences the results. Therefore, this dataset was excluded from the analysis and the mean slope profile and cross-correlations were recalculated. The resulting optimal lags are listed in table 3.2.

When evaluating the results it stands out that for the measurements starting
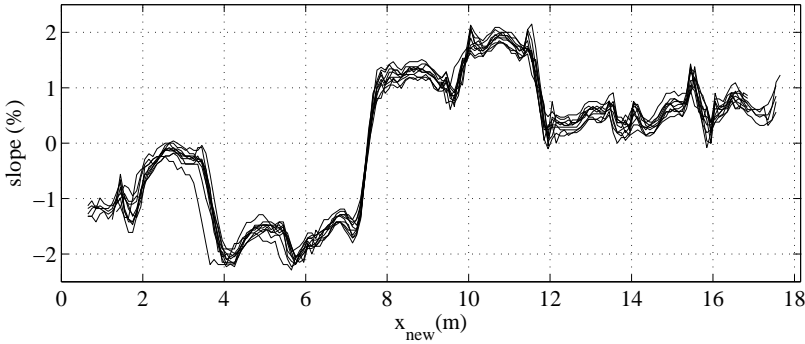
Figure 3.13: Measurement results after horizontal translation.

Table 3.2: The lags for which the greatest correspondence was found after removal of the invalid data, before and after adjustment of the starting position.

measurement started at manhole A			measurement started at manhole B		
tilt measure-ment	horizontal translation (m)	adjusted translation (m)	tilt measure-ment	horizontal translation (m)	adjusted translation (m)
1	0.1	0	6	-0.1	0
2	0.3	0.2	7	-0.1	0
3	0.1	0	8	-0.1	0
4	-	-	9	-0.1	0
5	0.1	0	10	0	0

at manhole A best correspondence was found at positive lags while for the measurements starting at the other manhole negative lags gave best correspondence. This bias is probably caused by a systematic error in the estimated starting position, $D_{initial}$. From the results it appears that that the distance between the lens and the beginning of the sewer should be estimated at $1.3\,m$ instead of $1.2\,m$. When applying this knowledge to the 9 slope measurements the optimal lags as listed in table 3.2 are found. Since no systematic deviation between the two independent sets of measurement data can be observed, it can be concluded that the distance is determined accurately.

Analysis of the uncertainty in the slope measurement

For the analysis of the uncertainty in the slope measurement 9 datasets are available (measurement 4 was excluded from the analysis). To eliminate random errors in the distance measurement, dataset 2 is translated horizontally over a distance of $0.2\,m$ (table 3.2).

Figure 3.14 shows the variance in slope measurement for the locations where 9 slope measurements were available. As can be seen the variance is clearly larger near the pipe joints. Therefore, when analysing the precision of the slope measurement, this data will be analysed separately.

To verify whether the error in the slope measurement is dependent on the measured slope, for every location the average slope is calculated. In figure 3.15 the variance is plotted as a function of the average slope. As can be seen, the variance is not correlated with the average measured slope. Therefore the error in the slope measurement is an absolute error.

The reason to measure the slope of the sewer is to attain the vertical profile of
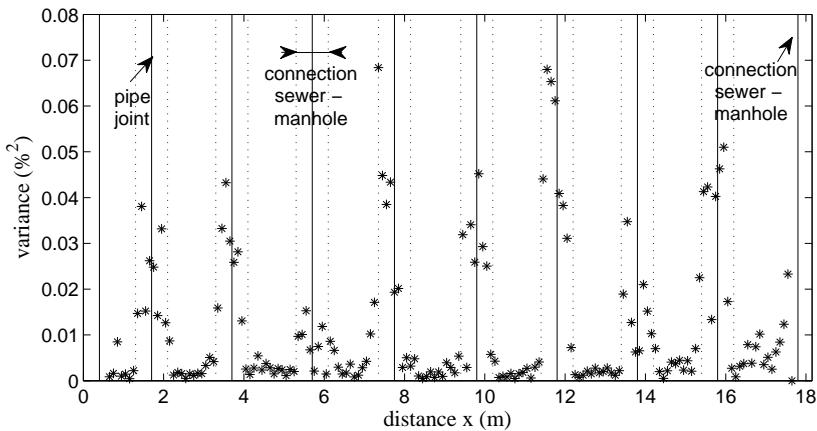
Figure 3.14: Variance in slope measurements along the sewer length.

the sewer. To analyse the uncertainty in the vertical profile of the sewer first the profile needs to be deducted from the slope measurements. This is accomplished by calculating for each measurement the corresponding rise over a distance of $0.1\,m$, the resolution of the distance measurement. Starting at $z = 0\,m$ at $x = 0\,m$, the slope measurement at $x = 0.05\,m$ can be used to define the vertical position at $x = 0.1\,m$. By integration along the whole sewer length, the sewer invert profile is obtained.

For this calculation, however, a slope measurement for each location is required. Since this is not the case, tilt values have to be estimated for the locations where it was not possible to measure the tilt. The missing values are estimated based on the assumption that each individual pipe of a sewer has, on average, the same slope (figure 3.16). By nature, this assumption is only valid for sewers made of rigid materials.

Following the method described, the profile of the sewer invert was determined for the 9 datasets. The resulting sewer profiles are depicted in the upper graph of
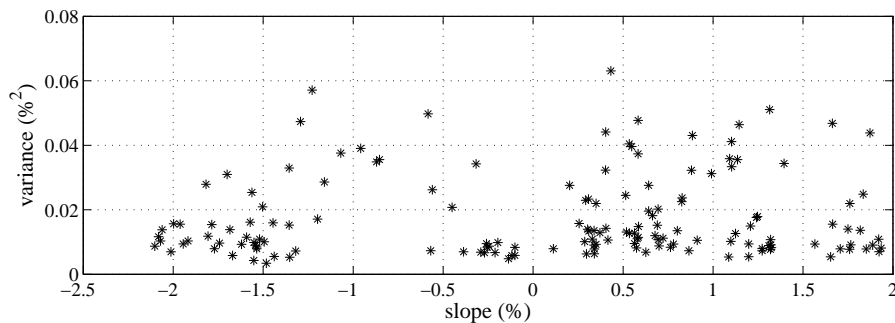
Figure 3.15: The variance in slope measurements as a function of the average measured slope. Data around pipe joints and individual pipes are combined.
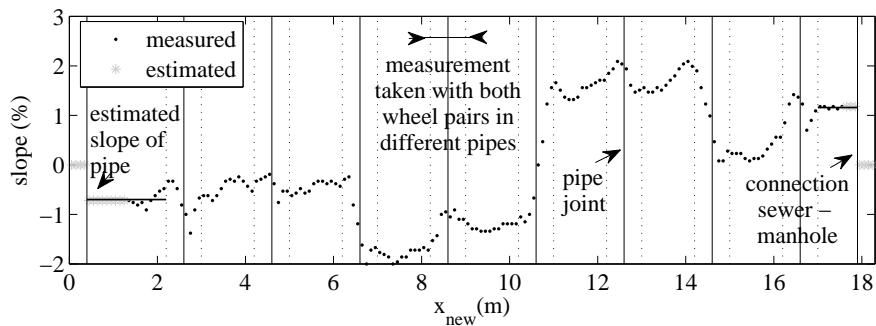
Figure 3.16: Measured and estimated values of slope measurement 9.

figure 3.17. In the lower graph of the same figure, the variance is shown. As can be seen the variance increases along the sewer length. This increase is caused by a systematic error in the slope measurement. Since this error is equal for each slope measurement within one dataset, the resulting error in the profile accumulates along the sewer length.

To analyse the uncertainties in the slope measurement first the systematic error is analysed; after elimination of the systematic error, the random errors are analysed.

Systematic error

The systematic error in the slope measurement is analysed by calculating the mean slope profile and comparing the 9 measurements with this mean profile. Like the analysis of the accuracy of the distance measurement the cross-correlation was used to find the most likely bias for which both datasets gave best correspondence. The results are listed in table 3.3. The maximum absolute bias for which the greatest correspondence was found is 0.14%.

To assess the systematic error in the slope measurement from these results, prediction intervals will be used instead of confidence intervals. Confidence intervals describe the uncertainty in the determination of the mean whereas prediction intervals describe the probability that future observations will fall within certain boundaries.
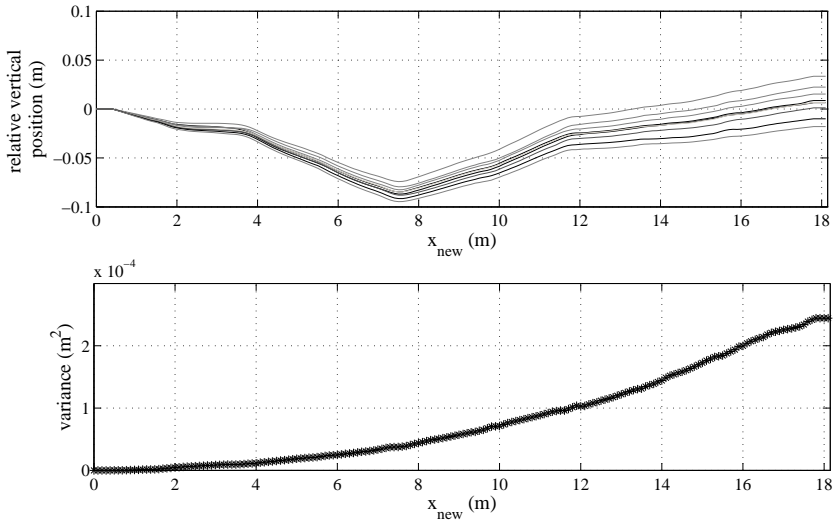
Figure 3.17: Upper graph: the resulting sewer invert profile for the 9 measurements. Lower graph: the variance in the vertical position along the sewer length.

The $(1 - \alpha)100\%$ prediction interval for the bias (y) is given by [Walpole and Myers, 1993]

$$\overline{y} - t_{\alpha/2}s_{sys}\sqrt{1 + \frac{1}{n}} < y < \overline{y} + t_{\alpha/2}s_{sys}\sqrt{1 + \frac{1}{n}} \qquad (3.15)$$

where $t_{\alpha/2}$ is a value of the t-distribution with $n - 1$ degrees of freedom.

For the values listed in table 3.3 the 95% prediction interval ($\alpha = 0.05$) with $n = 9$, $\overline{y} = 0.0005\%$, $t_{0.025} \cong 2.3$ for 8 degrees of freedom and

$$s_{sys} = \sqrt{\frac{1}{n - 1}\sum_{i-1}^{n}(y_i - \overline{y})^2} = 0.09\% \qquad (3.16)$$

the prediction interval is equal to $[-0.21, 0.21]$.

The practical meaning is that with 95% confidence one can predict that a slope measurement has a bias that falls within this range. It can be concluded that this result is consistent with the absolute error mentioned in the manual of $\pm 0.2\%$.

Random error

Apart from a systematic error, each individual measurement value is also subjected to a random error. This error can be caused by either the measurement equipment or irregularities in the measured object. To analyse the random error first the bias is eliminated (table 3.3).

In figure 3.14 the variance in slope measurements for each x-location are plotted. As can be seen the variance is much larger for the measurements obtained when each wheel pair was positioned in a different pipe. Therefore, two datasets

Table 3.3: The slope bias of each dataset of which the best correspondence with the average slope dataset was found.

measurement started at manhole A		measurement started at manhole B	
tilt measurement	slope bias (%)	tilt measurement	slope bias (%)
1	0.0058	6	-0.0893
2	0.0024	7	0.0002
3	-0.1448	8	0.0341
4	-	9	0.0962
5	-0.0421	10	0.1417

will be analysed: a dataset with measurements obtained with both wheel pairs in the same and in a different pipe.

For the dataset of values obtained with each wheel pair in a different pipe or 'joint dataset' the values at a distance of $0.3\,m$ or less from a joint were selected. Since the distance between both wheel pairs is $0.4\,m$, strictly all values at a distance of $0.4\,m$ or less should be selected. However, due to an error in the distance measurement it is very likely that this dataset would also contain measurements obtained with each wheel pair in the same pipe. For the same reason the dataset with each wheel pair in the same pipe or 'pipe dataset' will contain all measurement obtained at a distance of $0.5\,m$ or more from a joint.

Following the previously described reasoning the two datasets are created. Each dataset consist of a number of locations $j = 1 \cdots m$ with at each location at most 9 independent measurements $x_{i,j}$ with $i = 1 \cdots n$, $n \leq 9$. The number of measurements varies because the x-values where the slope could be measured are dependent on the starting location (manhole A of B) as can be seen in figure 3.12.

To analyse the shape of the distribution of the error, for the locations where 9 measurements were available ($n = 9$) the difference between a single measurement and the mean of all measurements at that location, $\bar{x}_j$, is calculated. The distribution of $x_{i,j} - \bar{x}_j$ for both the joint and pipe dataset are shown in figure 3.18.
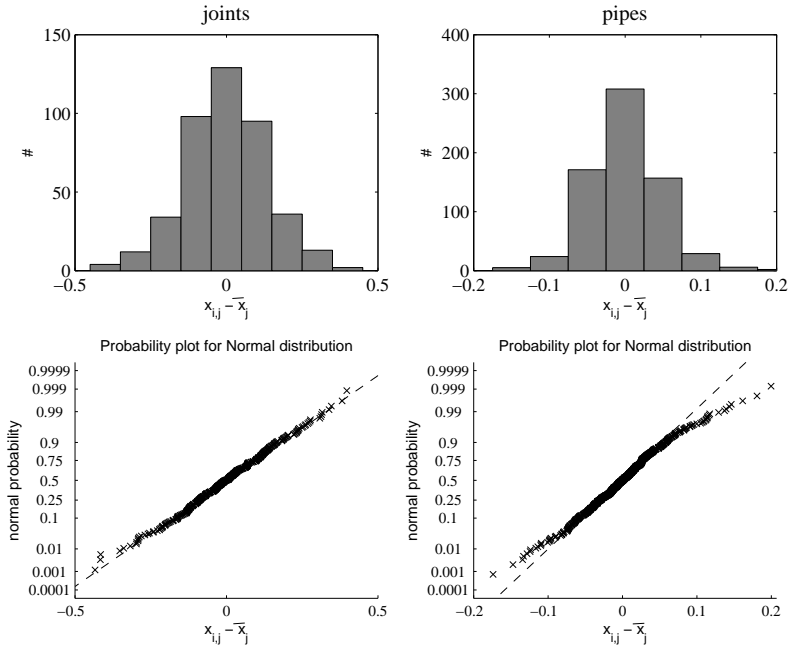
Figure 3.18: Distribution and probability plot of both datasets. Please note the difference in x-axis for the joint and the pipe dataset.

As can be seen in figure 3.18 the distribution of $x_{i,j} - \bar{x}_j$ is symmetrical for both the joint and pipe dataset. From this it can be concluded that the distribution of the random error is, as expected, symmetrical. From the probability plots it can be seen that the distribution of the joint dataset follows the normal distribution, the pipe dataset is less peaked in comparison to the normal distribution.

Because the number of measurements available at each location varies, the principle of pooled variance is used to calculate the variance in both datasets. This method can be used to estimate the variance for a set of samples that were taken in different circumstances where the mean may vary but the true variance remains the same and is calculated by:

$$s^2_{random} = \frac{\sum\limits_{j=1}^{m} \left((n_j - 1)s^2_j \right)}{\sum\limits_{j=1}^{m} (n_j - 1)} \tag{3.17}$$

with n_j the sample size of the jth sample, s^2_j the variance of the jth sample and m the number of samples being combined (84 for the joint dataset and 86 for the pipe dataset). This results in a variance of 0.021% for the joint dataset and 0.0026% for the pipe dataset. The corresponding standard deviations are 0.14% and 0.05%.

Analysis of the accuracy of the measurements

The accuracy of the slope measurement can be analysed by comparing the results of the slope measurements with the results of another independent measurement method such as sewer invert measurements. The sewer invert measurements were described paragraph 3.1 and in Dirksen et al. [2013]. The value by which both measurement techniques are compared is the difference in vertical position of the invert at both ends of the sewer, ΔH.

For the sewer invert measurements the difference in vertical position was obtained by subtraction of the most recently measured invert levels, these were taken in October 2010. To calculate ΔH for the slope measurements the sewer invert profile is deducted from the slope measurements. As explained previously, this is only possible when for each x location a slope measurement is available. In case no tilt value is available the average slope of the pipe is used. To accurately estimate the missing tilt values only slope measurements were used where for each pipe at least 3 measurements were available. In total the slope measurements of 92 sewers could be used for this analysis. The slope measurements were carried out from July until September 2010.

In figure 3.19 the difference in vertical position of the invert level at both ends of the sewer are compared for both measurement methods. To describe the relation, a linear model is fitted to the data by minimization of the squared error. As can be seen in the left graph of figure 3.19, three sewers have a relatively large difference in vertical position of the invert level and therefore considerably

influence the derived relation. Therefore, also the relation is determined without these three sewers; the result is shown in the right graph of figure 3.19.

Ideally the relation would be linear with slope 1 and offset 0. When calculating the 95% confidence bands for the slope for both datasets ([0.93 1.00] with the 3 extreme but correct measurements and [0.95 1.11] without the 3 extreme measurements) it is found that the ideal slope is within these bounds. For the offset, confidence bounds of [-0.013 -0.00075] and [-0.012 -0.00004] were found. Although the ideal offset does not lie within the latter bound, the offset is insignificant: only $0.007\,m$ for a sewer of, on average, $30\,m$, it can be concluded that the results of both independent measurement methods are consistent and therefore accurate.

3.2.3 Practical implications

To show the significance of the derived accuracy and precision of the several aspects of the slope measurement, confidence bands are calculated for the expected result (slope and sewer profile) of a single slope measurement. For this, a sewer was created of which the pipes were arranged with the average slopes of the pipes of the sewer that was used for the derivation of the accuracy and precision (figure 3.20). To calculate the confidence bands Monte Carlo methods are used. To determine the confidence interval (CI), 1000 slope measurements for the artificial sewer were derived by random sampling.

The following errors were applied:

- A systematic error, equal for all measurements within one slope measurement with a normal distribution with $\mu = 0$ and $s_{sys} = 0.09\%$.

- A random error, only for locations less than $0.4\,m$ from a joint with a normal distribution with mean equal to the slope of the artificial sewer and $s_{joint} =$
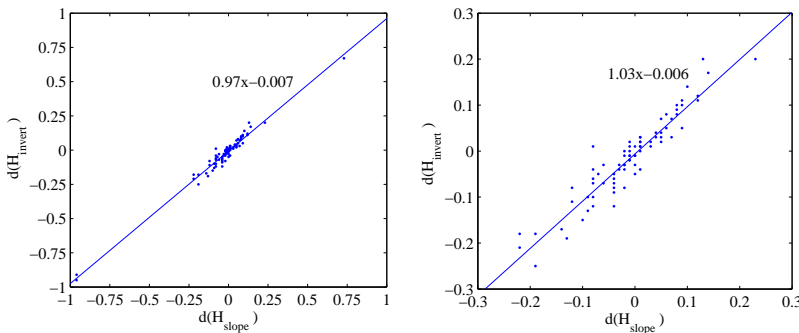
Figure 3.19: Relation between the difference in vertical position of the invert level at both ends of a sewer derived from the sewer invert measurement and the slope measurement. The right graph shows the relation without the three extreme measurements. All figures are in meters.

0.14%.

- A random error, only for locations more than $0.4\,m$ from a joint with normal distribution with mean equal to the slope of the artificial sewer and $s_{pipe} = 0.05\%$.

For each of the 1000 slope profiles the sewer invert profile was calculated and the resulting 95% CI's were derived. The results are presented in figure 3.20.

As can be seen, the CI for the slope profile is larger near the joints whereas the CI for the sewer invert profile is linearly increasing. The reason that the discontinuities of the slope measurements do not influence the CI of the sewer profile is that the errors in the slope profile are random and therefore cancel out. The increase in the 95% CI of the sewer invert level profile is caused by the systematic error, s_{sys}, equation 3.16. The 95% CI for the difference in sewer invert level at both ends of the sewer (ΔH) can be calculated by:

$$\pm \frac{2 \cdot s_{sys}}{100} L \tag{3.18}$$

with L, the distance from the starting manhole. For a sewer with a total length of $17.35\,m$ this results in a maximum 95% CI of $\pm 0.032\,m$. If a more reliable estimation of the total rise/fall of the sewer is available (e.g. based on sewer invert measurements), this can be used to correct the systematic error.
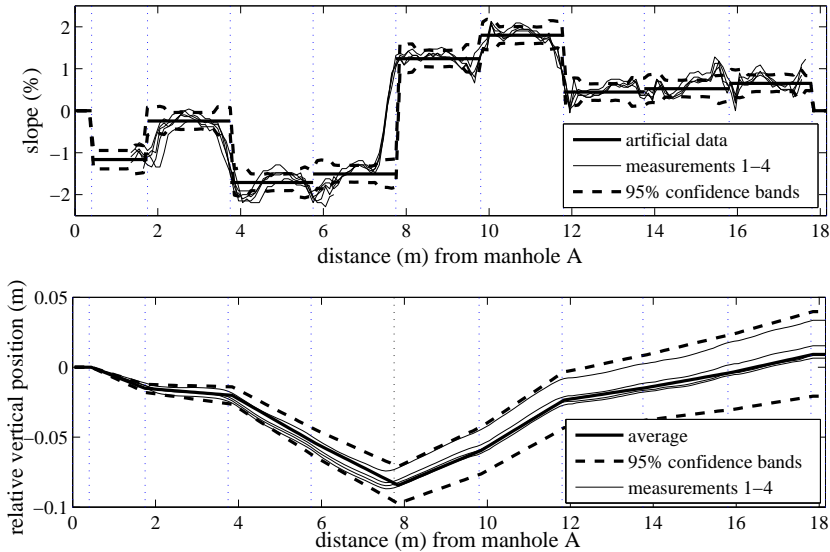
Figure 3.20: Confidence bands for the expected results of the measurement of a sewer with a profile similar to the measured sewer.

3.3   Conclusion and recommendations

The position of a sewer invert is determined by measuring the vertical position of the manhole cover using a leveling instrument and the distance between cover and sewer invert using a rod. The error of these measurements are respectively $s_{manhole} = 0.007\,m$ and $s_{distance} = 0.013\,m$, resulting in an error of $s_z = 0.016\,m$ for the sewer invert. Although in the last decades several alternatives have been developed (e.g. GPS, aircraft based lidar), leveling is still the most suitable method to accurately determine vertical positions in an urban environment.

Currently, monitoring settlement in urban areas requires a long monitoring campaign of costly and time consuming measurements. Therefore, settlement rates of most urban areas are unknown and application of the research is not likely to be expected in the near future. However, with the improvement of the interpretation of (historical) radar images, settlement analyses are expected to become less elaborate enhancing the use of settlement data for sewer asset management in areas with unstable ground conditions. Main challenge of all methods measuring settlement at ground level is how to cope with differences in ground level due to other reasons than ground settlement such as artificial ground elevation when renewing the road.

The electronic tilt meter integrated in a camera tractor is suitable for measuring the vertical profile of a sewer. Using the IBAK KRA85 camera tractor an error in the distance measurement of several centimetres can be attained when the camera is carefully installed in the sewer. The tilt meter integrated in the IBAK KRA85 tractor has a random error with $s = 0.05\%$. When both wheel pairs are positioned in a different pipe, the measurement results are influenced resulting in a larger random error of $s = 0.14\%$. Besides random errors, the measurement is also subjected to a systematic error with $s = 0.09\%$. The systematic error is caused by the calibration of the device. Since the systematic error is in the same order as the resolution it seems beneficial to improve the resolution to 0.01%.

Since the random errors are small and cancel out, *differences* in the slope of individual pipes can be measured fairly accurate. The determination of the difference in level between either end of a sewer is inaccurate because of the systematic error, therefore improvement of the calibration method is recommended.

Bibliography

Bishop, P., Misstear, B., White, M., Harding, N., 1998. Impacts of sewers on groundwater quality. Journal of the Chartered Institution of Water and Environmental Management 12, 216–223.

Budhu, M., 2007. Soil mechanics and foundations. John Wiley & Sons.

Butler, D., Davies, J., 2004. Urban Drainage. Spon Press.

Davies, J., Clarke, B., Wither, J., Cunningham, R., 2001. Factors influencing the structural deterioration of rigid sewer pipes. Urban Water 3, 73–89.

de Bruijne, A., Buren, J., Kosters, A., van der Marel, M., 2005. De geodetische referentiestelsels van Nederland - Definitie en vastlegging van ETRS89, RD en NAP en hun onderlinge relaties. Delft: Nederlandse Commissie voor Geodesie.

DeSilva, D., Burn, S., Tjandraatmadja, G., Moglia, M., Davis, P., Wolf, L., Held, I., Vollertsen, J., Williams, W., Hafskjold, L., 2005. Sustainable management of leakage from wastewater pipelines. Water Science and Technology 52 (12), 189–198.

Dheenathayalan, P., Cuenca, M., Hanssen, R., 2011. Different approaches for PSI target characterization for monitoring urban infrastructure. In: Proceedings of the 8 th International Workshop on Advances in the Science and Applications of SAR Interferometry, Frascati, Italy.

Dheenathayalan, P., Hanssen, R., 2011. Target characterization and interpretation of deformation using persistent scatter interferometry and polarimetry. In: Proceedings of the 5th international workshop on science and applications of SAR polarimetry and polarimetric interferometry, Frascati, Italy.

Dirksen, J., Baars, E., Langeveld, J., Clemens, F., 2013. Quality and use of sewer invert measurements. Structure and Infrastructure Engineering.First published on: 07 January 2013 (iFirst).

Ferretti, A., Prati, C., Rocca, F., 2000. Nonlinear subsidence rate estimation using permanent scatters in differential SAR interferometry. IEEE transactions on geoscience and remote sensing. 38 (5), 2202–2212.

Hanssen, R., Leijen, F., 2009. One-dimensional radar interferometry for line infrastructure. In: Proceedings of Geoscience and Remote Sensing Symposium 2009, Cape Town, South Africa.

IBAK software, 2009. Tilt Measurement.

Kumar, B., Sommerville, J., 2012. A model for RFID-based 3D location of buried assets. Automation in Construction 21, 121–131.

MacGougan, G., K., O'Keefe, K., Klukas, P., 2009. Accuracy and reliability of tightly coupled GPS/ultra-wideband positioning for surveying in urban environments. GPS Solutions 14 (4), 351–364.

Metje, N., Atkins, P., Brennan, M., Chapman, D., Lim, H., Machell, J., Muggleton, J., Pennock, S., Ratcliffe, J., Redfern, M., Rogers, C., Saul, A., Shan, Q., Swingler, S., Thomas, A., 2007. Mapping the underworld - state-of-the-art review. Tunnelling and Underground Space Technology 22, 568–586.

Otto, M., 2007. Chemometrics. Wiley-VCH Verlag GmbH & Co. KGaA.

Raad voor aarde en klimaat, (Accessed 2 March 2012) 2007. Bodembeweging in nederland.
URL `http://www.ncg.knaw.nl/subciebodembeweging/adviesbodembeweging.html`

Read, G., Vickridge, I. (Eds.), 1997. Sewers - rehabilitation and new construction: repair and renovation. Elsevier/Butterworh Heinemann.

Rice, J., 2007. Mathematical statistics and data analysis. Brooks & Cole.

van der Zon, N., (Accessed 3 Februray 2012) 2011. Kwaliteitsdocument AHN-2.
URL `http://www.ahn.nl`

Walpole, R., Myers, R., 1993. Probability and statistics for engineers and scientist. Macmillan publishing.

Wirahadikusumah, R., Abraham, D., Iseley, T., Prasanth, R., 1998. Assessment technologies for sewer system rehabilitation. Automation in Construction 7, 259–270.

Chapter 4

Analysis of (sewer) settlement in the city of Amsterdam

The Netherlands literally means 'low countries' or 'low lands'; large parts of the country, about 1/3 of the total area, are situated below sea level. An integrated system of dykes, waterways and pumping stations protects the county from flooding by maintaining a decreed water- and groundwater level. The artificially maintained low position of the Netherlands relative to sea level is caused by land subsidence coinciding with a period of post-glacial sea level rise.

As can be seen in figure 4.1 (left-hand side), the western part of the Netherlands experience significant ground settlement when confronted with a load of $1m$ of sand. This part of the Netherlands is a flat, low-lying delta, much of which was covered by highly compressible peat and clay soils. Over many centuries land use practices resulted in loss, decay, and consolidation of these soils and subsequent land subsidence [Hoeksema, 2007].

Despite adverse ground conditions, most Dutch cities are situated in the west. In order to be able to live and build in these swampy areas, ditches and canals are dug to drain the ground, houses have a pile foundation and ground conditions are improved by the application of extra layers of soil. However, drainage as well as the application of an extra load induce ground settlement and, as a consequence, pavements will eventually not level with house entrances (figure 4.2). This problem is in general overcome by raising the ground artificially. Paradoxically, this again causes settlement resulting in an almost indefinite cycle of settlement and artificial ground elevation.

In this thesis the city of Amsterdam will be used as a case study. Amsterdam is the capital and largest city of the Netherlands, located in the province of North Holland in the west of the country (figure 4.1, right-hand side). The city, which

has a population (including suburbs) of 1.36 million on 1 January 2008, comprises the northern part of the Randstad, the sixth-largest metropolitan area in Europe, with a population of around 6.7 million.

This chapter focuses on the assessment of settlement in the city of Amsterdam. To understand why ground settles, the chapter starts with a description of the subsurface of the Amsterdam region form a geological point of view. In the second part the settlement rate is analysed. For this analysis the sewer invert measurements as described in chapter 3: Monitoring Settlement, paragraph 3.1 are used.
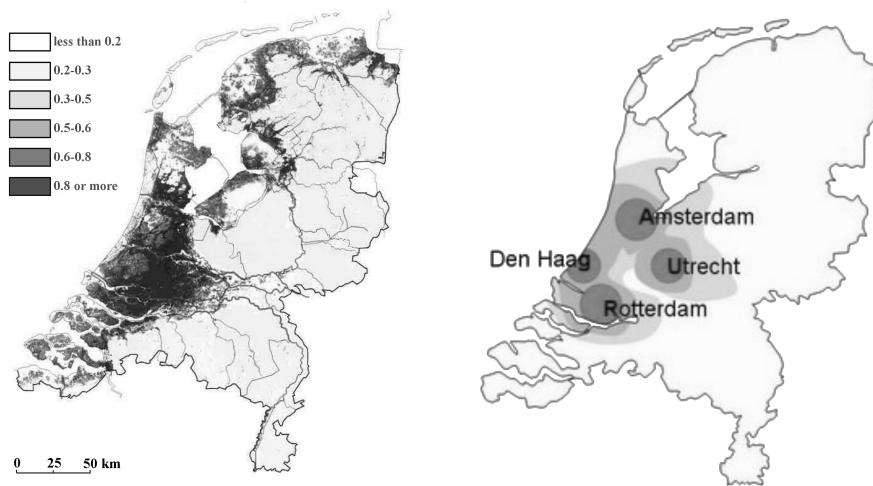
Figure 4.1: Left: expected settlement in meters when applying 1 meter of sand. Right: map of the Netherlands, the shaded area indicate the Randstad.

Figure 4.2: Creative solution to allow for entrance after ground settlement.

4.1 Description and formation of the Amsterdam subsurface

The subsurface of the Amsterdam area consist of a $10m$ Holocene peat layer and fine clastic tidal deposits underlain by a glacial basin mainly filled with lacustroglacial- and marine clay (figure 4.3). In order to understand the origin and characteristics of these layers, the processes (natural as well as non-natural) which formed these layers are described in the following. As standard in the Netherlands, the chronostratigraphy based on climatic variations as presented by Zagwijn [1991] is used.
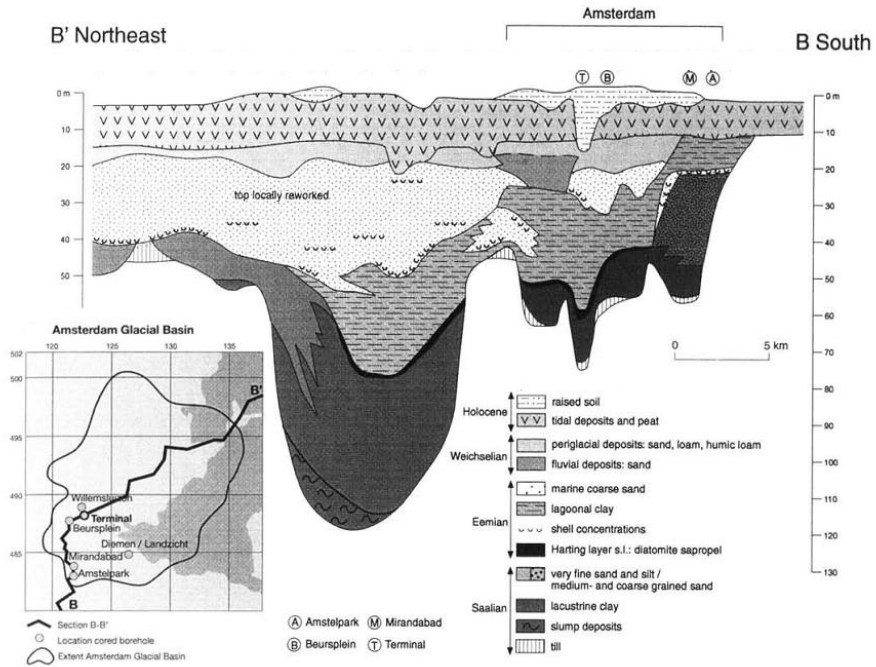
Figure 4.3: Cross-section of the Amsterdam glacial basin [De Gans and Wassing, 2000]. The axis on the left and the right are equal and indicate the depth of the layers in meters relative to NAP. The small figure on the bottom-left shows a map of the Amsterdam glacial basin with an indication of the location of the depicted cross-section. Dark areas on the map indicate water, the lighter areas are land (in the current situation).

4.1.1 Amsterdam area during the Pleistocene

The Saalian

The Saalian refers to the glacial period which started 238.000 years ago and ended 128.000 years ago. During its maximum extension, an ice cap reached into the central Netherlands, where piping and pushing by ice-tongues of glaciers excavated over 100 m deep basins including the Amsterdam basin. This basin is about $25\,km$ long and $15\,km$ wide, its maximum depth is $-125\,m$NAP. The city of Amsterdam is situated at on the top of the southern part of the basin. Based on the deduced lake level in the Amsterdam glacial basin, De Gans and Wassing [2000] suggest that a lake covered central Noord-Holland and the IJsselmeer during the late Saalian. During this period the basin was partly filled with lacusto-glacial clays. Along the southern margin of the basin, the lancustrine clay interferes with, and is overlain by, sands derived from the fringing ice-pushed ridges.

The Eemian

The interglacial following the Saalian is referred to as the Eemian. During the Eemian temperature levels raised and the Saalian land ice melted, resulting in a sea-level just above current levels. At the start of the Eemian, the basins formed during the Saalian reached over $-100m$NAP and, although they were partly filled with sediment during the late Saalian, they still formed considerable deeps when they were flooded in the Eemian [De Gans and Wassing, 2000].

The lowermost Eemian in the deep glacial basins (such as the Amsterdam basin) is formed by a black layer of sapropel and diatomaceous earth, informally called 'Harting layer'. This layer clearly marks the boundary between Eemian end Saalian deposits. On top of the Harting layer, a layer of clays and very silty clays that varies in thickness from a few to 30 meters is deposited. As appears from the fauna, most of the clays were deposited in a lagoonal setting shielded behind a threshold and/or barrier. The rate of sediment supply was low; lagoonal conditions were maintained over a long time span. The base of the overlying lagoonal Eemian clays is in the Amsterdam basin at about $-80\,m$NAP [Zagwijn, 1991].

De Gans and Wassing [2000] hypothesize that the due to subsidence, caused by the compaction of the clay, the barrier was recessed and the exchange with the open North Sea increased. Consequently the clays are overlain by a wedge of sands which are thought to derive from the ice-pushed ridges and brought into the basin by wave- and tide-induced transport. This wedge varies in thickness from almost 40 m in the Northern part of the basin to only a few meters in the core. The sands are absent in the southern part of the basin. The Eemian sands are usually rich in shells and shell fragments and can therefore be distinguished from the fine-graded Weichselian deposits. It is clear that, due to the deposition of sand, substantial compaction has occurred in both Saalian and Eemian clays of the Amsterdam basin.

The Weichselian

In Scandinavia and Northern Europe, the last glacial period occurring during the Pleistocene is in referred to as Weichselian stage. In contrast to the ice age before the Weichselian, the Saalien stage, the area of the Netherlands not covered with ice; the soil however was permanently frozen. Premafrost conditions were maintained even during summer time, prohibiting the infiltration of melt water. Instead a large river plain was formed smoothing the accidental morphology by fluvial action. The fluvial sand bed (first sand layer) is overlain by a complex unit composed of fine sands, loam, humic loam and peat layers. The maximum thickness of this unit is about 4 meters. The top of this formation consists of eolian deposits, they are referred to as 'cover sands' (second sand layer). For the Amsterdam Basin, fluvial and eolian sediments of the Weichselian age, locally reaching a thickness of almost 10 m, eventually levelled the basin.

4.1.2 Amsterdam area during Holocene

At the end of the Weichselian the level of the North Sea was low and a large part of the current North Sea was dry. During the Holocene the North Sea plain gradually filled with melt water, sea-level started to rise at a speed of about 0.5 meter every century.

The Holocene successions differs in a number of important respects from that of the Eemian, although both represent the transgression and highstand of an interglacial. In the first place, peats layers are formed during the Holocene and secondly the area was filled by sediment during the highstand. Due to the sedimentation the tidal basin could keep up with sea level rise several thousands of years before reaching highstand. The slightly westward tipping Weichselian river plain, smoothed during the Late Glacial, formed an ideal basement for the development of a barrier/back-barrier system (de Gans, 2000). As a result a freshwater zone was formed and peat layers were formed. Currently this peat layer has a thickness of 0.1 up to 0.3 m and is referred to as 'basal veen'.

Due to rising ground water levels and ground subsidence, the western part of the Netherlands was drowned and periods of transgression and regression followed. When the influence of rivers in the coastal zone increased, fresh water was provided resulting in the formation of peat layers. The so-called 'holland veen' varies in thickness from 1 up to 5 meters.

4.1.3 Human interference with geological processes

Human activities in the western part of the Netherlands started around the year 1000. Unsurprisingly activities coincide with a period of transgression. Amsterdam was founded over 750 years ago at the location where the small river Amstel discharged into an inland sea (later the river IJ). At this location a dam with a culvert was constructed to mitigate the inflow of seawater, and hence flooding,

during storm events. Due to the favourable location and the political situation Amsterdam flourished in the 14th century.

As described in the previous chapter, the top layer of the Amsterdam basin consisted of peat. Therefore, in order to live and build in these swampy areas, ground conditions needed to be improved. The origin of the soil used for elevation as well as the method to elevate changed over time depending on the availability of ground and technological possibilities to extract and transport the material.

Figure 4.4 shows a map of the centre of Amsterdam. To allow for city growth, two neighbourhoods were developed around 1615. On the map it can be seen the channels in the town centre follow a circular pattern with the dam square as the centre. Most small channels connecting the larger ones are laid-out perpendicular to the channels, like the spokes of a wheel. A clear exception is the Jordaan neighbourhood. As the Jordaan neighbourhood was meant to residence the less-fortuned, little money was spent on the development of the area. Where for the other, more upscale, neighbourhood the material that came free with the digging of the channels was used to elevate the ground level, ground conditions in the Jordaan area were hardly improved. The difference in ground level is still apparent today. As can be seen on the photographs of figure 4.4, the difference between the water level and the ground level is much smaller for the Jordaan area (same water level in both areas).

Differences in ground improvement are not only caused by the availability of money, also technological innovations played an important role. Whereas in the 18th century the soil from the channels was used to raise the ground level, at the end of the 19th century small trains were used to import sand from the

Figure 4.4: The Amsterdam city centre. On the map the neighbourhoods developed around 1615 are indicated.

dunes. Other areas such as the Waddendijk area (1930) were raised with dredged sediments (paragraph 4.2.1). But, due to the problems experienced with the use of dredged sediments (e.g. non-uniform composition), in 1930 it was decided to strictly use sand for ground improvement. For this artificial lakes, like the Sloterplas, were dug. As sand layers are quite deep, these lakes have depths up to 30 meters. Soil that could not be used for ground elevation was used to create parks.

One can imagine that the method as well as the material used for the ground elevation will have an influence on the current settlement rate.

This paragraph was mainly based on personal communication with Kees Hogenes and literature from Speet [2010] and Hogenes [1997].

4.2 Analysis of the settlement rate

Despite knowledge about the geology of the Amsterdam area and the awareness of it's settlement prone content, currently settlement rates are not monitored. Therefore, to be able to study the influence of settlement on the functioning of sewer systems, the first step is to analyse settlement rates. Fortunately, for the Amsterdam area time series of measurements of the sewer invert level can be used to estimate settlement rates.

In Amsterdam measuring the sewer invert level is general practice since the 1970s. At first the data was stored on maps, later computer programmes are used to store and visualize the data. Even though the historical maps contain valuable information, manual recovery of the data is very time consuming limiting the potential of that data source. Computer files of the Amsterdam sewer system also have a difficulty: because sewer invert measurements are currently only used to determine the present position, old values are overwritten when a new measurement becomes available.

Fortunately the contractor who took the measurements was able to provide copies of old measurement data files from 1995 to 2009. By scrutinizing these data files and using back-up copies of the general information files to provide information on for example location, date of construction and material, it was possible to recover on average 2 measurements for each sewer invert in the Amsterdam area.

In this paragraph this data will be used to assess the (differences in) settlement rate of the Amsterdam area. At first the settlement rates of the sewer invert levels in a small area (Waddendijk) are analysed. Since this area was also used for the analysis of the measurement error, measurement data of the historical maps are also available. Secondly a settlement map for the city of Amsterdam is developed based on digital available information only.

4.2.1 Analysis of settlement in the Waddendijk case study area

The Waddendijk area is a neighbourhood ($700m$ by $500m$) in the northern part of Amsterdam. The neighbourhood is situated in a former agricultural area. Before the area was prepared for construction in 1930, the area was surveyed by drilling of cored boreholes on 12 locations evenly distributed over the area. At most locations down to 5 meter depth was drilled; on two locations much deeper depth was attained, up to 14 meters. The sedimentary record of these two drillings are shown in figure 4.5.

As can be seen in figure 4.5 at first a layer of sand is found. This layer is most likely the result of earlier efforts to improve the subsoil and therefore does not have a geological origin. This sandy top layer is found at most locations (8 of the 12) and is on average 1.5 meters tick. From the sand layer up to a depth of 12 meters Holocene tidal deposits (clay, sand and silt) and organic material (peat) are found. The upper layer of the Holocene deposits comprise of a peat layer ('Holland veen'). In the case study area this layer has a thickness of $2 - 2.5\,m$. The peat layer is followed by layers of sandy clay and clayey sand. These layers belong to the Calais formation and where formed when the influence of the sea prevailed. At a depth of 12 to 13 m a small layer of sand can be found. This layer was formed during the Weichselian periglacial and is commonly referred to
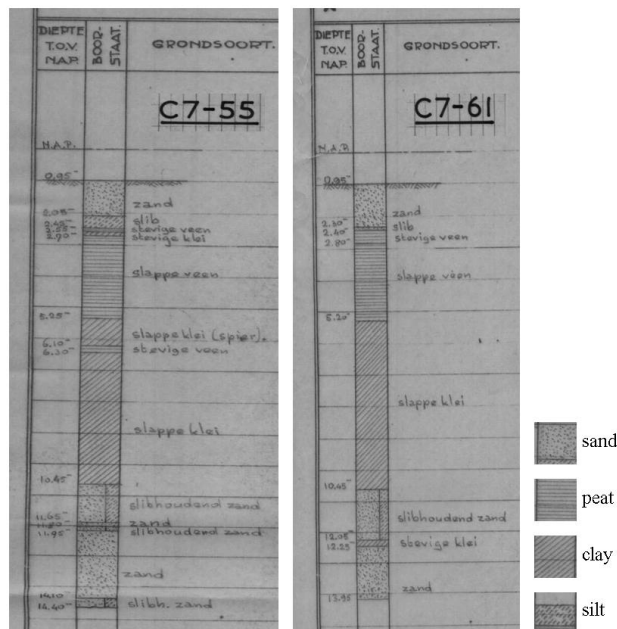
Figure 4.5: Sedimentary log, cored borehole, October 1929.

as the first sand layer. For most old buildings in Amsterdam this is the layer into which the timber piles are driven. The results of cone penetration tests (CPT) which were performed at a later stage (from 1963, 59 in total, figure 4.6 gives an example) show that this layer varies in thickness from 0 to 4 meters. From about $18\,m$ lies the second sand layer, which is well compacted and hence suitable for more heavily loaded concrete piles.

Based on the results of the survey of 1929 (figure 4.5) it was decided to improve ground conditions prior to construction activities. For this dredged sediments from the river IJ were used to elevate the ground level. Figure 4.7 shows the results of the drilling of a cored borehole and CPT at 6 neighbouring locations at 3 moments in time. It can be seen that after application of sediments the sand layer was thickened from $1.5\,m$ (based on the results of 12 cored borehole tests in 1929) to 3 - 4 m (based on the results of 11 cored borehole tests in 1949). However, although indicated as sand on the sedimentary log, the results of the CPT indicate that the resistance in these layers varies significantly (figure 4.6 and 4.7) indicating the presence of clay and silt. Because of the blue color of the dredged sediments the neighbourhood was soon nicknamed 'blauwe zand' or blue sand, a name which is still in use.
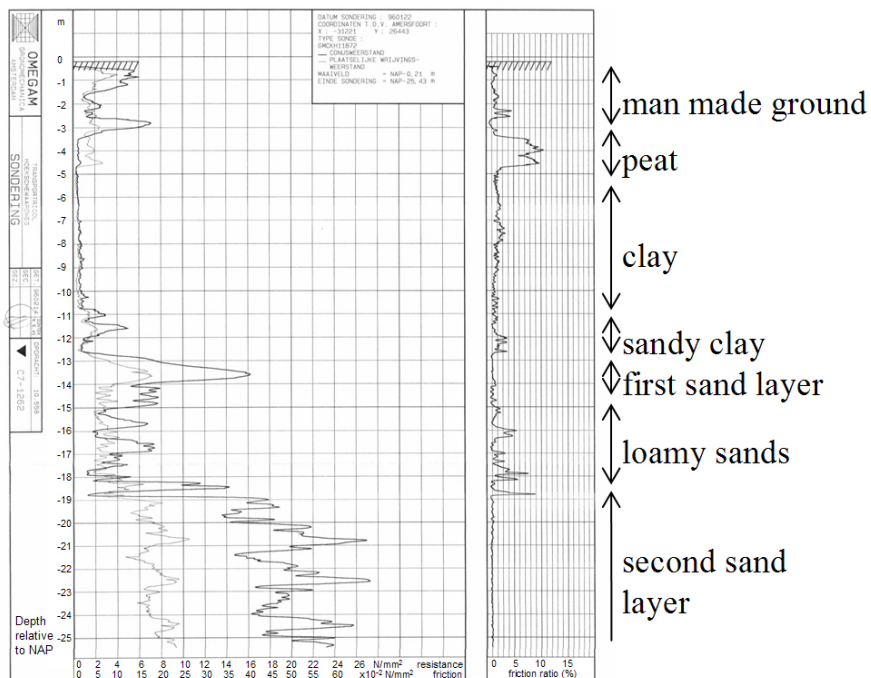
Figure 4.6: CPT result. Left hand graph: resistance (thick line) and friction (thin line), right hand graph: friction ratio. May 1996.

Soon after the deposition of the sediments in 1929, the construction of the houses started on 8 September 1930 followed by the arrival of the first inhabitants in 1931. Due to the short period (only 2 years) between ground application and construction, it is very likely that the primary consolidation process (the transfer of load from the excess porewater pressure to the soil particles by expulsion of water) was not finished at the moment of construction. Since this primary consolidation involves a considerable decrease in soil volume, it is very likely that soon after construction the ground settlement was significant. Photographs of subsided sheds taken in 1935 (only 4 years after construction was finished) confirm this suspicion (figure 4.8).
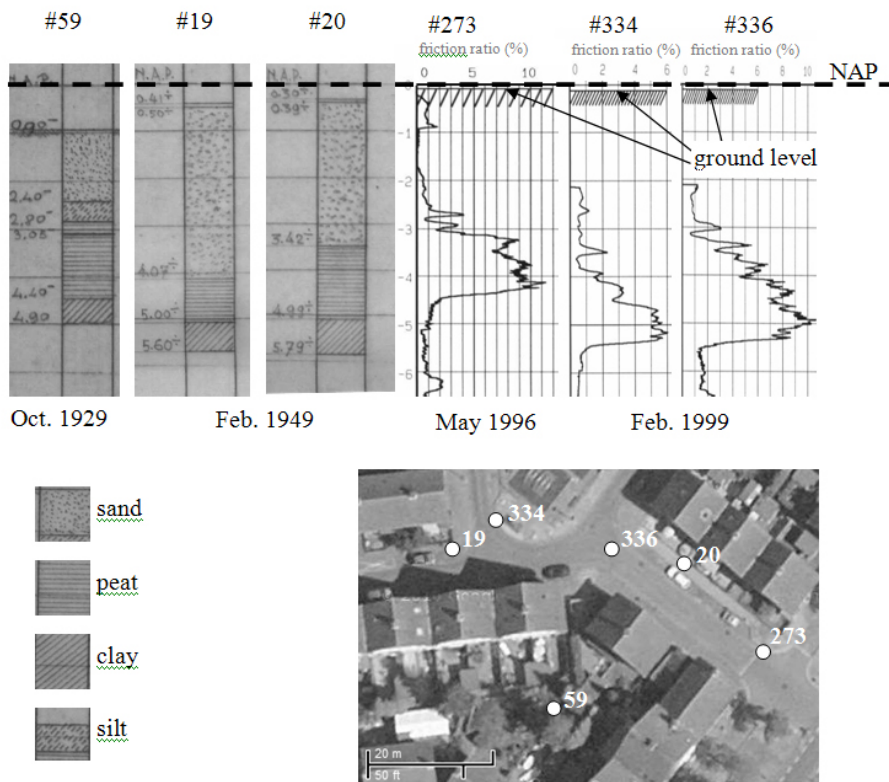
Figure 4.7: Top, from left to right: a graph indicating the soil composition before ground elevation, 2 graphs indicating the soil composition after elevation with dredged sediments and one graphs indicating the results of a cone penetration test in 1996 and two in 1999. The numbers above the graph refer to the drilling location shown on the map at the bottom of the figure.

Materials and methods

To analyse the current settlement rate of this area, historical maps and computer files are scrutinized resulting in 6 measurements for most sewer invert levels in the area:

- May 1983

- February 1990

- March 1993

- May 2000

- September 2004

- November 2011

Since the considerable time span between the first available measurement and the development of the area it is very likely that the primary consolidation process has finished and a linear model can be used [e.g. Budhu, 2007]. This assumption was verified in paragraph 3.1.2 where the adequacy of the linear model was tested using the F-test. Since only 19 of in total 288 time series failed the goodness-of-fit test ($\alpha = 0.95$) it is concluded that after primary consolidation, a linear model adequately describes the settlement process.

Figure 4.8: Left: difference in ground settlement between a structure with (brick house) and without (wooden shed) a piled foundation. The wooden bar indicates the level of the base of the shed after construction. Right: people jacking up a shed. Photographs taken in 1935.

Results

In paragraph 3.1.3 the calculation of the settlement rate and the resulting confidence interval was explained. For the time series of the 6 measurements in the Waddendijk area this resulted in an error of $\pm 1.4\,mm\,year^{-1}$ at the 95% confidence limit.

Figure 4.9 shows the settlement rate of the sewer invert levels in Waddendijk. The average settlement rate is $4.5\,mm\,year^{-1}$ but, as can be seen in the figure, the settlement rates in the eastern section of area are slightly higher $(4-5mm\,year^{-1})$ compared to the western section $(3-4\,mm\,year^{-1})$. Therefore, it is concluded that even within a neighbourhood, settlement rates might vary. When calculating neighbourhood average settlement rates, this natural variation should be taken into account as will be explained in the next paragraph.

An explanation for the variation of settlement rate within a neighbourhood might be found by studying the results of the CPT's and sedimentary logs taken in the Waddendijk area. As shown in the beginning of section 4.2.1, the thickness of the different layers in the subsoil can vary even within several meters.

4.2.2 Settlement map of the Amsterdam area

To calculate settlement rates for the whole Amsterdam area only digital available information is used. As a result, on average 2 measurements for each sewer invert level are available. The calculation of the settlement rate based on more than two measurements is described in paragraph 3.1.3; when only two measurements are
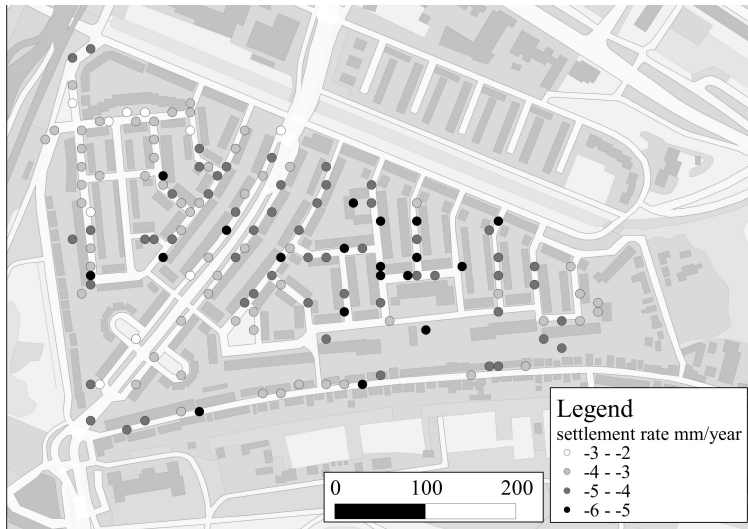
Figure 4.9: Estimated settlement rates in $mm\,year^{-1}$ (distance in meters).

available the settlement rate can be calculated by:

$$\hat{b} = \frac{z_2 - z_1}{t_2 - t_1} \tag{4.1}$$

with z_1 and z_2 the measured sewer invert levels at t_1 and t_2. The the corresponding 95% confidence interval due to the error in the measurement of the sewer invert level can be estimated by:

$$\hat{b} - 1.96 s_b \leq b \leq \hat{b} + 1.96 s_b \tag{4.2}$$

$$\hat{b} - 1.96 \frac{\sqrt{2s_z^2}}{t_2 - t_1} \leq b \leq \hat{b} + 1.96 \frac{\sqrt{2s_z^2}}{t_2 - t_1} \tag{4.3}$$

With an average time interval of 5 years between measurements and an error $s_z = 0.016\,m$ this results in an error at the 95% confidence limit of $9.1\,mm\,year^{-1}$. Due to this large error, calculated settlement rates of individual sewer inverts are quite meaningless.

Nevertheless, it might be possible to calculate reliable area average settlement rates. In order to do so, these areas should be large enough to contain sufficient estimates, but small enough not to have too much natural variation in settlement rate. Because it is a reasonable assumption that areas that are developed around the same time using similar methods have the same average settlement rate, settlement rates are averaged over neighbourhoods. The municipality of Amsterdam consists of 470 neighbourhoods with an average area of $5 * 10^5\,m^2$ or $0.5\,km^2$.

Materials

Figure 4.10 shows a map of the municipality of Amsterdam. Each dot represent a manhole of which the darkness indicates the number of recovered measurements. In the figure rectangular areas can be recognized. The boundaries of these areas coincide with the boundaries of (historical) maps. These maps are also used when planning and contracting the measurement of sewer invert levels.

To show how the area average settlement rates are calculated, the neighbourhood of Emanuel van Meteren is as an example. Because this neighbourhood covers 2 maps (KK1 and KK2), not all manholes are measured at the same time: the western manholes are measured on 1-12-1996 and 30-11-2002 and the eastern manholes on 11-12-1996 and 19-5-2003. Figure 4.11 shows the the estimated settlement rate for each sewer invert in Emanual van Meteren neighbourhood. In the figure also the boundary of the maps is indicated.

Figure 4.12 shows the histograms of the settlement rate estimations for the manholes in the western and eastern part of the neighbourhood. As can be seen for eastern part an unexpected high number of sewer invert levels has a settlement rate estimation of $0\,mm\,year^{-1}$. As this phenomena was also observed for most other (sub-) neighbourhoods it is very likely that a large part of the measurement files also contain old measurements. To reduce the number of incorrect settlement

rate estimations, the number of $0\,mm\,year^{-1}$ settlement rate estimations is adjusted so that it does not exceed the number of settlement rate estimations one category higher or lower than $0\,mm\,year^{-1}$.

To correct for unrealistic extreme observations, outliers are removed until all data lie within three standard deviations $(\mu\pm3\sigma)$ of the remaining data. On average this resulted in the removal of 1.5% of the available settlement rate estimates within one (sub-) neighbourhood. The histograms of the resulting datasets for the Emanuel van Meteren neighbourhood are also shown in figure 4.12.

Since all further calculations are only possible when the data is normally distributed, the assumption that the data is normally distributed is verified. For all remaining (sub-) neighbourhoods a dataset is created containing the estimations of the settlement rate:

$$\mathrm{M} = \begin{bmatrix} b_1 \\ \vdots \\ b_m \end{bmatrix} \tag{4.4}$$

with m, the number of settlement rate estimations within a (sub-) neighbourhood.
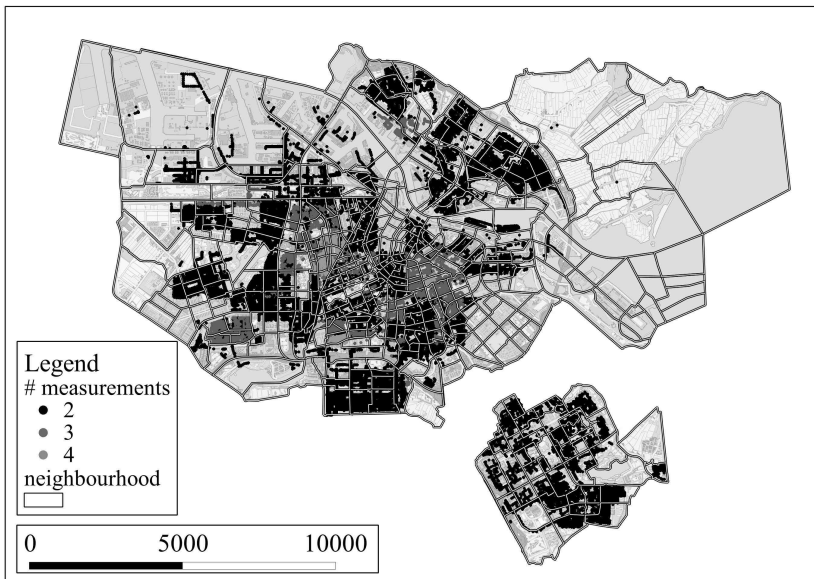
Figure 4.10: Number of available measurements for each manhole (distance in meters).
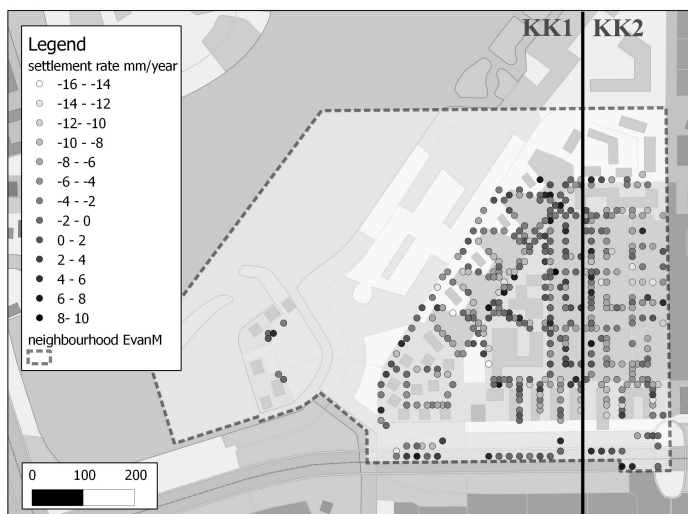
Figure 4.11: Neighbourhood Emanuel van Meteren (distance in meters).
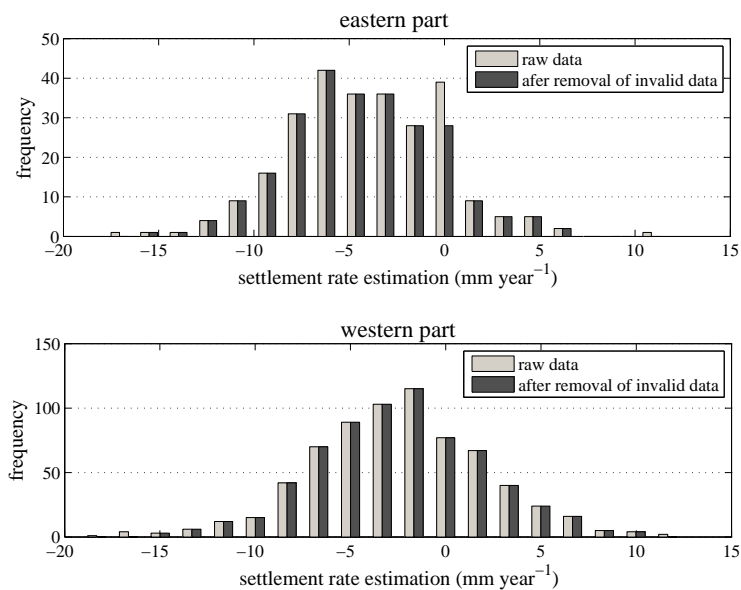
Figure 4.12: Distribution of settlement rate estimations for the eastern and western part of neighbourhood Emanuel van Meteren.

The Chi-square goodness-of-fit test was used to test the null hypothesis that the data in vector M are a random sample from a normal distribution with mean and variance estimated from M, against the alternative that the data are not normally distributed. When only 2 measurements are available for each sewer invert, like in the Emanual van Meteren neighbourhood, the dataset M is discrete. For these discrete datasets the unique values in the dataset are used as bin centres. For datasets with more than 20 unique values, the standard number of bins, 10 is used. For a significance level $\alpha = 0.05$ it was not possible to reject the null hypothesis for most datasets (452 of 529), including the datasets of both Emanuel van Meteren sub-neighbourhoods.

Methods

For the remaining 452 (sub-) neighbourhoods the area average settlement rate is calculated:

$$\hat{\mu}_b = \mathrm{E}\left(\mathrm{M}\right) = \frac{1}{\mathrm{m}} \sum_{\mathrm{i}=1}^{\mathrm{m}} \mathrm{b_i} \qquad (4.5)$$

To verify if the estimation of the area average settlement rate was reliable, the 95% confidence interval for the estimated average area settlement rate is calculated:

$$\hat{\mu}_b - 1.96 s_{\mu_b} \leq \mu_b \leq \hat{\mu}_b + 1.96 s_{\mu_b} \qquad (4.6)$$

$$\hat{\mu}_b - 1.96 \frac{s_{total}}{\sqrt{m}} \leq \mu_b \leq \hat{\mu}_b + 1.96 \frac{s_{total}}{\sqrt{m}} \qquad (4.7)$$

$$(4.8)$$

s_{total} is calculated by:

$$s_{total}^2 = \mathrm{Var}\left(\mathrm{M}\right) = \frac{1}{\mathrm{m}} \sum_{\mathrm{i}=1}^{\mathrm{m}} (\mathrm{b_i} - \bar{\mathrm{b}})^2 \qquad (4.9)$$

with m the number of available settlement rate estimations. When the confidence interval is very large compared to the average settlement rate, the calculated average does not give any information. Therefore the (sub-) neighbourhoods where the 95% confidence interval exceeds $1\,mm\,year^{-1}$ are excluded. Due to this constraint another 163 neighbourhoods were left out. The excluded neighbourhoods were in general neighbourhoods with a limited number of settlement rate estimations ($m \approx 50$).

In table 4.1 the estimations of the area average settlement rate for the eastern and western part of the Emanuel van Meteren neighbourhood are listed. From the results it can be seen that, although the separation into sub-neighbourhoods was not based on physical properties, both sub-neighbourhoods do have a significant difference in area average settlement rate. This suggests that the division of the Amsterdam area based on neighbourhoods probably does not give the most optimal results.

As observed when studying the settlement rates of the Waddendijk neighbourhood (paragraph 4.2.1), settlement rates can vary within a neighbourhood. This spatial variance can be estimated by calculating the difference between the variance of the settlement rates estimations (total variance, s_{total}^2) and the expected variance due to the measurement error (measurement variance, s_m^2). Since the measurement variance depends on the moment of measurement, settlement rate estimations of sewer inverts that have different moment of measurement can not be combined into one dataset. This is the main reason for not combining the sub-neighbourhoods like the eastern and western part of the Emanuel van Meteren neighbourhood into one dataset.

To estimate the spatial variation in settlement rate also the variance due to the measurement error needs to be estimated. When two measurements are available, the variance due to the measurement error is equal to:

$$s_m^2 = s_b^2 = \left(\frac{\sqrt{2s_z^2}}{t_2 - t_1} \right)^2 \quad \text{(see also equation 4.3)} \tag{4.10}$$

if there are three or more measurements, s_b^2 can be calculated by:

$$s_m^2 = s_b^2 = \frac{s_z^2}{\sum\limits_{i=1}^{n} (t_i - \bar{t})^2} \quad \text{(equation 3.12 paragraph 3.1.3)} \tag{4.11}$$

with t_i the moment in time when the sewer invert level was measured and n, the total number of measurements for one sewer invert. From these these formulas it is clear that the variation due to the measurement error depends heavily on the maximum time interval between measurements $(t_n - t_1)$.

The total variance is estimated from the dataset with settlement rate estimations (M) by equation 4.9. Like the estimation of the area average settlement rate, also for the estimation of the total variance a 95% confidence interval can be calculated [Rice, 2007]:

$$\frac{(m-1)s_{total}^2}{\chi(1 - \frac{\alpha}{2}, m-1)^2} \leq \sigma_{total}^2 \leq \frac{(m-1)s_{total}^2}{\chi(\frac{\alpha}{2}, m-1)^2} \tag{4.12}$$

Table 4.1: Analysis of the settlement rate in the Emanuel van Meteren neighbourhood.

	area average settlement rate $mm\,year^{-1}$	$\pm$ 95% confidence interval $mm\,year^{-1}$
KK1	-2.4	± 0.3
KK2	-4.3	± 0.5

For both the Emanuel van Meteren sub-neighbourhoods the calculated properties are listed in table 4.2. As expected the spatial variation for the western and largest sub-neighbourhood is the highest. It should be emphasised that the spatial variance relates to the settlement rate of individual sewer inverts.

Table 4.2: Analysis of the spatial variance in the Emanuel van Meteren neighbourhood.

	total variance with 95% CI $(mm\,year^{-2})$ s^2_{total}	variance due to measurement error $(mm^2\,year^{-2})$ $s^2_m = s^2_b$	spatial variance with 95% CI $(mm\,year^{-2})$ $s^2_{spatial} = s^2_{total} - s^2_m$
KK1	$17.4 < 19.3 < 21.5$	14.2	$3.2 < 5.1 < 7.3$
KK2	$12.7 < 15.0 < 18.0$	12.3	$0.3 < 2.7 < 5.7$

Figure 4.13: Settlement rate for the (sub-) neighbourhoods of Amsterdam (distance in meters).

Results

Figure 4.13 shows the resulting settlement map for the city of Amsterdam. For some neighbourhoods it was possible to estimate the area average settlement rate. The manholes in these areas are indicated by a dot of which the intensity gives an indication of the area average settlement rate.

In appendix B a list of all the (sub-) neighbourhoods and their average area settlement rates is included. For some (sub-) neighbourhoods the total variation was less than the estimated variation due to the measurement uncertainty. For these (sub-) neighbourhoods the spatial variation is indicated as < 0. Since this situation is physically not possible, causes should be found in (additional) inaccuracies in the data.

Comparing the estimated spatial variance of the (sub-) neighbourhoods listed in appendix 7.4 it stands out that while for some neighbourhoods the estimated spacial variance is very low (< 0) for others it is quite large (up to $30\,mm\,year^{-2}$. As the distribution of settlement rates of all (sub-) neighbourhoods listed in appendix 7.4 is normal, it not likely that splitting these neighbourhoods in different areas would result in a smaller spacial variance. Further research should indicate if the settlement rate in these neighbourhoods is really very heterogeneous.

4.3 Conclusion and recommendations

Ground settlement in the city of Amsterdam ranges from $0-10\,mm\,year^{-1}$. There are two reasons why it is not expected that settlement rates will decrease in the near future. First Amsterdam is built on top of $60\,m$ of compressible soil and second the municipality is keen on keeping up with the settlement by applying extra layers of sand. The constant settlement rate was confirmed by analysis of the settlement rates of one area in Amsterdam. For this area it was found that the linear model (time invariant settlement rate) fits the 30 year dataset for the vast majority of measurement locations.

In comparison to other settlement prone delta cities like Jakarta, $84\,mm\,year^{-1}$ [Djaja et al., 2004], Bangkok, $15\,mm\,year^{-1}$ [Aobpaet et al., 2009] and Changzhou City, maximum $147\,mm\,year^{-1}$ [Wang et al., 2008], a settlement rate of $0-10\,mm\,year^{-1}$ might seem irrelevant but taking into account that sewers are expected to function over 60 years, even a settlement rate of only $5\,mm\,year^{-1}$ will result in a total of $300\,mm$ over the live span of a sewer. Considering that sewers are in generally operated under gravity in low gradient settlement prone coastal areas and that sewers with a shallow foundation are in general connected to, or cross, structures with a pile foundation, even a settlement rate of a few millimetres each year can have serious consequences.

Settlement rates for the Amsterdam area were defined based on, on average, two measurements of the sewer invert level with a time interval of 5 years. Despite the lack of accuracy of a settlement rate estimation for an individual sewer invert, it is shown that a high density of these inaccurate estimates can be used to

calculate area average settlement rates. In this thesis, the area over which the settlement rates are averaged were neighbourhoods. It is very likely that by defining areas based on physical properties (spacial variability of the layering of the ground) instead, the spatial variance can be reduced, thus improving the results.

The main reason why the settlement rate estimations of individual locations had such a large confidence interval is not the fact that only two measurements were available but the short time lag between the first and the last measurement. Using the equations 3.13 (>2 measurements) and 4.3 (2 measurements) the confidence interval of the settlement rate estimation of an individual sewer invert level for an intended monitoring campaign can be calculated. Table 4.3 gives the confidence intervals for a scenarios with different measurement intervals and $s_z = 0.016\,m$.

As can be seen in table 4.3, at least 30 years of measurements are needed for accurate estimations of settlement rates for individual locations. Because of this considerable time span, it is advised not only to put a lot of effort in gathering measurement data but also in the analysis in the layering of the subsoil to find areas where it can be expected that settlement rates do not vary significantly. For the Amsterdam situation, the recovery of the data of the historical maps is advised.

Table 4.3: The resulting 95% confidence intervals of the estimation of the settlement rate of an sewer invert when measuring the sewer invert level (with $s_z = 0.016\,m$) at different time intervals.

measurement at moment t in years					resulting 95% confidence interval $(mm\,year^{-1})$
0	5	10	20	30	
x	x				9.0
x	x	x			4.4
x		x			4.5
x				x	1.5
x		x	x	x	1.4

84

Bibliography

Aobpaet, A., Cuenca, M., Hooper, A., Trisirisatayawong, I., 2009. Land subsidence evaluation using inSAR time series analysis in Bangkok metropolitan area. In: Fringe 2009 Workshop. Frascati, Italy.

Budhu, M., 2007. Soil mechanics and foundations. John Wiley & Sons.

De Gans, W., Wassing, B., 01 2000. Geology and related geotechnical aspects of the underground of Amsterdam. Zeitschrift der Deutschen Geologischen Gesellschaft 151 (1-2), 9–20.

Djaja, R., Rais, J., Abidin, H., Wedyanto, K., 2004. Land subsidence of Jakarta metropolitan area. In: 3rd FIG Regional Conference. Jakarta, Indonesia.

Hoeksema, R., 2007. Three stages in the history of land reclamation in the Netherlands. Irrigation and Drainage 56 (Issue Supplement 1), S113–S126.

Hogenes, C., 1997. Costelijk Stadswater. Stadsdrukkerij/Dienst Riolering en Waterhuishouding Amsterdam.

Rice, J., 2007. Mathematical statistics and data analysis. Brooks/Cole.

Speet, B., 2010. Historische Atlas van Amsterdam. SUN-Historische atlassen.

Wang, G., You, G., Shi, B., Yuc, J., Tuck, M., 2008. Long-term land subsidence and strata compression in Changzhou, China. Engineering Geology 104 (1999), 109–118.

Zagwijn, W. H., 1991. Geologie van Nederland, deel 1 Nederland in het Holoceen. SDU Uitgeverij.

Chapter 5

Differential settlement of sewer pipes

When settlement occurs it is very likely that due to inhomogeneities sewer pipes move relative to each other (figure 5.1 C). As these movements can cause for example open joints, disconnected pipes, in- and ex-filtration and fractures, differential settlement is frequently mentioned as a cause for sewer deterioration [for example DeSilva et al., 2005, Bishop et al., 1998, Davies et al., 2001, Read and Vickridge, 1997].

Reviewing literature on differential settlement of (sewer) pipes, several theoretical models can be found [Iimura, 2004, Moghaddas Tafreshi and Tavakoli Mehrjardi, 2008, Frantziskonis and Breysse, 2003]. These ambitious models, however, require a large set of input parameters which hampers the validation and therefore application. Especially the evaluation of the parameter describing the variability associated with the properties of soils, the scale of fluctuation, proves to be
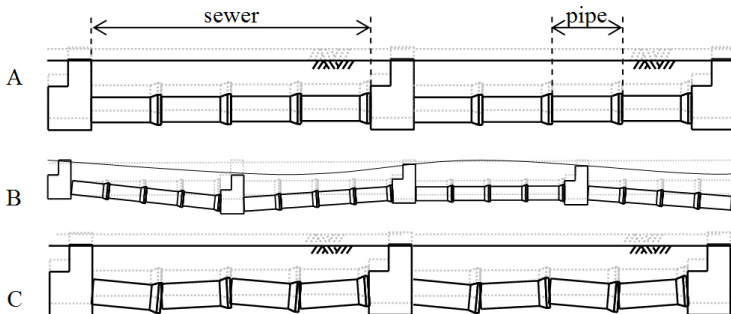
Figure 5.1: Differential settlement: A) no settlement difference, B) network level: settlement differences between manholes, C) pipe level: differential settlement of pipes.

challenging [Jaksa et al., 1999]. Finally, Buco et al. [2008] reported on another input parameter; the stiffness of the joints. Using an experimental apparatus, joint behaviour under various loading conditions was tested.

To the author's knowledge no articles have been published on the influence of settlement on the position of (sewer) pipes using empirical data. It is therefore unclear if, how and under what conditions differential settlement of sewer pipes has an impact on the functioning of a sewer system. To get a first insight into these relations, the slopes of the sewer invert of more than 100 sewers made of different materials were analysed. Based on this initial assessment, the settlement process of the sewer type most sensitive to settlement, namely sewers with a shallow foundation connected to a manhole with a pile foundation, were studied in more detail.

For the measurement of the slope, the electronic tilt meter integrated in the IBAK KRA85 camera tractor is used. This measurement technique and the uncertainty of the resulting sewer invert profiles were previously discussed in chapter 3: Monitoring Settlement, paragraph 3.2. To interpret and understand the results, the chapter starts with a paragraph on the design and layout of sewer systems in Amsterdam.

5.1 Sewer system design in Amsterdam

Figure 5.2 shows the layout of the sewer system in the Waddendijk case study area. In Amsterdam there are many of these small catchment. Each catchment comprises of a pumping station and a gravity sewer system. Once collected at the pumping station, the waste water is transported under pressure to the waste water treatment plant. The reason to divide the system into many small catchments is that Amsterdam is a flat area.

With the exception of older sewer systems like the Waddendijk system, sewer systems in Amsterdam are mainly separated. Nevertheless, the layout of both systems concerning the collection and transport of foul water does not differ substantially.

A special characteristic of the Amsterdam sewer system are sewers with a pile foundation. Pile foundations are used for all sewers from $-1.8m$ below ground level. The reason is that the peaty subsoil below the artificially applied sand layer (average thickness $2\,m$) can not provide enough support for a shallow foundation. As the waste water is transported by gravity, the sewers closest to the pumping station are the deepest and hence pile founded. In general, pile founded sewers only have a transport function; houses are connected to sewers with a shallow foundation.

When applying structures with and without a pile foundation in a settlement prone area, problems are likely to develop when connecting both types of structures. To mitigate the impact of the settlement differences, sewers connecting a manhole with a pile foundation to a manhole with shallow foundation (or hinge sewer) are specially designed in Amsterdam. Figure 5.3 shows the cross-section

of this design. The idea is that the pipe closest to the manhole with a pile foundation would act as a hinge, therefore this sewer is referred to as hinge sewer. To allow for proper discharge over time the initial slope of this pipe is higher (1% compared to 0.2%).
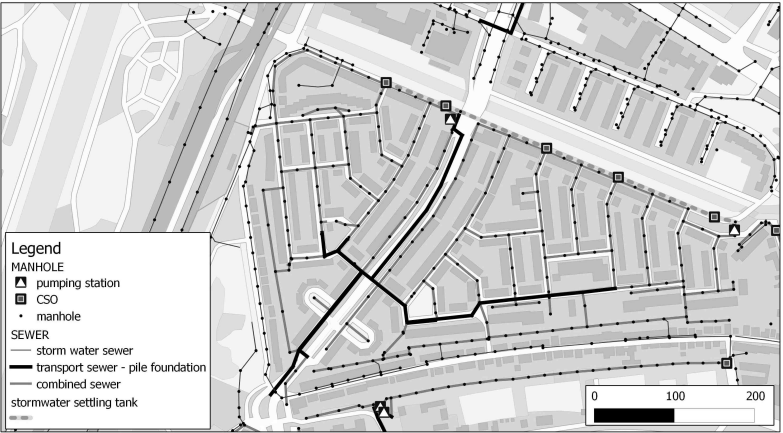
Figure 5.2: Typical layout of a combined sewer system in Amsterdam (distance in meters).
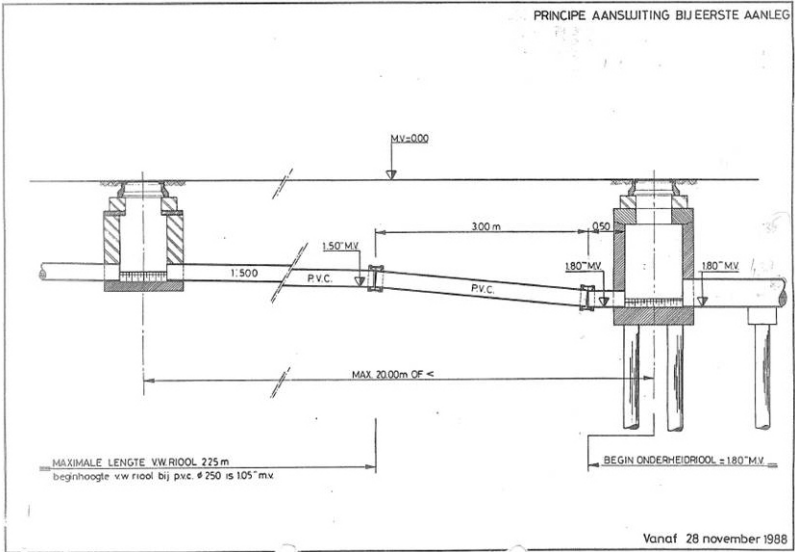
Figure 5.3: Design of the hinge sewer, a sewer with a shallow foundation connected to a manhole with a deep foundation.

5.2 Results of initial assessment

In figure 5.4 the sewers that were analysed from July until September 2010 are highlighted. For this initial assessment, a diverse set of sewers was selected. In table 5.1 some characteristics of the analysed sewers are listed. With the exception of the number of studied hinge sewers (sewers with a shallow foundation connected to a manhole with a deep foundation), the subset of analysed sewers is a representative sample of the sewers in the Waddendijk case study area. Although the sewers in the Waddendijk area are also made of PVC, the manholes are made of either masonry or concrete.
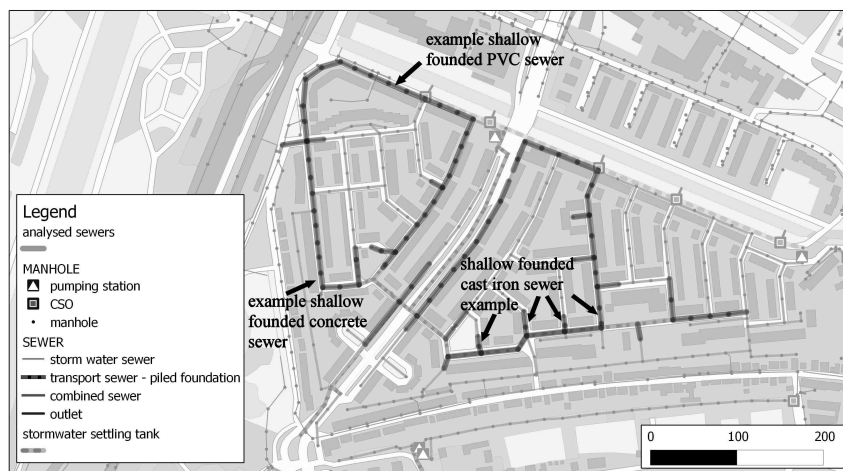
Figure 5.4: Analysed sewers (distance in meters).

Table 5.1: Some characteristics of the analysed sewers (composed: sewer made of pipes with different lengths).

type of foundation	material	year of construction	length of pipes	number
shallow	concrete	1952-2003	1/1.5/2/2.5	60
	PVC	1979/2000	5	9
	cast iron	1979	composed	3
pile	cast iron	2000/1997	6	6
hinge sewer	concrete	1997-2000	1/2.5	5
	PVC	1977-1999	5/composed	6
	cast iron	1974/1980	6/composed	3

5.2.1 Shallow foundation

Concrete

Figure 5.5 shows an example of the profile of a concrete sewer with a shallow foundation. The sewer was constructed in 1977 and has a diameter of $300\,mm$. The location of the sewer is indicated in figure 5.4.

As can be seen figure 5.5, no slope measurements are available for locations closest to a manhole. The reason is that in Amsterdam the manholes of combined sewer systems have a sediment trap (e.g. invert manhole is lower than invert sewer). Due to this trap, it is not possible to drive the camera tractor along the whole length of the sewer. To attain the vertical profile along the whole length of the sewer, tilt values are estimated for the locations where it was not possible to take a measurement. The missing values are estimated based on the assumption that each individual pipe segment of a sewer has, on average, the same slope (see also chapter 3).

In the upper graph of figure 5.5 it can be seen that the largest changes in slope occur at the location of a joint; in between joints the sewer has almost the same slope. Therefore, as expected, it can be confirmed that pipes made of concrete are rigid. Nevertheless, significant but small deviations from the average slope can also be recognized between the joints (for example the pipe at a distance of $6.5-8.5\,m$ from the centre of the manhole, figure 5.5). Because similar deviations
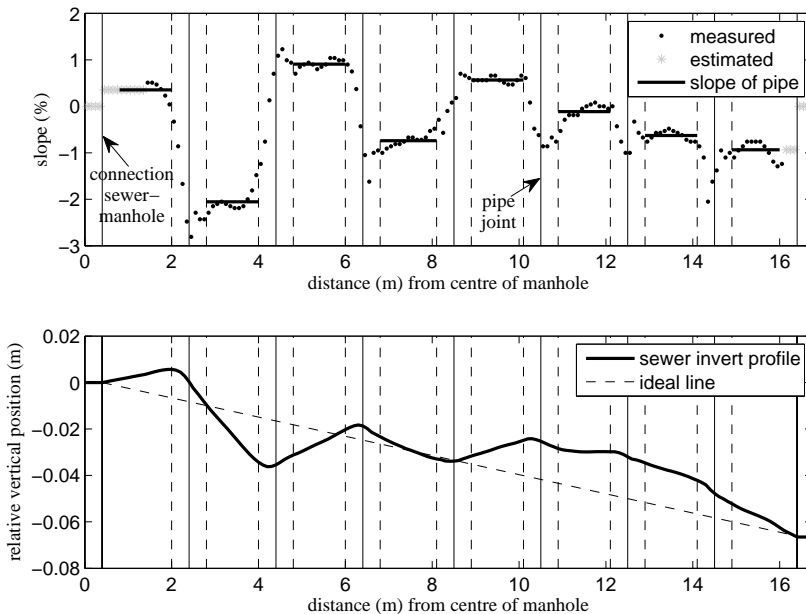
Figure 5.5: Example of a concrete sewer with a shallow foundation.

were also present in each measurement of the sewer measured 5 times from each direction as discussed in paragraph 3.2.2 (figure 3.13), it can be concluded that even concrete pipes are not always perfectly straight.

To verify if the profile of a sewer is influenced by (differential) settlement, a property should be defined that reflects the bumpiness (i.e. the deviation from the ideal line) of a sewer. For this, two parameters are developed: the average and maximum difference in slope between two neighbouring sewer pipes. Both properties are equal to 0% when a sewer profile follows the ideal line. It is expected that values increase over time due to differential settlement. For the sewer shown in figure 5.5, these properties are equal to respectively 1.2% and 3.0%.

For 5 of the 60 concrete sewers with a shallow foundation it was not possible to calculate both properties: one sewer was made of only one pipe and 4 sewers consisted of pipes of only 1 meter which is not long enough to collect sufficient slope measurements for each pipe to calculate an average slope. For the remaining sewers, the settlement rate of the sewer was calculated by averaging the settlement rate of the manholes on both ends of the sewer. When no reliable estimation of the settlement rate of a manhole is available (CI $> 1\,\mathrm{mm\,year^{-1}}$), the average settlement rate of the Waddendijk case study area of $4.5\,mm\,year^{-1}$ was used.

The left graph of figure 5.6 shows the relation between both properties (average and maximum slope difference), the gray scale indicates the total settlement (average settlement rate multiplied by the age of the sewer). As can be seen the average and maximum slope are correlated but do not increase with an increasing total settlement.

To verify if the total length of the sewer influences the average and/or maximum slope difference between two neighbouring pipes, the right graph of figure 5.6 shows the relation between the total length of a sewer and the average slope difference. As in the left figure, the gray scale indicates the total settlement. From
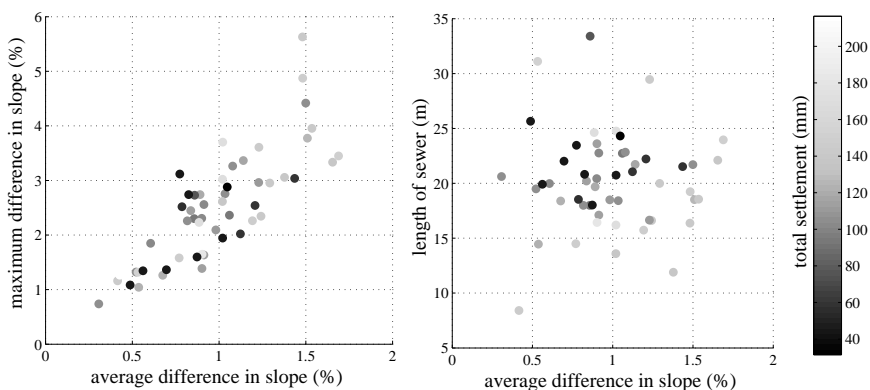
Figure 5.6: Relation between the average and maximum slope difference between neighbouring pipes and average slope difference and sewer length, the gray scale indicates the total settlement.

the graphs it is concluded that the total length of a sewer does not influence the average and the maximum slope difference between two neighbouring pipes.

Also the shape of the profile of the sewer invert was compared to the ideal line. Three different shapes were identified:

- sewer bending downwards and upwards (examples in figures 5.5 and 5.13)

- upward bending (example of a PVC sewer with this shape can be seen in figure 5.7)

- downward bending

Categorizing the whole set of 60 sewer profiles of concrete sewers with a shallow foundation revealed that the profile of 32 sewer inverts can be characterized as down and upward bending, 13 as upward and 15 as downward. Because no distinct shape could be recognized it is concluded that the settlement rate of manholes and sewers is generally the same.

PVC

Figure 5.7 shows the profile of a PVC sewer with a shallow foundation. The diameter of this sewer constructed in 2000 is $297\,mm$. When comparing this profile to the profile of the concrete sewer it stands out is that, as expected, sewer
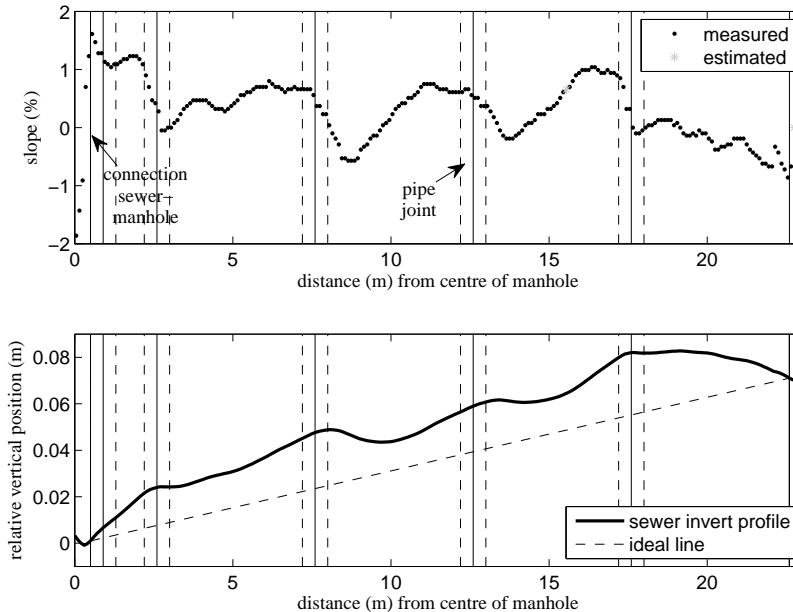
Figure 5.7: Example of a PVC sewer with a shallow foundation.

pipes made of PVC are flexible and are also able to bent in between joints. But, like concrete sewers, the slope of the PVC sewer also changes at the location of the joints.

As indicated in table 5.1 only 9 sewers with a shallow foundation made of PVC are analysed. With the exception of one sewer built in 1979, these sewers were constructed in 2000. In general the shape of the profile of the sewer invert and the ideal line were similar. For the sewer shown in figure 5.7 the maximum difference between the ideal line and the profile is only $27mm$.

To verify whether the settlement process of PVC sewers differ considerably from the settlement of concrete sewers, the results of the 8 PVC sewer constructed in 2000 (age at inspection 10 years) with a shallow foundation were compared to the results of 8 concrete sewers also constructed in 2000 with a shallow foundation. For all sewers the maximum difference between the ideal line and the measured profile was determined. The results are listed in table 5.2. The independent two-sample t-test was used to check if the calculated values differ significantly for both materials. Based on the test it can be concluded that, although the average maximum difference is larger for the concrete sewers ($23mm$ compared to $19mm$), the averages do not differ significantly at the 5% significance level.

Cast iron

As indicated in table 5.1 only 4 sewers made of cast iron with a shallow foundation have been analysed. The location of these sewers is indicated in figure 5.4. In general cast iron sewers are only used with a pile foundation or as hinge sewers. The analysed cast iron sewers used to be hinge sewers too, but with the renewal of the pile founded sewer in 1997 the part of the cast iron sewer closest to the pile founded manhole was also renewed. To connect the new concrete hinge sewer to the old cast iron sewer a new manhole was constructed.

Figure 5.8 shows the measurement result of the cast iron sewer indicated in figure 5.4. Like the other analysed cast iron sewers with a shallow foundation,

Table 5.2: Maximum difference between the ideal line and the measured profile.

PVC		concrete	
sewer ID	difference (mm)	sewer ID	difference (mm)
295	18	325	22
296	18	396	15
316	22	398	24
317	27	399	41
318	37	400	46
319	15	402	31
322	14	404	32
323	40	379	24

this sewer was constructed in 1979 with a diameter of $400\,mm$. As can be seen in the figure, cast iron sewers, like sewers made from concrete, are rigid and hardly show any deformations in between joints.

Because the subset of cast iron sewers with a shallow foundation is too small, the invert profiles of these sewers are not further looked into. Besides, this type of sewers (cast iron, shallow foundation, connected to manholes with a shallow foundation) are hardly present in the Amsterdam sewer system.

5.2.2 Pile foundation

In comparison to sewers with a shallow foundation, pile founded sewers are different in several aspects: sewers as well as sewer pipes are much longer, have a larger diameter and the manholes do not have a sediment trap. Figure 5.9 shows the result of the measurement of a sewer with a pile foundation. This sewer, like most analysed sewers with a pile foundation, was constructed in 1997; only one sewer constructed in 2000 was analysed. All analysed sewers with a pile foundation are made of cast iron.
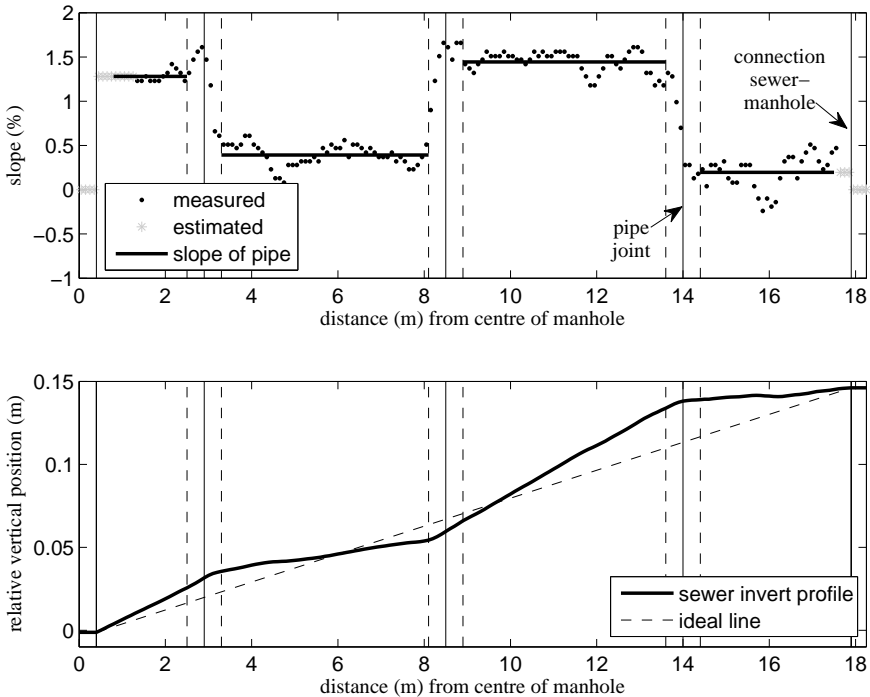
Figure 5.8: Example of a cast iron sewer with a shallow foundation.
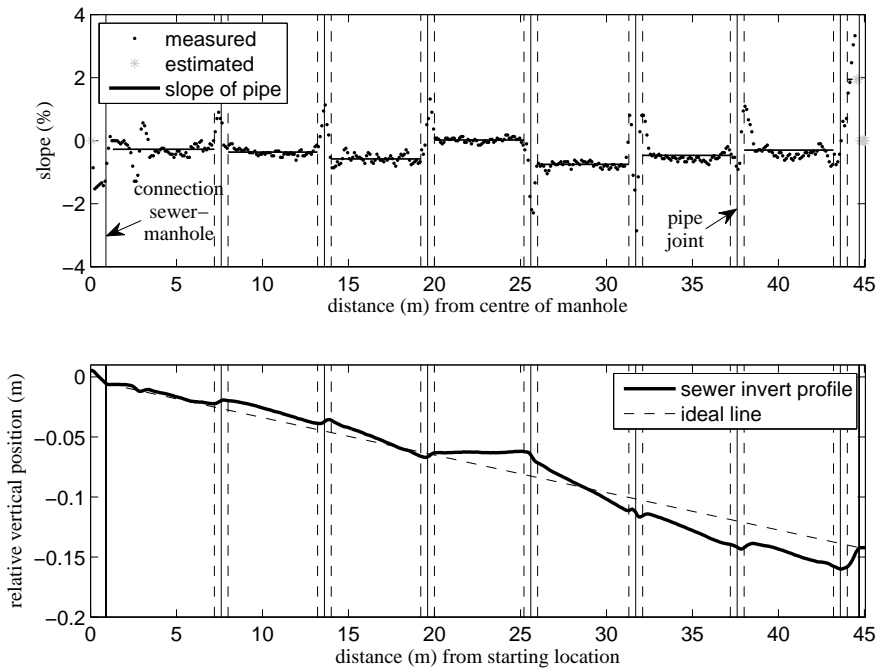
Figure 5.9: Example of a cast iron sewer with a pile foundation.
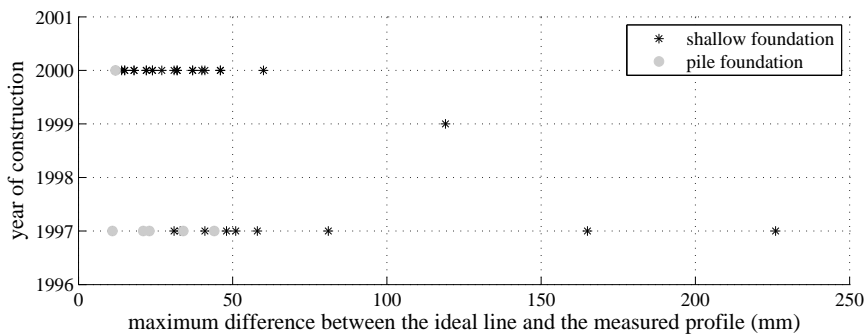
Figure 5.10: Comparison between sewers with and without a pile foundation on the maximum difference between the ideal line and the invert level.

Despite a pile foundation, the sewer pipes of the sewer shown in figure 5.9 are not perfectly aligned. Figure 5.10 shows the maximum difference between the ideal line and the profile for the pile founded sewers as well as sewers with a shallow foundation. All sewers were constructed between 1997 and 2000. As can be seen in the figure, despite their length, sewers with a pile foundation follow more closely the ideal line in comparison to the analysed sewers with a shallow foundation.

5.2.3 Hinge sewers

As can be seen in table 5.1 the slope profile of 14 hinge sewer have been analysed. The total can be divided into three groups: 4 concrete sewers that were recently constructed (1997-2000), 6 PVC sewers constructed in 1997 and 4 somewhat older sewers constructed in 1974-1980 made of different materials.

Analysis of the slope profiles of the recently constructed concrete sewers revealed that the shape of only one of these sewers resembles the design of hinge sewers as shown in 5.3. The maximum difference between the ideal line and the profile of the sewer invert of the remaining 3 sewers are 36, 32 and 60 mm which is not considerably different compared to the values for concrete and PVC sewers constructed in 2000 as listed in table 5.2.

Of the 6 analysed PVC hinge sewers constructed in 1997, 4 are less than $10m$ long; the remaining two resemble the design of hinge sewers. Nevertheless, the slope profile measurement revealed that, although only 13 years old, all sewers started to sag right before the manhole with a pile foundation. In figure 5.11 shows some photographs taken with the inspection camera in the direction of the manhole with a pile foundation. As can be seen, about 10% of the sewer is permanently filled.

The older hinge sewers were constructed in 1974, 1977, 1980 and 1980. At the moment of measurement these sewers were 36, 33, 30 and 30 years old which is relatively young for sewers that are expected to last at least 60 years. Nevertheless, visual inspection revealed that two of these sewers were already repaired by replacing the part of the sewer closest to the pile founded manhole. The profiles

Figure 5.11: Photographs of hinge sewers made of PVC and constructed in 1997 showing small sags just in front of the manhole with a deep foundation.

of the sewer invert of the other two hinge sewers are shown in figure 5.12. As can be seen a significant sag is present in front of the manhole with a pile foundation. Due to this sag the PVC sewer has at the lowest point a filling percentage of 50%; as the diameter of the cast iron sewer is much larger ($400mm$ compared to $200mm$) the filling percentage in the cast iron sewer is maximal 20%. Nevertheless, even after hydraulic cleaning a significant amount of settled deposits was found in the cast iron sewer.

5.2.4 Relation between defects and (differential) settlement

To verify if there is a relation between the differential settlement of sewer pipes and the development of defects, the sewers were also visually inspected. Because the probability that a defect is missed by the inspector is large (probability $\approx 25\%$ as concluded in chapter 2), the footage was analysed at least twice and only defects that are clearly visible will be further looked into.

In this paragraph only defects that are possibly related to the differential settlement of sewer pipes are used for the analysis. These are: 'fissure', 'infiltration', 'ingress of soil' and 'deformation' for PVC sewers only. Although clearly linked to the differential settlement of pipes, the defect 'displaced joint' will not be further analysed. The reason is that during inspection it proved impossible to unambiguously define what is, and what is not a 'displaced joint'.
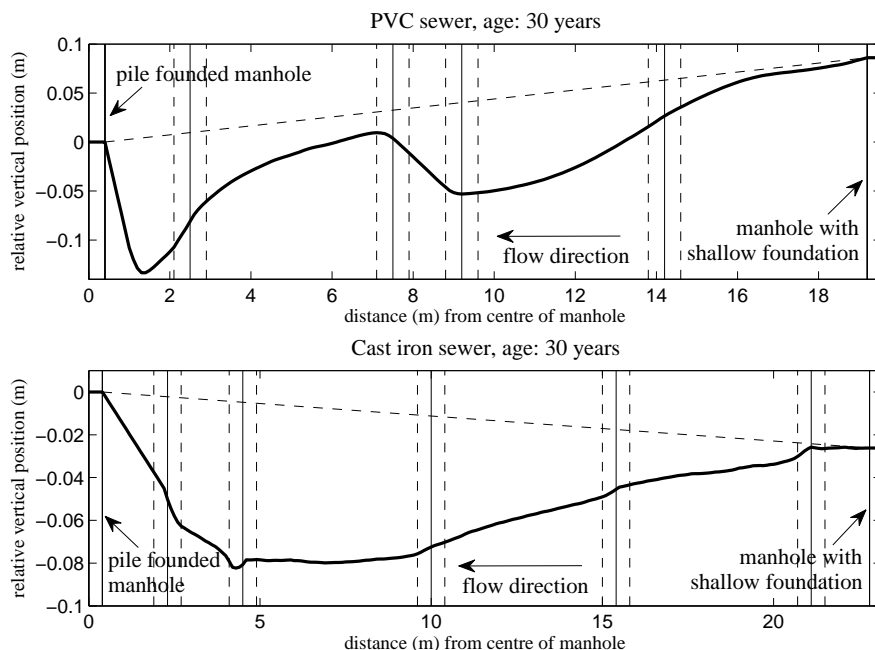
Figure 5.12: Sewer invert profile of two hinge sewers.

In general, not many defects were found in the analysed sewers of the Waddendijk case study area. What stands out is that severe (clearly visible) defects were only found in sewers made of rigid materials. Only one PVC sewer was flattened (defect: 'deformation') probably because this sewer is positioned just above a sewer with pile foundation.

To verify if the occurrence of defects is related to the displacement of sewer pipes, the inspection footage of two joints with the largest difference in slope between the two connecting pipes were analysed thoroughly. Figure 5.13 shows the vertical profile of the sewer invert of both sewers. In the graphs the average slopes of pipes on both sides of the joint with the largest slope difference are indicated. The maximum difference in slope for the shallow founded concrete and the cast iron sewer are respectively 5.9 and 8.7%.

On the right hand side of the graphs in figure 5.13, photographs of the inside of the sewer showing the specific joint are depicted. It can be seen that despite the drastically deformed sewer invert profiles, the inside of the sewers does not look very abnormal. For the concrete sewer, no defects were found besides a filling percentage of 20%. Inspection of the cast iron sewer revealed that water was dripping at the location of the joint. As groundwater tables in Amsterdam are generally high (1-2 meter below ground level) it is very likely that groundwater infiltrates into this sewer.

The most severe condition that was found in the sewer system of Waddendijk was a combination of the defects 'infiltration' in and 'ingress of soil' that was found in two hinge sewers and one shallow founded sewer. Only for one of these
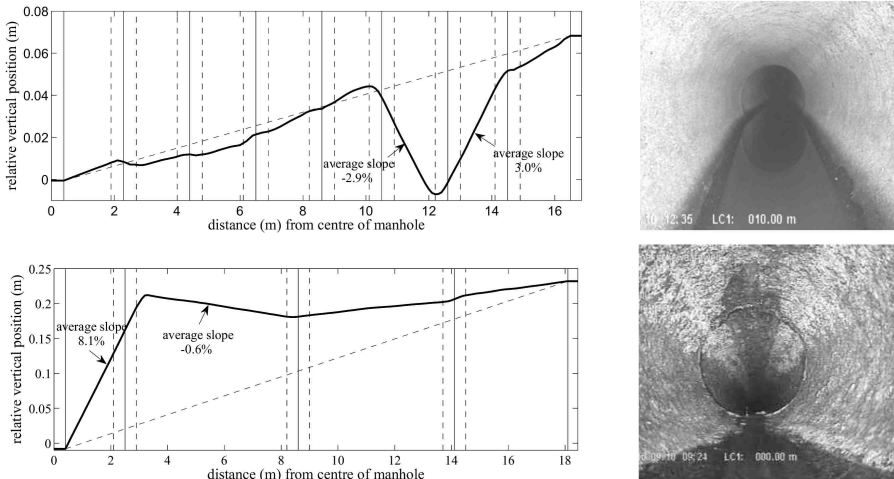
Figure 5.13: Concrete sewer (upper graph and picture) and cast iron sewer (lower graph and picture) with the largest difference in slope of between neighbouring pipes.

sewers the occurrence of the defects might be related to the angle of the pipes. For this sewer the defect occurred close to the pile founded manhole. The difference in slope between the pipes at each side of the leaking joint was 5-6%. For the other hinge sewer the defects occurred close to the manhole with a shallow foundation at the joint of a pipe with a length of only 30 cm. Because this very short pipe was found at the end of the sewer it is likely that a sewer pipe was shortened mechanically when, at construction in 2000, the sewer did not fit directly between both manholes. The last location where the defects 'infiltration' in combination with 'ingress of soil' were found was in a concrete sewer. For this concrete sewer some of the pipes were replaced with PVC pipes. At the connection of a PVC pipe with a concrete pipe water and sand were gushing into the sewer.

Finally the defect 'fissure' was found twice. In both instances it concerned a surface crack at the spigot end of a pipe. As the slope difference of the pipes at each side of the joint with the surface crack was small it is very likely that the surface crack was caused by careless installation of the pipes.

5.3   Detailed analysis of hinge sewers

From the initial analysis of the sewer invert profile of 100 sewers in the Waddendijk case study area, it was found that for most analysed sewers differential settlement of sewer pipes have (not yet) resulted in the development of defects. Most remarkable observation was the sagging of the relatively new (age 13) PVC sewers just before the manhole with a deep foundation. Consultation with the sewer cleaning and inspection personnel revealed that sags occur frequently before manholes with a deep foundation and that these location are notorious for its frequent blockage.

To study the sagging of hinge sewers, the slope profile of 74 hinge sewers was measured. It was chosen to select only sanitary sewers made of PVC in separate sewer systems. The reason to chose PVC is that these, due to their flexibility, are able to follow the ground settlement better and therefore probably develop sags in an earlier stage compared to sewers made of rigid materials. Besides, most hinge sewers in the Amsterdam area are made of PVC. The reason to focus on sanitary sewers of separate sewer systems is that these are probable most sensitive to blockage due to small diameters and unfavourable conditions (water quality and quantity).

This paragraph focusses on structural aspects only: settlement, differential settlement, sags and defects. Chapter 6 will elaborate on the consequences of (differential) settlement on the functioning of sewer system including the relation between sags and blockage frequency.

5.3.1 Materials and methods

Selection of sewers

Only sanitary sewers of separate sewer systems made of PVC were selected for this analysis. In addition, some other aspects were taken into account:

- Neighbouring sewers should be least of the same age or older.

- The diameter should be equal to $235\,mm$ (standard size for PVC sewers).

- It is aimed to select sewers of different ages.

- Sewers were selected form different neighbourhoods in Amsterdam.

In total 74 hinge sewers were analysed. For 7 sewers, however, it was not possible to drive the camera tractor along the whole length mainly due to too sharp vertical and/or horizontal bends. For another 9 sewers inspection revealed that the pile founded sewer was just renovated and that the part of the hinge sewer closest to the pile founded sewer was replaced with new pipes. Because the sewer invert profile of some of these sewers pointed out a specific and interesting problem, the results will be discussed in a separate paragraph (paragraph 5.3.3). The total set of sewers was analysed from September 2011 until November 2011. It took a full team (camera vehicle, a vacuum truck with integrated sludge tank and a water jet cleaner) 15 days to take all necessary measurements.

Analysis of the settlement rate

To estimate the settlement rate of the analysed sewers all available measurements (digital available data as well as measurements only available on historical maps) of the sewers invert level are used (see paragraph 3.1 for more information about these measurements). Nevertheless, for most sewers insufficient data was available for a reliable estimation $(CI < 1\,mm\,year^{-1})$. To reduce the error, it was decided to average the settlement rates of sewer inverts within a certain distance from the analysed sewer. Averaging settlement rates over an area was previously successfully applied to calculate neighbourhood average settlement rates in paragraph 4.2.2.

The distance from within the sewer inverts are selected should be large enough to contain sufficient estimates but small enough not to include too much natural variation in settlement rate. Analysis of a semi-variogram can help to decide on the radius. As the gathering of data from the historical maps is very time-consuming, it is not feasible to calculate the semi-variogram for each analysed sewer. Therefore the settlement data from sewer system of the Wadddendijk case study area is used to decide on a suitable radius. The settlement rates of the sewer inverts in this system were previously described in paragraph 4.2.1.

Variograms are widely used in geostatistical practice to describe spacial correlations of observations. In mathematical notation the variogram is defined as

$$2\gamma(D) = \frac{1}{n} \sum (g(x) - g(x + D))^2 \tag{5.1}$$

with $2\gamma(D)$ the value of the variogram for distance D, $g(x)$ the measurement value at location x and $g(x + D)$ the paired measurement value at a distance D from measurement $g(x)$ and n the number of pairs that you have. To interpret the results usually γ is plotted against D resulting in a semi-variogram. In the ideal situation, γ is zero when D is equal to zero. When measurements are taken further apart (D increases), the difference between the measurement values increase and so γ. When the distance becomes very large the measurement values will become independent of one another and the semi-variogram value will become more or less constant [see e.g. Clark, 1979].

The left graph of figure 5.14 shows the frequency distribution of the settlement rates in the Waddendijk case study area. As an be seen the data is skewed which will present problems when calculating the semi-variogram due to impact of the extreme values. To overcome this problem, the root of the absolute difference is used instead of the squared difference [Cressie and Hawkins, 1980].

$$Y(D) = \frac{1}{n} \sum \sqrt{g(x) - g(x + D)} \tag{5.2}$$

The resulting semi-variogram (Y) is shown in the right graph of figure 5.14. Because the dataset is large, the calculated values of Y are grouped into classes of $20m$, in the graph the class averages are shown. The semi-variogram of the Waddendijk case study area appears not to intersect the y-axis at zero. This is called the nugget effect and is the result of an uncertainty in the estimation of the
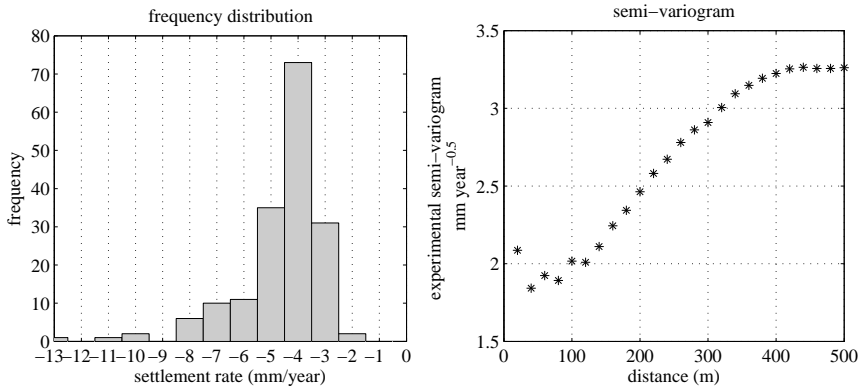
Figure 5.14: Frequency distribution and the experimental semi-variogram of the settlement rates in the Waddendijk case study area.

settlement rate. Until $D = 120\,m$ the nugget effect appears to dominate, from $D = 120\,m$ the semi-variogram appears to follow the spherical or 'ideal model'.

To find a suitable radius not only the increase in variation should be taken into account, but also the number of available data points. Analysis of the distances between manholes in the Waddendijk case study area showed that with a radius of 75, 100 and $125\,m$ on average respectively 7, 12 and 18 manholes can be found. For the situation with manholes measured twice with an interval of 5 years (see equation 4.3) this implies that the settlement rate can be predicted with an 95% confidence interval of respectively 1.2, 0.75 and $0.5\,mm\,year^{-1}$ (possible increase in variation with increasing radius not taken into account). Because the error does not reduce significantly between 100 and $125\,m$ and to reduce the amount of work (collecting the historical invert levels is laborious) a radius of $100\,m$ was chosen.

Measurement routine

To be able to study relevant aspects of the settlement process of the hinge sewers the following measurements/action were (under)taken:

- Visual inspection of condition (structural condition and fouling) of both manholes.

- Measurement of the water level in both manholes.

- If possible, inspection of the sewer before cleaning, starting from the manhole with a shallow foundation.

- Cleaning of the sewer.

- Inspection of the clean sewer, starting at the manhole with a shallow foundation.

- Measurement of the sewer invert profile.

This paragraph focuses on the impact of settlement on the position and structural condition of the sewer. For this the results of the sewer invert profile measurement and the inspection of the clean sewer are used. As will be explained, the measurement of the water level in both manholes is used to interpret the sewer invert profile measurement. It was chosen to start the inspection at the manhole with a shallow foundation so that the part of the sewer closest to the manhole with a pile foundation can be inspected completely.

Slope measurement

Figure 5.15 shows the result of a slope measurement. Because the bottom of the manhole with a pile foundation is at a different level compared to the level of the sewer invert, it was not possible to measure the slope along the whole length of the sewer. As the sewer pipes are made of flexible material it was not possible to

estimate missing data based on the average slope of a pipe. To estimate missing slope measurements close to the manhole with a deep foundation, the location of the beginning of the stagnant water zone as shown on the inspection footage of the clean sewer was used as will be explained.

For the example in figure 5.15, the photograph of the inside of the sewer shows that the filling starts just before the joint at $6.8m$ from the centre of the manhole. To verify if the water level indicates the beginning of the sag, it was checked whether the sag is completely filled. As can be seen in figure 5.15, the missing slope values close to the manhole with the pile foundation were estimated so that the profile of the sewer invert match the observation.

To estimate missing data close to the manhole with a shallow foundation, the slope as shown on the inspection video just after the positioning of the inspection camera in the sewer was used. For the situation where the manhole with a shallow foundation is lower than the manhole with a pile foundation, the water level measurement at the manhole with a shallow foundation is used to estimate the missing slope values.

5.3.2 Results

A total of 58 sewer invert profiles are available for the analysis of the differential settlement of hinge sewers. For each of these sewers the settlement rates of the sewer invert levels at a maximum distance of $100\,m$ were calculated. To verify if
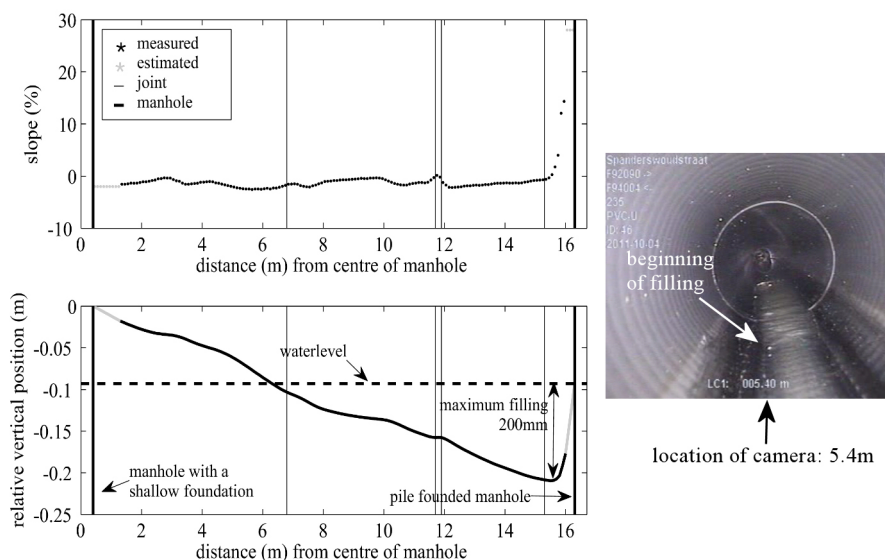
Figure 5.15: Example of the sewer invert profile of a hinge sewer. The photograph on the right shows the location of the beginning of the sag.

the average is a robust estimation of the settlement rate of the sewer, the relation between the average and the median settlement rate was studied (figure 5.16). For the calculation of the average settlement rate all values in the dataset can be used (left graph) but one can also choose to ignore the lowest and highest settlement rate of the dataset (right graph).

From the graphs it is concluded that the median and average are strongly correlated indicating that averaging gives robust results. Furthermore, not taking into account the lowest and the highest value gives slightly better results; average difference between mean and median reduces from $0.5\,mm\,year^{-1}$ to $0.4\,mm\,year^{-1}$. Therefore, the settlement rates calculated with this procedure (mean of the dataset without the highest and lowest value) are used for further analysis.

From figure 5.16 it can also be seen that, as intended with the selection of sewers in different areas, the settlement rates of the analysed sewers are diverse.

Analysis of the sewer invert profile

Within the 58 analysed hinge sewers also two newly constructed sewers were present. Like the recently reconstructed sewers analysed in the Waddendijk case study area (discussed in paragraph 5.2.3), the shape of these sewers did not resemble the hinge sewer design (figure 5.3): the last 3 meters before the pile founded manhole did not have a significant higher slope. The lack of a distinct difference in slope, however, is not the main concern. On the long term, the lack of fall (drop in level) of the hinge sewer will have more significant implications. For the two analysed new sewers this drop was only 28 and $66\,mm$ which should be at least $300\,mm$ according to the design. With a settlement rate of respectively -7.4 and $-8.6\,mm\,year^{-1}$ this implies that over respectively 4 and 8 years time the sag will reach the manhole with a shallow foundation. Bringing the system back
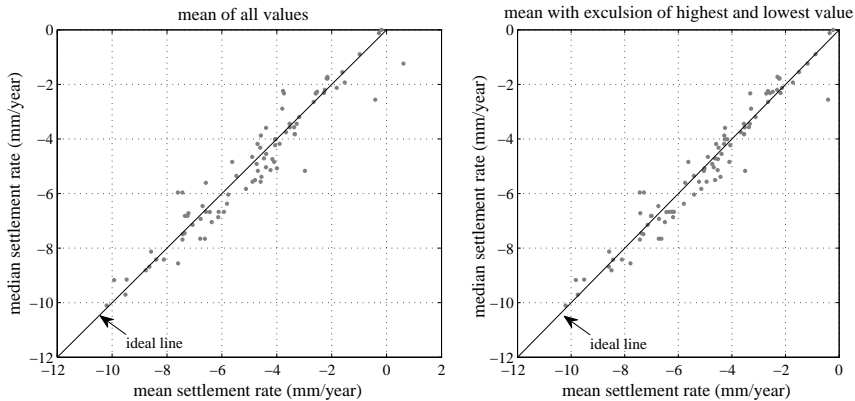
Figure 5.16: Relation between mean and median settlement rate.

to its desired state (no filling) would therefore not be possible by the renewal of the hinge sewer only, but requires renewal of all sewers upstream.

To verify whether the difference in level between the beginning and end of a hinge sewer (or fall) was also too small for the other analysed hinge sewers as well, the fall of the analysed sewers was determined based on the sewer invert profiles. In figure 5.17 the difference in level is plotted against the total settlement. In this figure the equation and line of the linear fit by minimization of the squared difference is also shown. When assuming that the distribution of the fall at construction is symmetrical with average 0, the linear fit represents the relation between the fall and the total settlement. As the manhole with a pile foundation does not settle, the fall should decrease with the same rate as the total settlement increase. In the figure it can be seen that, as expected, the slope of the linear fit is almost -1. The intercept of the linear fit indicates the average fall at construction (total settlement $= 0$). As can be seen the average fall at construction is only $172\,mm$ which is considerably less than the formal design rules ($300\,mm$).

Figure 5.18 shows four examples of sewer invert profiles at different stages of the settlement process. In this figure it can be seen how the shape of hinge sewers changes due to the settlement difference between the sewer and the pile founded manhole. To allow for easy comparison both axis of all four graphs are equal. It should be stressed that these sewers were selected based on their resemblance with the original design of hinge sewers. Especially the relatively straight part at the beginning of the sewer up to around $5\,m$ before the manhole with a deep foundation was not observed for all (new and old) hinge sewers.

Analysis of the sewer invert profiles of all analysed sewers showed that, although PVC is a flexible material, the largest difference in slope occurs at the joints. This phenomenon can clearly be observed for the sewer invert profiles shown in figure 5.18.
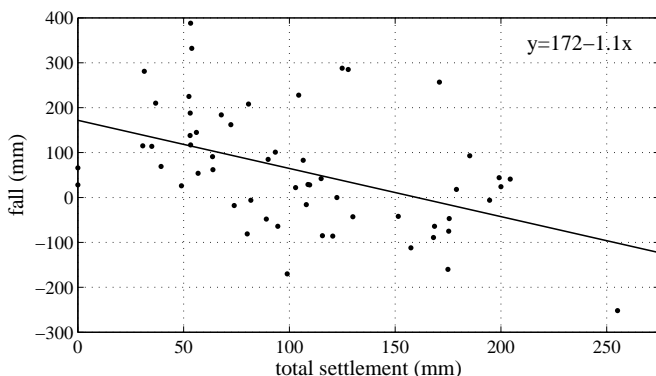
Figure 5.17: Relation between the total settlement and drop in level over the length of the hinge sewer.

It can also be seen that the filling (maximum depth of the sag) increases with increasing total settlement. In figure 5.19 the relation between filling and total settlement for all analysed hinge sewers is shown. In general the filling increases with increasing total settlement but there are large differences for individual sewers. Reason for this variation can probability be found in the design and construction of the connection of the sewer to the manhole with a deep foundation as one can imagine that the force needed to rotate the sewer connected to the pile founded manhole can be very different for each sewer.
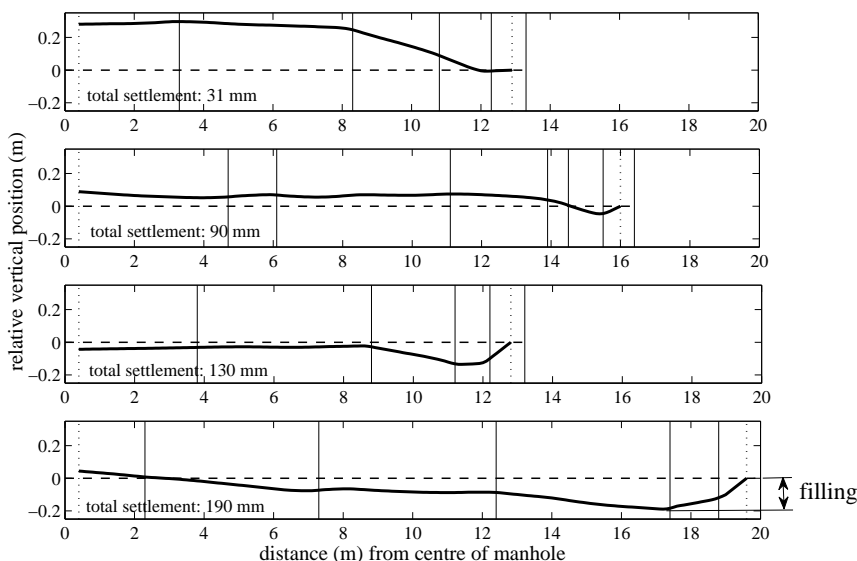
Figure 5.18: Examples of sewer invert profile at different stages of the settlement process. The flow direction is from left to right; the pile founded manhole is on the right.
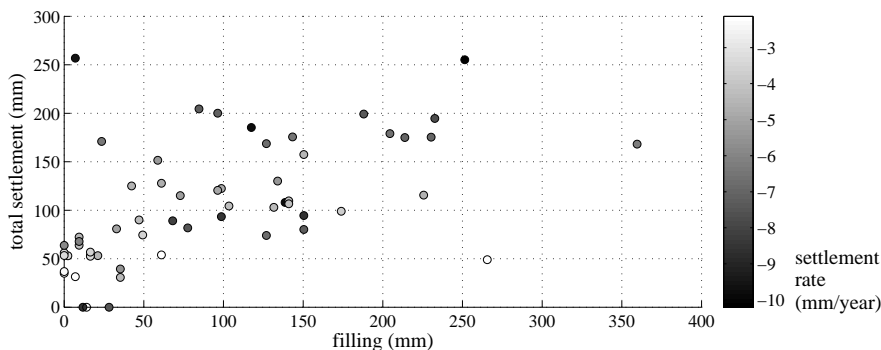
Figure 5.19: Relation between the total settlement and the filling. The gray scale gives an indication of the estimated settlement rate.

For the sewers shown in figure 5.18 at first the sewer closest to the manhole with a pile foundation rotates. Up to a certain angle the force needed for this rotation increases to a level where it is more favourable to deal with the differential settlement by rotating the next pipe. For other hinge sewers different slopes of the last sewer pipe were found. For some sewers it appeared even that this joint was completely stiff (slope measurement close to pile founded manhole almost zero).

Another influencing factor on the settlement process of hinge sewers is probably the length of sewer pipes and the way that they are arranged. Like the sewers in figure 5.18, for most sewers the part closest to the manhole with a deep foundation was composed of several short pipes. As the largest slope difference are found at the location of joints, the length of these pipes determine the shape of the invert profile after significant settlement.

Defects

To assess the relation differential settlement and the development of defects, the footage of the inspection camera was carefully examined. For the sewers with a high filling percentage (over 70-80%) it was not possible to collect good images for the complete sewer as the camera lens fouls when submerging.

For all analysed sewers most severe defects were found close to the manhole with a deep foundation. Figure 5.20 gives some examples of sewers with severe defects. The left and the middle photograph show two examples of displaced joints. Although displaced joints were frequently observed, in the majority of cases infiltration of groundwater and/or ingress of soil were not observed. The joint in the left photograph is an example of this. For this sewer the change in slope caused the pipes move closer to each other at the upper part. As can be seen this resulted in the deformation of the PVC pipe. Nevertheless no water was seen to enter the sewer at the moment of inspection. The photograph in the middle gives an example of an open joint at the lower part of the sewer. This was the only sewer where infiltration of groundwater was observed.

The photograph on the right gives an example of a different defect, namely deformation. Heavily deformed pipes at the connection to the manhole with a
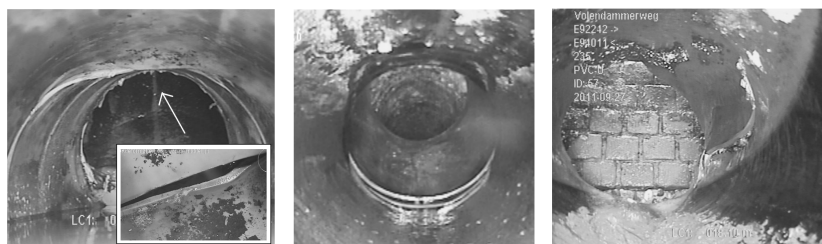
Figure 5.20: Examples of hinge sewers with severe defects.

deep foundation were found for 9 hinge sewers. Analysis of the slope measurement revealed that for all of these 9 sewers the slope of the sewer close to the manhole was relatively steep (slope $> 15\%$). The location of the the last joint before the pile founded manhole was not different compared to the other analysed hinge sewer. Two of these deformed hinge sewers were cracked like the one shown in the figure.

5.3.3 Other findings

In addition to the 58 previously discussed hinge sewers also 9 sewers were analysed in an area where the pile founded sewer (including manholes) was recently renewed. When inspecting the hinge sewers it was found that the last part of these sewer was also renewed as can be seen in the photograph of figure 5.21. When analysing the sewer invert profiles of these sewers a peculiar bump was found for 4 of these sewers. Figure 5.21 shows the sewer invert profile of one of these sewers.

Looking further into the specific characteristics of these 4 sewers it was found that all of these sewers were located at the southern side of the pile founded sewer. Therefore the thought raised that the bump was caused by some line structure next to the pile founded sewer. Detailed analysis of the historical maps of the area showed that the new pile founded sewer was located just north of the old sewer.
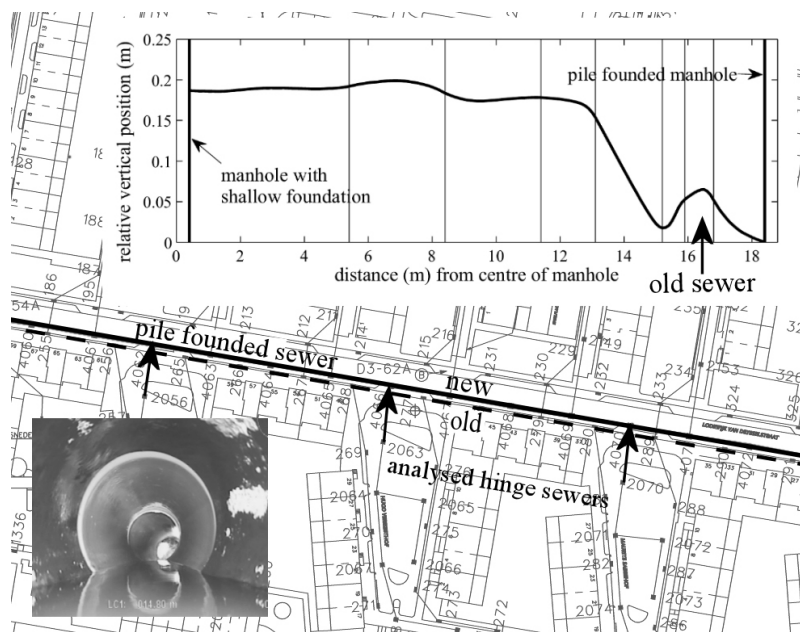
Figure 5.21: Sewers crossing an old pile founded sewer.

Consultation with the contractors revealed that, when renewing a pile founded sewer, the old sewer is generally not removed. As was done in the analysed area, the new pile founded sewer is laid just next to the old one.

The complications of this practice are clear from the measured sewer invert profiles: as the old hinge sewers on one side of the pile founded sewer have to cross the old pile founded sewer, a bump is, or becomes, apparent. Eventually this will almost certainly lead to defects such as deformation, open joints and cracks.

5.4   Conclusion and recommendations

As mentioned in the introduction of this chapter, it was expected that due to inhomogeneities of the soil, sewer pipes move relative to each other and that these movements most likely will result in defects. Detailed analysis of 91 sewers with a shallow foundation revealed that both expectations could not be confirmed. As the sewers were only analysed once, this conclusion is based on the comparison between the sewer profiles of old and new sewers. For a more detailed analysis it is recommended to measure the sewer invert profile of the same sewer several times over a period of time.

It is concluded that with a settlement rate of $5\,mm\,year^{-1}$, the movement of sewer pipes relative to each other is insignificant in comparison to the imperfections of a newly constructed sewer. That sewers are not always installed perfectly also became clear with the analysis of the hinge sewers as the vertical profile of recently constructed hinge sewers did not resemble the vertical profile of the design. For almost all analysed hinge sewers it was found that at installation the difference in level between the beginning and end of the hinge sewer was less than the required $300mm$.

Analysis of the structural condition of the sewers did reveal some defects. The majority of these defects, however, could not be related to the (differential) settlement of the sewer pipes. The only sewers that showed significant changes in the sewer invert profile and structural condition with increasing settlement are hinge sewers. For these sewers it was found that due to the difference in settlement between the manhole with a pile foundation and the sewer with a shallow foundation, sags are formed just before the manhole with a deep foundation. At the connection with the pile founded manhole, severe defects such as cracks and deformation were found in several sewers.

To manage these hinge sewers effectively it is advised to inspect and measure the sewer invert profile regularly. As the condition of this sewer is related to settlement, the time interval between inspections/measurement can be based on the (expected) settlement rate. Also the inspection and measurement of the sewer invert profile of newly constructed sewers is recommended. This is advised not only to check the work of the contractor but also to be able to compare the results of a condition assessment at an older age with the situation after construction.

Bibliography

Bishop, P., Misstear, B., White, M., Harding, N., 1998. Impacts of sewers on groundwater quality. Journal of the Chartered Institution of Water and Environmental Management 12, 216–223.

Buco, J., Emeriault, F., Kastner, R., 2008. Full-scale experimental determination of concrete pipe joint behavior and its modeling. Journal of Infrastructure Systems 14 (3), 230–240.

Clark, I., 1979. Practical Geostatistics. Applied Sciences Publishers LTD.

Cressie, N., Hawkins, D., 1980. Robust estimation of the variogram: 1. Mathematical Geology 12 (2), 115–125.

Davies, J., Clarke, B., Wither, J., Cunningham, R., 2001. Factors influencing the structural deterioration of rigid sewer pipes. Urban Water 3, 73–89.

DeSilva, D., Burn, S., Tjandraatmadja, G., Moglia, M., Davis, P., Wolf, L., Held, I., Vollertsen, J., Williams, W., Hafskjold, L., 2005. Sustainable management of leakage from wastewater pipelines. Water Science and Technology 52 (12), 189–198.

Frantziskonis, G., Breysse, D., 2003. Influence of soil variability on differential settlements of structures. Computers and Geotechnics 30 (3), 217–230.

Iimura, S., 2004. Simplified mechanical model for evaluating stress in pipeline subject to settlement. Construction and Building Materials 18 (6), 469–479.

Jaksa, M. B., Kaggwa, W. S., Brooker, P. I., 1999. Experimental evaluation of the scale of fluctuation of a stiff clay. In: Stewart, R., Melchers, M. G. (Eds.), 8th Int. Conf. on the Application of Statistics and Probability. Vol. 1. A. A. Balkema, Rotterdam, Sydney, pp. 415–422.

Moghaddas Tafreshi, S. N., Tavakoli Mehrjardi, G., 2008. The use of neural network to predict the behavior of small plastic pipes embedded in reinforced sand and surface settlement under repeated load. Engineering Applications of Artificial Intelligence 21 (6), 883–894.

Read, G., Vickridge, I. (Eds.), 1997. Sewers - rehabilitation and new construction: repair and renovation. Elsevier/Butterworh Heinemann.

Chapter 6

Influence of settlement on the functioning of the sewer system

This chapter extends the paper 'Settlement as a driver for sewer rehabilitation.' published in Water Science and Technology [Dirksen et al., 2012] and the paper 'The impact of fat, oil, and grease deposits on the performance of sanitary sewers' sent in for presentation at the 7th conference on Sewer Processes and Networks.

Additional to the deterioration of the structural condition as studied in the previous chapter, differential settlement can also lead to fouling (accumulation of solid pollutants) of the system. Fouling includes the deposition of sediments and the attachment of deposits on the surface of the pipe. As both processes are likely to occur with low velocities and long retention times, the presence of sags and therefore settlement will influence the fouling of the system.

The impact of settlement on the flooding frequency is not studied because, giving the current Dutch regulations, it is very unlikely that changes in the vertical position of the sewer system elements will have an influence on the frequency of flooding. For combined systems Dutch regulation imposes constraints regarding the hydraulic and environmental performance. For the hydraulic performance, the system should be able to discharge a standard design storm [e.g. rain event 5, return period T=1 year, volume $16.8mm$, values adopted from Rioned foundation, 2013] by maintaining a water level of 0.1 to $0.3mm$ below ground level. Since the Netherlands is a flat area, the majority of the system will be surcharged in case of a large storm event. The environmental performance is defined as a maximum annual CSO discharge per hectare of $50\,kg\mathrm{COD}\,ha^{-1}$ [Rioned foundation, 2013]. This criterion is translated into a minimal storage capacity which, in general results in a system that is over-dimensioned with regard to the hy-

draulic performance constraints. Therefore, only the influence of settlement on the environmental performance of combined sewer systems is studied.

For the combined sewer system of the Waddendijk area, the influence of settlement on the storage capacity (paragraph 6.1.1) and the pollution potential (paragraph 6.1.2) is analysed. The 58 studied hinge sewers are used to analyse the relation between sags and the frequency of blockages in the sanitary sewers of separate sewer systems (paragraph 6.2).

6.1 Combined sewer systems

Figure 6.1 shows the layout of the sewer system and the settlement rates of the Waddendijk case study area. As discussed previously (chapter 5, paragraph 5.1), sewers from $-1.8m$ below ground level have a pile foundation.

Figure 6.2 exemplifies the future implications of applying sewers with and without a piled foundation by showing the longitudinal profile of the sewer indicated in figure 6.1. As can be seen, sewers located upstream of the manhole with a piled foundation (manhole 1 in figure 6.1 and 6.2) will gradually settle to a level below this manhole. Since these locations are permanently filled, the storage capacity of the system reduces. Furthermore, due to decreasing flow velocities, sediments are likely to deposit, increasing the pollution potential of the system in case of a CSO (combined sewer overflow) event.
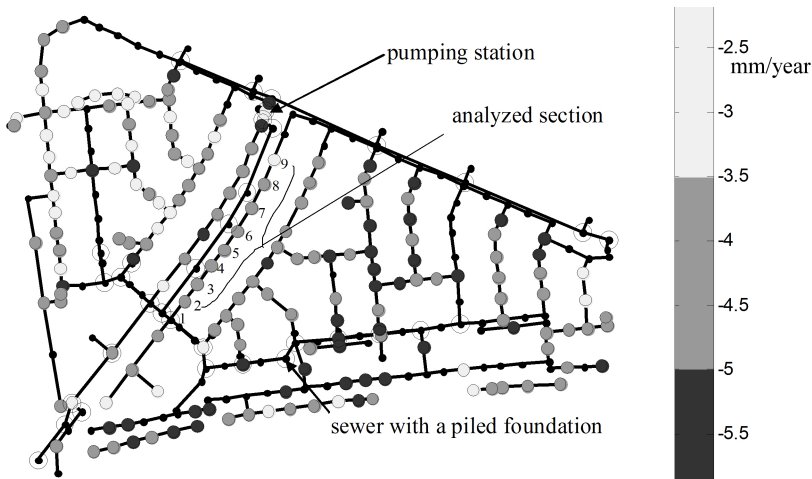
Figure 6.1: Estimated settlement rates in $mm\,year^{-1}$. Manholes are depicted by a dot; the gray scale of the large dots indicates the settlement rate. The small black dots represent manholes for which not enough data was available to give a reliable estimate. Manholes with a piled foundation can be recognized by an larger open circle.

To analyse changes in the functioning of the system due to the development of locations with stagnant water, future sewer invert levels were estimated using the linear model (previously discussed in paragraph 4.2):

$$\hat{z} = a + bt \text{ (see also equation 3.1)} \tag{6.1}$$

with a and b (settlement rate) estimated by the measurement data of a sewer invert. When no reliable estimation could be given (less than 5 measurements), the sewer invert was assumed to settle at the average settlement rate (for this area $4.5\,mm\,year^{-1}$, paragraph 4.2.1). Figure 6.3 shows an example of the measurement data of a sewer invert level and the linear model. It was assumed that the overflow weirs and pumping station do not settle since these are pile supported.

Figure 6.4 shows the estimated future water levels at the location of the manholes. It can be seen that the number of locations with stagnant water and the water depth increases over time. Because the storm water settling tank along the northern side of the area cannot drain by gravity, these manholes are also indicated as locations with stagnant water. For the calculation of the static storage capacity, lost storage and volume of stagnant water (figure 6.5), the volume in the storage tank was not taken into account.
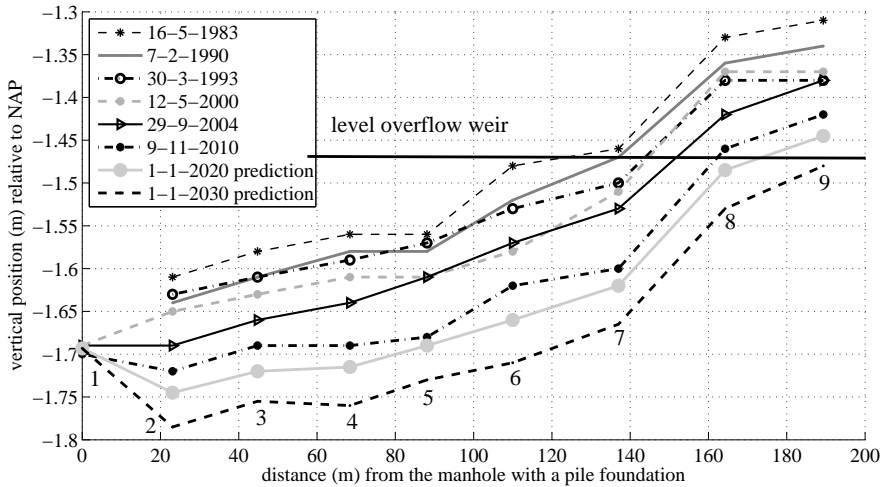
Figure 6.2: Longitudinal profile of sewer invert of the sewer section indicated in figure 6.1.
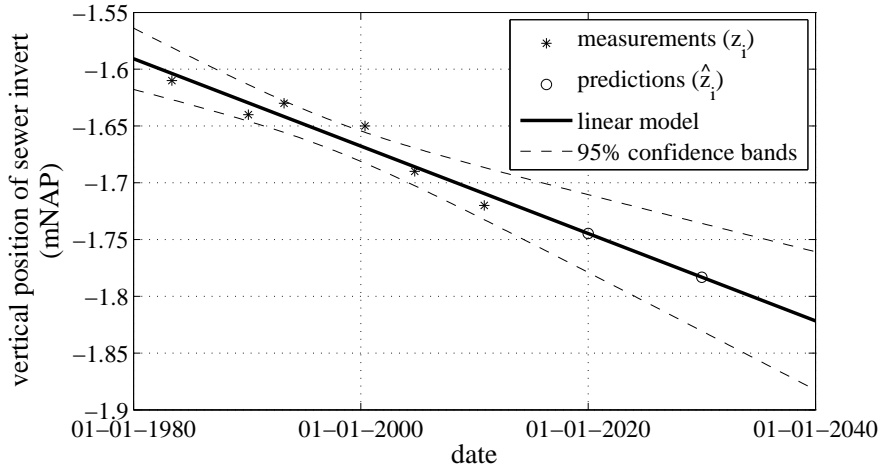
Figure 6.3: Measurement data of an individual sewer invert. The dashed lines indicate the 95% confidence bands for the estimation of y values (solid line).
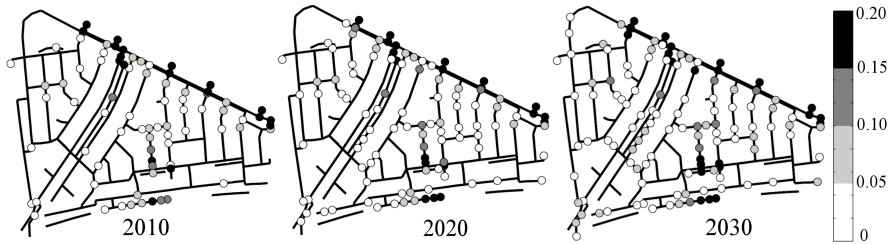
Figure 6.4: Estimated water levels (m).
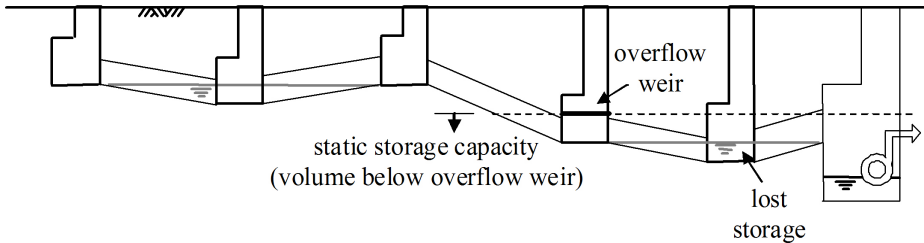
Figure 6.5: Cross-section of a combined sewer system with two locations of stagnant water. As indicated only the locations of stagnant water that are part of the static storage are accounted as lost storage.

6.1.1 Influence of settlement on the storage capacity

To study the influence of settlement on the storage capacity, the static storage was compared to the lost storage for the estimated future sewer invert levels. The static storage capacity was defined as the in-sewer storage below the lowest overflow weir at $-1.47m$NAP. As explained in figure 6.5, the volume of the static storage that can not drain by gravity, is referred to as the lost storage. For the calculation of the volumes it was assumed that the sewers are straight.

The calculated volumes are listed in table 6.1. As can be seen, the lost storage is only a small percentage (1-2%) of the static storage capacity. As expected the lost storage increases. The increase in static storage is nonetheless larger, because in 2010 a large part of the system is situated above the overflow weir (for example manholes 8 and 9, figure 6.2). Therefore, it is concluded that, for this particular sewer system, settlement has a positive influence on the static storage capacity.

To give an indication of the uncertainty of the calculated values presented in table 6.1, the variance of the estimated future invert levels were calculated. The variance for an estimated sewer invert level $\hat{z}_t$ at moment t_j based on historical measurements can be calculated by:

$$Var(\hat{z}_j) = Var(\hat{a}) + (t_j - \bar{t})^2 Var(\hat{b}) \tag{6.2}$$

with

$$Var(\hat{a}) = \frac{s_z^2 \sum_{i=1}^{n} t_i^2}{n \sum_{i=1}^{n} t_i^2 - \left(\sum_{i=1}^{n} t_i\right)^2} \text{ (Rice [2007])} \tag{6.3}$$

and

$$Var(\hat{b}) = \frac{s_z^2}{\sum_{i=1}^{n} (t_i - \bar{t})^2} \text{ (Rice [2007])} \tag{6.4}$$

with $s_z = 0.016\,m$ (paragraph 3.1.2) and n the number of measurements. As appears from the formulae 6.2-6.4, the variance depends on the number and time interval between measurements (by n and $t_i...t_n$), the moment for which the

Table 6.1: Network characteristics.

year	static storage (m^3)	lost storage (m^3)	stagnant water (m^3)
2010	1140.8	15.3	17.3
2020	1190.1	17.6	20.4
2030	1245.7	23.4	27.4

variance is calculated (by t_j) and the error in the measurement (by s_z). Therefore, the variance for the predicted sewer inverts 2 to 9 as shown in figure 6.2 are all equal: $1.3 \cdot 10^{-4} m^2$ for 9-11-2010, $3.2 \cdot 10^{-4} m^2$ for 1-1-2020 and $5.9 \cdot 10^{-4} m^2$ for 1-1-2030. In figure 6.3 the 95% confidence intervals $(1.96\sqrt{Var(\hat{z_j})})$ for estimation of (future) sewer invert levels is indicated.

To calculate the variance for the predicted sewer invert levels of the sewers with a deep foundation (e.g. sewer invert 1 in figure 6.2) it is assumed that these do not settle. Therefore the variance is only dependent on the number of measurements. The variance can be calculated by:

$$Var(\hat{z}) = \left(\frac{s_z}{\sqrt{n}} \right)^2 \tag{6.5}$$

To analyse the influence of the uncertainty of the predicted sewer invert levels on the calculated storage capacity, lost storage and volume of stagnant water Monte Carlo (MC) simulation is used. To apply this method a normal distribution is assumed with the calculated variances. The results after 500 simulations are presented in table 6.2.

When comparing the results of the MC simulation (table 6.2) with the results based on the most likely future invert levels (table 6.1) it stands out that the average volume for the lost storage and stagnant water are larger for the MC simulations. An explanation for this is that due to the application of a random error, the sewer profile becomes bumpier in comparison to the most likely future invert level. Since a downward bend as well as an upward bend will result, in most situations, in stagnant water zones, the volume of stagnant water increases with an increasing number of bends.

It should be noted that the confidence intervals of this analysis are highly dependent on the size and layout of the studied sewer system.

6.1.2 Influence of settlement on the pollution potential

As explained in Gromaire et al. [2001], in-sewer pollutant stocks can be a major source of particles and organic matter during wet weather flows. Since at locations of stagnant water sediments are likely to deposit, the formation of stagnant water

Table 6.2: Results of the MC analysis.

year	average static storage (m^3)	95% CI	average lost storage (m^3)	95% CI	average stagnant water (m^3)	95% CI
2010	1141.0	1.7	16.6	2.0	18.7	2.0
2020	1190.1	1.6	20.1	2.6	23.1	2.6
2030	1245.8	1.7	28.0	3.2	32.4	3.3

zones influences the amount of sediments in the system and consequently the pollution potential in case of a CSO event.

The quality of the sediment in the deposits can vary significantly. In order to estimate the potential impact of the increase in in-sewer pollutant stocks, three situations are taken into account. Local depression is filled with:

- dry weather flow (DWF)

- fresh organic material

- old sewer sludge

For the concentrations of COD (Chemical Oxygen Demand) the values given in Langeveld [2004] (DWF, 0.6 kgCOD m^{-3}) and Ristenpart [1995] (old, 34.96 kgCOD m^{-3}, and fresh organic sludge, 114.7 kgCOD m^{-3}) are used. The results are presented in table 6.3.

It can be seen that the volume of stagnant water, and consequently the sediment built-up, increases considerably. To verify the significance of the additional fouling, the values in table 6.3 are compared with the Dutch regulation for maximum annual CSO discharge per ha ($50\,kg$COD ha^{-1}, for this system $50 \cdot 11 = 550\,kg$COD $year^{-1}$). From this comparison, it is concluded that the increase in COD for the case of old and fresh organic sludge is significant. Because the calculations are based on rough assumptions about the amount and quality of the sediments it can only be concluded that the pollution *potential* is significantly influenced by differential settlement. Whether pollutants accumulate at locations of stagnant water and exit the system via an overflow weir depends on many local factors e.g. the antecedent dry weather period, location of the stagnant water zone, type of storm event, quality of the dry weather flow. Nonetheless the influence of in sewer pollutant stocks on the quality of wet weather flows should not be underestimated [e.g. Gromaire et al., 2001].

6.2 Separate sewer systems - blockage frequency

In Amsterdam all sewers are on average cleaned every 5 years. In half of these instances the sewer is also inspected. Nevertheless, blockages occur frequently in

Table 6.3: Increase in pollution potential.

year	stagnant water (m^3)	DWF (kgCODm^{-3})	old sludge (kgCODm^{-3})	fresh organic (kgCODm^{-3})
2010	17.3	10	600	2000
2020	20.4	12	700	2300
2030	27.4	16	950	3100

the sanitary sewers of Amsterdam. To assess the number of blockages, the number of reactive cleaning activities for each type of system are studied. The results are presented in table 6.4. As can be seen, the majority of the sewer systems in Amsterdam are separate; only the older systems (mainly in the city centre) are combined. Despite their relative young age, separate systems block more often per km sewer.

As concluded based on the analyses of 58 hinge sewers in separate sewer systems, sags develop due to the difference in settlement between manholes with a deep foundation and hinge sewers with a shallow foundation (paragraph 5.3). As previously mentioned in paragraph 5.3, these locations are notorious for its frequent blockage.

When unblocking these hinge sewers with hydraulic jet cleaning lumps of hard yellowish material are often observed. The cleaning personnel suspects that this material originates from fat and oils used for the preparation of food. It is therefore thought that the accumulation of FOG deposits in the sagging hinge sewers contributes for a large part to the blockages in separate sewer systems in Amsterdam.

In literature several studies on the characterization of the chemical and physical properties of FOG deposits can be found. Keener et al. [2008] and Williams et al. [2012], for example, report on the chemical and physical properties of FOG deposits recovered from sanitary sewers. He et al. [2011] studied the FOG formation process by lab experiments. Among other things, a link between FOG properties and water hardness was found. All studies agree on the fact that FOG deposits are the result of a chemical reaction.

Because these studies mainly focus on chemical aspects, hardly any information is given on the location and appearance of FOG deposits in real sewer systems. Some general remarks about the sampling locations are given:

- FOG deposits typically accumulate slightly above the low-flow water mark. [Williams et al., 2012, Keener et al., 2008, Water Research Centre, 2009]

Table 6.4: Frequency of blockage for different types of systems in the city of Amsterdam.

type of sub-system	number of subsystems	km sanitary sewer	km combined sewer	reactive cleaning activities 2006-2010	
				total	$year^{-1} km^{-1}$
combined sewer system	31	12	481	1062	0.45
separate sewer system - sanitary sewer	264	785	<1	2518	0.65
combination of both	16	45	37	199	0.5

- FOG's form a layer in pumping pits [Franke et al., 2011, Williams et al., 2012]

- FOG problem locations are often found downstream of catering establishments [Williams et al., 2012, Keener et al., 2008]

- FOG deposits display an adhesive character and can become securely bound to interior pipe walls [Keener et al., 2008]

To find effective measures for FOG prevention, this study will elaborate further on the occurrence of FOG deposits by studying the location and appearance of FOG deposits in sewers and analysing blockage frequencies.

In the next two paragraphs it is explained how citizen call data and the resulting reactive maintenance activities are used to analyse the blockage frequency of the 58 studied hinge sewers. The sewer invert profile and the maximum filling of these sewers were previously described and studied in paragraph 5.3. Examples of other studies where customer complaints were successfully analysed to assess sewer system performance can be found in ten Veldhuis and Clemens [2011], Jin and Mukherjee [2010] and Arthur et al. [2008].

Recalling from chapter 5, the studied hinge sewers are all sanitary sewers of separate sewer systems, have a diameter of $235mm$ and are made of PVC. As these sewers were mainly selected to study the differential settlement of the sewer pipes, no special attention is given to the location of the hinge sewers relative to catering establishments. Analysis of the neighbourhoods when inspecting the sewers showed that all studied hinge sewers are located in residential areas. Apart from an occasional snack bar no catering establishments were present.

6.2.1 Materials

To analyse the number of blockages, two databases are available in Amsterdam: a customer complaints database and database of all (reactive and proactive) maintenance activities. Archiving call data and maintenance activities started at the end of 2004.

Each entry in the customer complaints database consists of the time and date of the call, a description of the location (in most cases a street address), an indication of the problem by a classification and, for some entries, a description of the problem. Table 6.5 gives some examples of entries from the database of customer complaints.

For the classification of the reported problems, 21 classes are used. Examples are: blocked gully pot, odour, surface water pollution and blocked sewer. Because most inhabitants are not able to discriminate between all types of problems, decision trees are used to establish the most likely type of problem. When an inhabitant complains about water on the street, for example, the simple question: "where is the water located or coming from: a round manhole in the middle of the street or from a gully pot with a small square lid and holes in the side?"

is used to determine whether the complaint is classified as a 'blocked sewer' or 'blocked gully pot'.

The database of maintenance activities also uses classes to give an indication of the type of activity. In total 63 classes are used. This research only includes activities classified as:

- 102-proactive cleaning sanitary sewers,

- 105-clean various sewers,

- 203-clean and inspect sanitary sewers, and

- 303-unblock sanitary sewer

The location of the maintenance activity is also stored in the database. For most activities an address in the direct vicinity of the maintained object is recorded but, when a maintenance activity is the result of a complaint, usually the address of the complaint is copied. For the proactive activities (102 and 203) the name of the sewer system (in most cases the name of the street where the pumping station is located) is used to describe the location. Because it is very likely that for some sewers cleaning was not possible (e.g. manhole inaccessible) one can not establish exactly which sewers in that sewer system were actually cleaned. In table 6.6 some examples of entries from the database of maintenance activities are listed.

Because both databases (customer complaint and maintenance activities) are neither set-up nor maintained for the purpose of assessing the functioning of the sewer system, it is unlikely that it contains all relevant information. Besides, because addresses are used instead of sewer object identification numbers, errors can be made when trying to establish which sewer was referred to.

Additional to the analysis of the maintenance and complaint databases, the videos of the inspection before cleaning are also studied. Although it is not

Table 6.5: Examples of entries from the customer complaints database.

ID	street	no.	date	problem number	notes
14569	Spanderswoud-straat	77	18/12/2007 21:42	21 (blocked sewer)	causing a lot of trouble
4334	Elisabeth Boddaretstraat	10	11/02/2006 13:08	21 (blocked sewer)	sewerage is entering storage unit
8490	Plesmanlaan	14	8/11/2006 09:43	21 (blocked sewer)	
2819	Elisabeth Boddaretstraat		26/10/2005 14:58	20 (blocked gully pot)	location: playground

possible to exactly determine the last moment of cleaning and hence the duration over which the present FOG deposits were built-up, inspection of the uncleaned sewer might give information about the conditions under which FOG deposits are formed.

6.2.2 Methods

To analyse the blockage frequency of the 58 analysed hinge sewers, both databases were examined. Because information provided by sewer inspection and cleaning personnel is probably more reliable, the database of maintenance activities is used as a starting point. The only strategy to relate maintenance activities to the hinge sewers is by comparison of addresses. First step is to find the inspected hinge sewers on a map and register the name of the street. Because a blockage in a hinge sewer can also cause problems further upstream in the sewer system, the street names of the sewers up to $150m$ upstream are also looked up.

Second step is to select all maintenance activities in these streets and, if a reference is made to a call, the relevant information from the customer complaints database is added. Last step is to thoroughly analyse the gathered information and decide for each activity whether it is likely that it had to do with that specific hinge sewer.

Figure 6.6 shows an example of a hinge sewer. This sewer is located in the Elisabeth Boddaretstraat. As can be seen, sewers in the Plesmanlaan also discharge via this hinge sewer. In table 6.7 all maintenance activities and relating customer complaints that might concern this hinge sewer are listed.

Table 6.6: Example of entries from the maintenance activities database.

ID	street	no.	date	classification	id of complaint	notes
61491	Bramzeil	99	29/12 2007	303 (unblock sanitary sewer)	14654	hinge sewer
4221	Waalburger-singel	121	17/11 2004	303 (unblock sanitary sewer)		high water level in manhole
2444	Dijkmans-huizenstraat	143	12/10 2004	105 (clean various sewers)		FOG deposits cleaned twice
110542	Buikslotermeer-plein		28/10 2010	203 (clean and inspect sanitary sewers)		
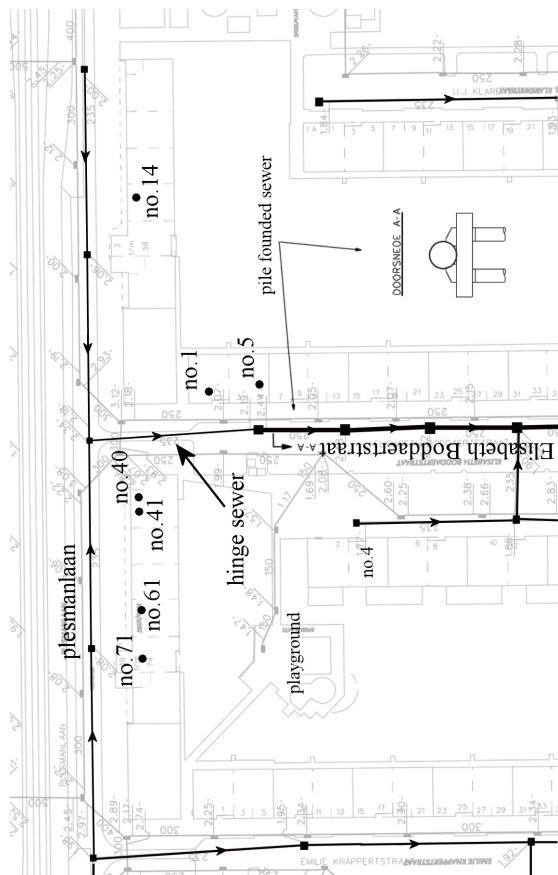
Figure 6.6: Example of a hinge sewer. On the map the addresses of the maintenance activities are indicated.

124

Table 6.7: All entries from the maintenance activities database which might concern the hinge sewer in the Elisabeth Boddaretstraat (figure 6.6).

entry ID	street	no.	date	class	notes	ID of complaint	street	no. problem number	notes
1	7839	E.B.straat	5	18-1-2005	303	next to no.4				
2	8136	Plesmanlaan	40	22-1-2005	303					
3	8137	Plesmanlaan	71	23-1-2005	303	lot of FOG deposits				
4	21938	E.B.straat		26-10-2005	303		2819		20(blocked gully pot)	location: playground
5	41605	Plesmanlaan	14	8-11-2006	303		8490	Plesman-laan 14	21(blocked sewer)	
6	43926	E.B.straat		21-12-2006	303	clean foul sewer, hurry				
7	44433	Ottho Heldringstraat		10-1-2007	102					
8	44920	E.B.straat		23-1-2007	105					
9	73533	E.B.straat	1	10-9-2008	303					
10	73591	Plesmanlaan	41	16-9-2008	303		17969	Plesman-laan 41	21(blocked sewer)	Chris
11	96029	Plesmanlaan	41	15-12-2009	303		24366	Plesman-laan 41	21 (blocked sewer)	
12	97370	Plesmanlaan	61	5-2-2010	303		24876	Plesman-laan 42	21 (blocked sewer)	
13	116160	E.B.straat		1-3-2011	105	additional proactivecleaning. Clean foul sewers from corner Plesmanlaan-E.B.straat until H. Dunantstraat				

After a thorough analysis of the selected activities, 4 entries are excluded. For the first entry in the table the maintenance personnel indicated that the sewer in front of no.4 was cleaned. As shown on the map of figure 6.6, no.4 is on the opposite side of the street closer to a different sewer. For entry 4 the complaint specified that there was a problem at the playground where, according to the map (figure 6.6), only storm sewers are located. Finally, entries 6 and 8 are too vague, it is therefore unclear whether these activities concern this hinge sewer.

Excluding entries 1, 4, 6 and 8, seven activities remain. Looking into the date of these activities, it stands out that the activities listed as entry 2 and 3 took place two days in a row. Therefore it is very likely that the first cleaning activity did not solve the problem adequately. As both activities probably concern the same problem these two activities will be counted as one reactive cleaning activity.

Figure 6.7 shows the cleaning activities on a time line. It can be seen that the interval between blockages is maximum 2 years. In total the sewer was blocked 5 times over the last 7 years. As the time interval between the last cleaning activity and the inspection of the sewer is only half a year it is expected that, at the
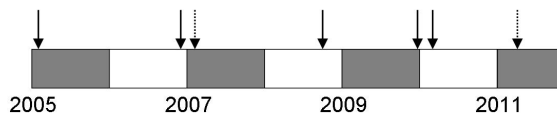
Figure 6.7: Time line of reactive (solid) and proactive maintenance (dashed) activities for the hinge sewer in the Elisabeth Boddaretstraat. At the end of the time line (October 2011) the sewer was inspected for this research.
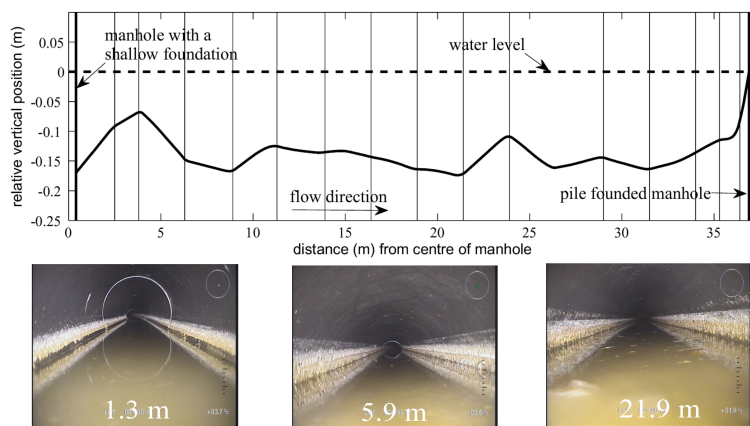
Figure 6.8: Top: sewer invert profile of the hinge sewer in the E.B.straat. Bottom: photographs of the inside of the sewer before cleaning.

moment of inspection in October 2011, the sewer was relatively clean.

Figure 6.8 shows the sewer invert profile along with some photographs of the inside of the sewer before hydraulic cleaning. As expected the sewer is relatively clean. Over the whole length of the sewer FOG deposits are observed at the air-water interface. The degree of filling of this sewer is more or less constant over the length; maximum filling percentage is 74%. The sewer was constructed in 1984 and settled $99mm$. Inspection of the sewer after cleaning did not reveal any structural defects.

6.2.3 Results

Using the method as explained in the previous paragraph, the blockage and cleaning history of all studied hinge sewers was assessed. As the database became in use in November 2004 the number of blockages in almost 6 years time (November 2004 and October 2011) were counted. Figure 6.9 shows the relation between the maximum water level in the hinge sewer (filling) and the number of blockages.

From the results is it clear that there is a relation between the maximum filling and the number of blockages. It can be seen that sewers with a filling less than $90mm$ (40%, diameter $235mm$) block rarely; sewers with a filling percentage of more than 50% are likely to block more often. The reason why not all sewers with high filling percentages block frequently can probably found in differences in discharge behaviour of the customers.

In the figure also the number of proactive cleaning activities are indicated. As the analysed period is 7 years, most sewers were cleaned twice. Some analysed sewers have been cleaned four times as these sewers are located in a sewer system that is known to block frequently. To analyse whether proactive cleaning helps to prevent blockages, figure 6.10 shows the blockages of the analysed hinge sewers in the Buikslotermeerplein sewer system on a time line. In this sewer system 38 hinge sewers were analysed; in total these sewers blocked 32 times.
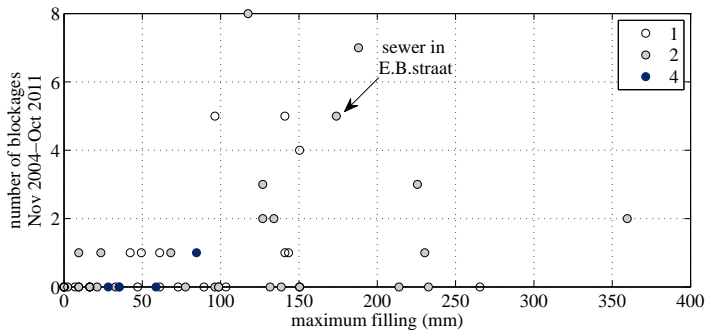
Figure 6.9: Relation between filling and blockage frequency. The gray-scale indicate the number of proactive cleaning activities.

As can be seen, the sewers in the Buikslotermeer sewer system were cleaned proactive in April/May 2005 and were cleaned and inspected at the end of 2010. As the cleaning and inspecting is quite laborious the last action took 4 months to complete: from October 2010 until January 2011. As can be seen in the figure, the blockages occur less frequent when the system is recently cleaned. After the last cleaning action no blockages have been reported for almost a year. It is very likely that when cleaning is combined with inspection, the sewer is cleaned better in comparison to cleaning only.

It was also found that reactive cleaning activities are not always effective. Like the hinge sewer in the Elisabeth Boddaretstraat (discussed in paragraph 6.2.2), for several other hinge sewers it was also found that two or three reactive maintenance activities were reported within a few days. This indicates that problems are most likely not, or not adequately solved the first time. As explained in the previous paragraph, reactive maintenance activities reported within a few days are counted as one blockage.

Analysis of the inspection videos of the hinge sewers before cleaning showed that 8 of the 58 analysed hinge sewers did not show any FOG deposits on the pipe wall. Detailed analysis of these sewers revealed that these sewers were either constructed in 2011 or that via these hinge sewers a limited number of houses (maximum 10) is served. In all other sewers, including other sewers serving a small number of houses, FOG deposits were present. Figure 6.11 shows some examples.
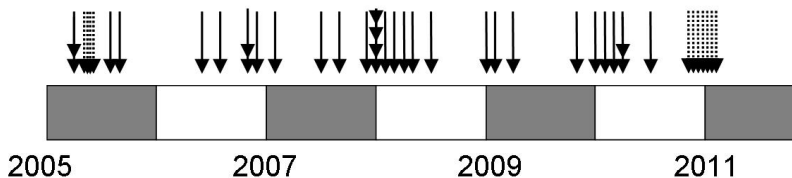
Figure 6.10: Time line of reactive (solid) and proactive maintenance (dashed) activities in the sewer system Buikslotermeerplein. At the end of the time line (October 2011) the sewer was inspected for this research.
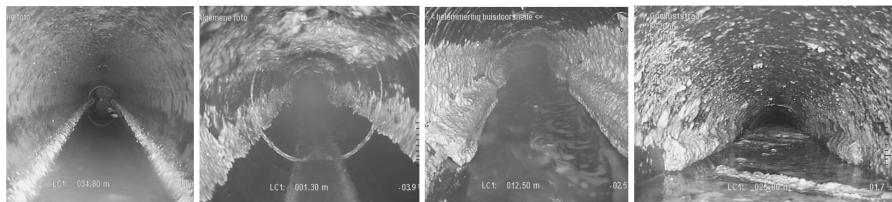
Figure 6.11: Some examples of FOG deposits.

The first photograph on the left shows a sewer with some FOG deposits at the water line. This was a common image at locations with water levels up to a few centimetres. The second photo shows a sewer were the sewage is flowing rapidly. In this situation no FOG deposits are present at the water line. On the soffit of the pipe however, a layer of FOG deposits is present. Most likely these deposits were formed when, probably due to a blockage downstream or pump failure, water levels were higher. From the photo it can be seen that the deposits were formed on two occasions with different water levels: about 50% and 75% of the diameter. It can clearly be seen that FOG deposits are only attached to the surface of the pipe above the water line.

The last two photos show sewers that are almost blocked. In both photos it can be seen that the FOG deposits at the air-water interface vary in thickness along the length of the sewer. This variation is probably caused by the occasionally detachment of deposits. In the fourth photo a bar-shaped piece of FOG deposits is just floating in front of the camera. As FOG deposits are quite rigid, these lumps of FOG deposits can easily get stuck potentially causing complete blockage of the sewer in the near future.

In all cases, the amount of FOG deposits increases with increasing water depth. Figure 6.12 shows the profile of the sewer invert of a sewer with a filling percentage of 100%. Above and below the graph are some photos of the inside of the sewer,
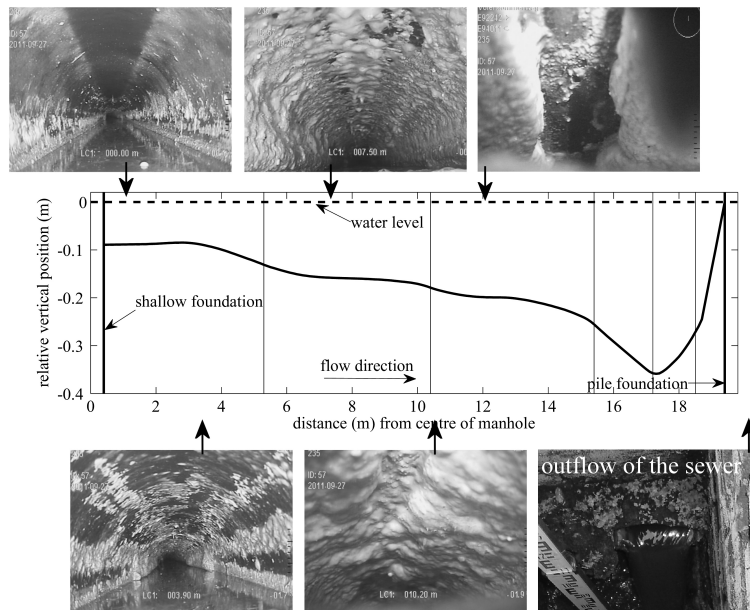
Figure 6.12: Inspection result of a sewer with a filling percentage of 100%. The graph represents the vertical cross section of the sewer.

the arrows indicate the location where the photograph was taken. As can be seen the amount of FOG deposits increases. At low water levels FOG deposits accumulate slightly above the water line (photograph at $3.9m$). At a distance of $7m$ deposits are formed on the soffit of the pipe indicating that the water level was higher for some period of time, most likely caused by a partial blockage down stream.

At the moment of inspection the pipe was not yet fully blocked as can be seen at the outflow of the sewer. By looking from the downstream manhole in the sewer it was established that the downstream part is free of FOG deposits. This phenomenon was also observed at other locations of which figure 6.13 shows two examples.

The first example (the upper two photographs of figure 6.13) shows a concrete sewer that was almost completely blocked as can be seen in the upper left photograph showing the upstream manhole. Inspection of the sewer from a manhole at the downstream end gives the possibility to find out what was blocking the sewer. The result is shown in the upper right photo. In this picture a lump of FOG deposits can be seen. The shape of the lump suggest that it probably consists of bar shaped FOG deposits which are, as indicated previously, sometimes detached from the surface. It can also be seen that downstream of the blockage no FOG deposits are present. Most likely a partial blockage of the pipe functions as a FOG retainer keeping the downstream part clean. The photos at the bottom of figure 6.13 show another example of the same phenomenon.

In addition to FOG deposits, settled deposits were found in 11 of the 58 anal-
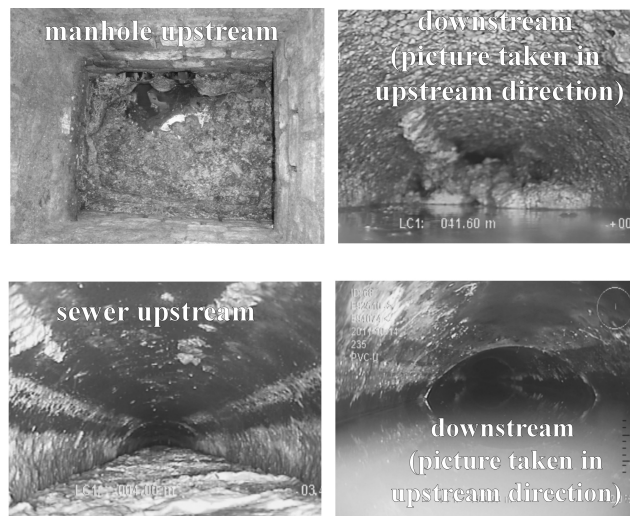
Figure 6.13: Two examples of sewers with a (partial) blockage. Of each sewer there are two photo's: one upstream and one downstream of the blockage.

ysed hinge sewers. As settled deposits are typically present below the waterline, only a significant amount of settled deposits can be detected with a visual inspection. For most of the 11 sewers with settled deposits it was not possible to inspected the complete sewer: as the camera tractor acts as a scraper, deposits are accumulated until the camera is not able to push the pile any further. In figure 6.14 some photographs of such piles are shown.

6.3   Conclusion and recommendations

As shown for the Waddendijk case study area, even a settlement rate of $4 - 5\,mm\,year^{-1}$ can have an considerable impact on the functioning of a combined sewer system. For this system, due to settlement differences between sewers with and without a pile foundation, a significant volume of stagnant water will develop within 20 years time. As shown based in rough assumptions about foul content at these locations with stagnant water, the pollution potential in case of a storm event increases significantly.

To get a better insight in the influence of differential settlement on the performance of combined sewer systems, it would be worthwhile to study the influence of locations with stagnant water on the dynamic process of deposition of sediments during dry weather and the resuspension of sediments in case of a storm event.

For combined sewer systems a different problem arises due to the differential settlement of sewers. By studying the fouling and blockage frequency of 58 sewers with different sags it was found that FOG deposits accumulate at locations with stagnant water and that sewers with sags block more frequently. For PVC sewers with a diameter of $235\,mm$ it was found that sewers with a filling percentage of less than 40% block rarely; sewers with a filling percentage of more than 40% are likely to block more often.

As not all sewers with a high filling percentage were found to block frequently, it is concluded that the blockage frequency is also strongly dependent on other factors, e.g. the discharge behaviour of the customers. As it is neither cost effective nor morally acceptable to monitor every person's discharge behaviour it is unlikely that a sewer manager will be able to predict which sewers are likely
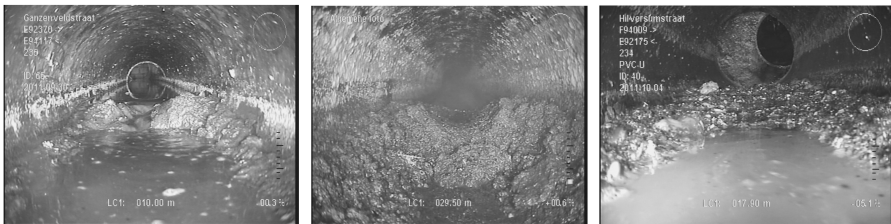
Figure 6.14: Some examples of settled deposits.

to block and which aren't. It is therefore recommended to keep better records of proactive and reactive maintenance activities and use these to study and improve current, mainly reactive, management practices. For proactive management the inspection frequency can be adjusted to the settlement rate (e.g. first inspection after $70\,mm$ of settlement).

Bibliography

Arthur, S., Crow, H., Pedezert, L., 2008. Understanding blockage formation in combined sewer networks. Water Management 161 (4), 215–221.

Dirksen, J., Baars, E., Langeveld, J., Clemens, F., 2012. Settlement as a driver for sewer rehabilitation. Water Science and Technology 66 (7), 1534–1539.

Franke, W., Ettl, M., Roldan, D., Kuhn, G., Langholm, A., Amar, M., 2011. Fat, oil and grease - Sewer contamination prevention strategies and double-dosage concept for fat traps and pressure mains. Water Practice & Technology 6 (2).

Gromaire, M., Garnaud, S., Saad, M., Chebbo, G., 2001. Contribution of different sources to the pollution of wet weather flows in combined sewers. Water Research 35 (2), 521–533.

He, X., Iasmin, M., Dean, L., Lappi, S., Ducoste, J., de los Reyes, F., 2011. Evidence for fat, oil, and grease (FOG) deposit formation mechanisms in sewer lines. Environmental Science & Technology 45, 4385–4391.

Jin, Y., Mukherjee, A., 2010. Modeling blockage failures in sewer systems to support maintenance decision making. Journal of performance of constructed facilities 24 (6), 622–633.

Keener, M., Ducoste, J., Holt, L., 2008. Properties influencing fat, oil and grease deposit formation. Water Environment Research 80 (12), 2241–2246.

Langeveld, J., 2004. Interactions within wastewater systems. Ph.D. thesis, Delft University of Technology.

Rice, J., 2007. Mathematical statistics and data analysis. Brooks/Cole.

Rioned foundation, 2013. Leidraad Riolering (Guidelines for sewers). Rioned foundation.

Ristenpart, E., 1995. Sediment properties and their changes in a sewer. Water Science and Technology 31 (7), 77–83.

ten Veldhuis, J., Clemens, F., 2011. The efficiency of asset management strategies to reduce urban flood risk. Water Science and Technology 64 (6), 1317–1324.

Water Research Centre, 2009. Cp290 Fats, Oils and Grease (FOG). Tech. rep., WRc, London.

Williams, J., Clarkson, C., Mant, C., Drinkwater, A., May, E., 2012. Fat, oil and grease deposits in sewers: Characterization of deposits and formation mechanisms. Water Research 46 (19), 6319–6328.

Chapter 7

Concluding remarks

For efficient and effective sewer asset management knowledge about the interrelation between defects, dysfunctioning and impacts is necessary. In addition to these relations, also a relation exist between defects and the cause of defects. In areas with significant ground settlement the majority of dysfunctions will probably be related to (differential) settlement of sewer pipes.

The objective of this thesis is to assess the potential and accuracy of methods to monitor (differential) settlement and to apply these methods to study the influence of settlement on the functioning of the sewer system (elements). With knowledge of the failure mechanisms related to settlement, decision making for sewer asset management in areas with soft soil conditions can be improved.

7.1 Visual inspection of sewers

Throughout Europe, decisions on sewer rehabilitation and replacement are mainly based on visual inspection reports according to the EN 13508-2. The use of visual sewer inspection as the primary investigation technique, however, has major drawbacks. Analysis of inspector examination results of sewer inspection courses in Austria and the Netherlands, field data from four municipalities in the Netherlands and one municipality in Germany, and the results of repetitive interpretation of the inspection results of the same sewer in France showed that inspection results are poorly reproducible. Therefore, it is very likely that any final decision or result of a deterioration model based on this data source is only tentatively linked to the actual (or future) condition of the inspected sewer pipe. Consequently, sewer management based on visual inspection data only will likely result in ineffective management. To improve the accuracy of visual sewer inspection data, it is recommended to take into account the limitations of using a 'human sensor'.

7.2 Monitoring settlement

Settlement differences can occur at different spatial scales. In this thesis two scales are discriminated: differential settlement on network level and differential settlement of sewer pipes. To analyse settlement on network level, the vertical position of a sewer invert is determined by measuring the position of the manhole cover using a levelling instrument and the distance between cover and sewer invert using a rod. Analysis of time series of historical measurements of 150 sewer inverts in the Waddendijk case study area in Amsterdam revealed that the error in the determination of the sewer invert level is $s_z = 0.016\,m$.

Based on the digital available sewer invert measurements, average settlement rates for the neighbourhoods in Amsterdam were calculated. It was found that settlements rates vary from $0 - 10\,mm\,year^{-1}$. For the Waddendijk case study area, settlement rates were calculated based on all available data (digital measurement files and historical maps). For the majority of sewer inverts 6 measurements were available that were measured over a period of almost 30 years. It was found that a linear model fits the data and therefore can be used to predict future sewer invert levels. For this dataset with a measurement error of $s_z = 0.016\,m$, the resulting 95% confidence interval for the estimation of the settlement rate of a sewer invert equals $\pm 1.4\,mm\,year^{-1}$. To increase the accuracy of the estimation of the settlement rate the measurement period should be increased. Because measurement campaigns lasting over 30 years are necessary to give a reliable estimation for the settlement rate of an individual sewer invert, spacial averaging is recommended. In order to find a suitable scale, semi-variograms can be studied. Additionally, analysis of the geological composition of the subsoil can be used to find areas for which the same average settlement rate can be expected.

As settlement rates are currently not monitored in urban areas, the use of settlement rates for sewer asset management in areas with unstable ground conditions is not expected in the near future. However, with the improvement of the interpretation of (historical) radar images, settlement analyses are expected to require shorter measurement periods and become less elaborate enhancing the availability and use of settlement data.

The electronic tilt meter integrated in a camera tractor is suitable for measuring the vertical profile of a sewer. By measuring the vertical profile of a sewer 5 times from each direction the errors were studied. It was found that the tilt meter has a random error with $s = 0.05\%$. When both wheel pairs are positioned in a different pipe the random error increases to $s = 0.14\%$. Because the system needs to be calibrated manually, the measurement is also subjected to a systematic error with $s = 0.09\%$. Because the random errors are small and cancel out, differences in the slope of pipes can be measured fairly accurate. The determination of the difference in level between either end of a sewer is inaccurate because of the systematic error, therefore improvement of the calibration method is recommended. Since the systematic error is in the same order as the resolution it seems beneficial to improve the resolution to 0.01%.

7.3 Influence of settlement on the functioning of sewer systems

To analyse the movement of sewer pipes relative to each other due to differential settlement, the sewer invert profile of sewers of different materials in a case study area (average settlement rate of $4.5\,mm\,year^{-1}$) was measured. The results showed that, for this area, the relative movement of pipes (age 0-35 years) without a pile foundation was insignificant compared to the imperfections in the sewer invert profiles of newly constructed sewers. Or, in other words, new sewers are as bumpy as older sewers. Also the majority of defects identified by careful analysis of the inspection footage could not be related to settlement (differences).

As settlement differences on pipe level are likely to be larger when average settlement rates are higher, the results might not be representative for areas with higher settlement rates. The analysis of the hinge sewers showed that differences in settlement rates of $\pm 5\,mm\,year^{-1}$ have a significant impact on vertical profile of the sewer as well as the development of defects. Studying sewer invert profiles along with a careful evaluation of inspection footage proved to be an effective method to give a first insight into the occurrence and consequences of settlement differences.

Looking into the influence of settlement on the functioning of sewer systems it was found that the use of sewers with and without a deep foundation results in the development of locations of stagnant water. For combined sewer systems sediments settled at these locations can significantly influence the pollution potential. As the location of stagnant water zones can be predicted, effective measures can be developed (for example cleaning these spots regularly).

For the sanitary sewers of separate sewer systems it was found that sewers with filling degree over 40% are more susceptible to blockages. As not all sewers with a high filling were found to block frequently, it is concluded that the blockage frequency is also strongly dependent on other factors, e.g. the discharge behaviour of the customers. It is therefore recommended to keep better records of proactive and reactive maintenance activities and use these to study and improve current management practices.

7.4 Recommendations

In this thesis the potential and accuracy of methods to study (differential) settlement is assessed. As the methods are only applied to a limited dataset in one area, it is difficult to draw any general conclusions. Nevertheless, the results show that even within an area with a limited settlement rate ($\pm 5\,mm\,year^{-1}$), settlement significantly influences the performance of the sewer system. To further explore the potential of the use settlement information to guide sewer asset management in areas with soft soil conditions, it is recommended to apply the methods to sewer systems in other areas as well.

In order to improve asset management of the sewers in the city of Amsterdam the following actions are advised:

- digital storage of the times series of sewer invert measurements,

- improvement of settlement map by including knowledge of the expected settlement based on the composition of the subsoil,

- when designing a sewer it is recommended to maximize the difference in level between the beginning and end of a hinge sewer,

- inspection and measurement of the sewer invert profile of newly constructed sewers,

- development of an inspection strategy for hinge sewers based on the settlement rate,

- keep better records of proactive and reactive maintenance activities,

- keep records of (used and unused) pile founded sewers,

- use the number and type of reactive maintenance activities as an important input (driving force and performance requirement) in the sewer management process.

Appendices

Appendix A: paper van der Steen et al.

Visual sewer inspection: detail of coding system versus data quality?

A.J. van der Steen[a]; J. Dirksen[ab]; F.H.L.R. Clemens[a]
[a]*Department of Civil Engineering and Geosciences, Delft University of Technology, Delft, the Netherlands* [b]*Waternet, Amsterdam, the Netherlands*

In order to provide information about the decisions on proactive and reactive maintenance, sewers are visually inspected. Previous research showed that quality of visual inspection data is questionable. A coding system prescribes which and how defects should be recorded. This article studies the influence of the coding system on quality of inspection data. A database with the examinations of the Dutch sewer inspector course is studied. Through time, ten photos of the inside of a sewer were evaluated according to two different coding systems: the concise NEN3399:1992 and the more detailed and extensive NEN3399:2004. This article compares both coding systems by evaluating candidate responses to photos showing sewers with clearly visible defects. Results show that added detail in the coding system of 2004 leads to more mistakes. Therefore it can be concluded that the increase in detail does not lead to more information.

Keywords: sewers and drains; inspection; errors; assessment; accuracy

1. Introduction

One of the main techniques to assess the quality and functioning of a sewer system is visual inspection. Visual inspection can support sewer management in deciding on proactive and reactive maintenance and evaluating the quality of the delivered work by contractors [Butler and Davies, 2011]. Because large investments are involved in sewer asset management, it is of importance that the sewer manager can rely on the quality of visual inspection reports. Nevertheless, according to several researchers the quality of the data is questionable [Dirksen et al., 2013].

In order to improve the quality, it is necessary to pinpoint the causes that influence the quality of visual sewer inspection data. The inspection procedure is prescribed by standards. An important element of these standards is the coding system that lists the number and type of aspects that have to be examined. The set-up of the coding system may have influence on the quality of inspection data. Therefore, the question is studied if, and in which manner the coding system has an influence on the quality of inspection data.

To answer this question, a database of 19 years of Dutch sewer inspector examinations is studied. Through time, the same ten photos of the inside of a sewer are evaluated according to two different coding systems: the NEN3399:1992 [NEN 3399:1992, 1992] and the NEN3399:2004 [NEN 3399:2004, 2004]. The NEN3399:1992 is a concise standard and the NEN3399:2004 is a more detailed and extensive standard. The influence of the coding system on the quality of sewer

inspection data is evaluated by comparing for both coding systems the ability of graduated candidates to recognize defects on the photos. Coding system properties that have an influence on the quality are identified by studying significant changes in the percentage of candidates that failed to recognize clearly visible defects.

This paper is a follow-up of the research presented by Korving [2004], Korving and Clemens [2004], Dirksen [2006] and Dirksen et al. [2013]. Whereas for these studies only the examinations were available, for the study presented in this paper it was also possible to analyze the photos used for the examination.

2. Inspection coding systems

The Dutch inspection coding systems which are used in this study are the NEN3399:1992 and its successor: the NEN3399:2004. Both coding systems have a different set-up. The NEN3399:1992 'Sewerage systems outside buildings - Classification system for visual inspection of objects' [NEN 3399:1992, 1992] consists of 18 aspects ordered in 3 main groups A,B and C, respectively leak tightness, stability and flow (gradient). When an aspect is observed, it has to be assigned a classification 1 to 5. The classification describes the nature of presence or gives a quantification. Class 1 refers to an aspect that is hardly or not observable, class 5 means that the aspect is present in its maximum appearance [NEN 3399:1992, 1992]. In practice there is discussion about the recording of class 1 aspects (see appendix). Table 1 lists the possible aspects and codes according to the NEN3399:1992.

Table 1: Inspection coding system NEN3399:1992.

	code	aspect	classification
leak-tight-ness	A1	infiltration of groundwater	1,2,3,4 or 5
	A2	ingress of soil from surrounding ground	1,2,3,4 or 5
	A3	longitudinal displacement	1,2,3,4 or 5
	A4	radial displacement	1,2 and 5
	A5	angular displacement	1 or 5
	A6	intruding sealing ring	1,3 or 5
	A7	intruding sealing material	1,2,3,4 or 5
stability	B1	damage	1 or 5
	B2	surface damage by corrosion or mechanical action	1,2,3,4 or 5
	B3	fissure	1,2,3,4 or 5
	B4	deformation of cross sectional shape	1,2,3,4 or 5
flow (gradient)	C1	intruding connection	1,3 or 5
	C2	root intrusion	1,2,3,4 or 5
	C3	fouling	1,2,3,4 or 5
	C4	encrustation of grease or other deposits (except for sand)	1,2,3,4 or 5
	C5	settled deposits	1,2,3,4 or 5
	C6	other obstacles	1,2,3,4 or 5
	C7	water level	1,2,3,4 or 5

The NEN3399:1992 is withdrawn when the European coding system 'EN 13508-2: 'Investigation and assessment of drain and sewer systems outside buildings-Part 2: Visual inspection coding system' was enacted [EN13508-2, 2003]. This European coding system is developed to enable cross-border competition and data exchange. Therefore, the aspects within the European coding systems were not selected based on a thorough research on what is possible but are merely a summation of all aspects within the existing national coding systems. As a consequence the European coding system therefore became very extensive.

Each country was allowed to decide which aspects from the European coding system they want to apply. The coding and description of these aspects has to be in accordance with the European standard. For the Netherlands, the national implementation of the European standard resulted in the NEN3399:2004 'Sewerage systems outside buildings-Classification system for visual inspection of objects' [NEN 3399:2004, 2004]. The NEN3399:2004 coding system is presented in table 2.

In the EN13508-2 aspects are described by a main code consisting of three letters and one or two characterization(s). Furthermore most aspects require a measured quantification. The first letter of the main code describes the application of the code, for instance B for pipeline or D for manhole inspection. The second letter describes the type of code, there are several groups: A,B,C and D, respectively related to fabric, operation, inventory or other. The third letter of the main code distinguishes between the aspects themselves. The characterization describes the nature of the main defect, it extends the description. For example the code BAA A stands for: 'deformation flexible pipes'; 'vertical' (the height of the pipe has been reduced). The quantification is based on a measurable variable like a length or a cross sectional area reduction. The value has to be recorded. In the NEN3399:2004 this quantification is captured in a classification, a class 1-5 has to be assigned to the aspect.

When table 1 and table 2 are compared it is clear that the NEN3399:2004 contains more aspects than the NEN3399:1992. Furthermore, most aspects are described in more detail by a required characterization resulting in a substantial increase in possible combinations. For instance, in the NEN3399:1992 the aspect other obstacles (C6) only requires a classification (1-5) based on the observed reduction of the cross section of the pipe. According to the NEN3399:2004, the aspect other obstacles (BBE) requires both a characterization (A, B, C, D, E, F, G, H or Z) and a classification (1-5). The possible characterizations for the aspect other obstacles are defined as: brick or masonry unit lying in invert (A), pieces of drain or sewer pipe are lying in the invert (B); another object is lying in the invert (C), protruding through the wall (D), wedged in the joint (E), entering through a connection/junction pipe (F), external pipes or cables built through

Table 2: NEN3399:2004 coding system, inspection from within the pipeline. Codes used in the examination of the course 'Visual inspection of sewers' are printed in bolt [NEN 3399:2004, 2004].

	code	aspect	characterization 1/2	classification
fabric	**BAA**	deformation flexible pipes	A or B	1,2,3,4 or 5
	BAB	fissure	A,B,C or D	1,2,4 or 5
	BAC	break/collapse		1,2,4 or 5
	BAD	defective brickwork or masonry	A or B	1,2,3,4 or 5
	BAE	missing mortar		1,2,3,4 or 5
	BAF	surface damage	A,B,C,D or E	1,2,3,4 or 5
	BAG	intruding connection		1,2 or 3
	BAH	defective connection		1,2,3,4 or 5
	BAI	intruding sealing material	A or Z	A:1,2,3,4 or 5 Z:1,3 or 5
	BAJ	displaced joint	A,B or C	A&B:1,2,3,4 or 5 C:1 or 5
	BAK	lining defect	A,B or C	1,2,3,4 or 5
	BAL	defective repair		1,2,3 or 5
	BAM	weld failure		1,2,3 or 5
	BAN	porous pipe		1 or 5
	BAO	soil visible through defect		1 or 5
	BAP	void visible through defect		1 or 5
operation	**BBA**	roots	A,B or C	1,2,3,4 or 5
	BBB	attached deposits	A,B,C or Z	1,2,3,4 or 5
	BBC	settled deposits	A,B,C or Z	1,2,3,4 or 5
	BBD	ingress of soil	A,B,C,D or Z	1,2,3,4 or 5
	BBE	other obstacles	A to H or Z	1,2,3,4 or 5
	BBF	infiltration		1,2,3,4 or 5
	BBG	exfiltration		1 or 5
	BBH	vermin		1 or 5
inventory	**BCA**	connection	A to H or Z; A or B	
	BCB	local repair	A,B,C,D,E,F or Z	
	BCC	curvature of sewer	A or B; A or B	1 or 5
	BCD	start node	A to F or Z	
	BCE	finish node	A to F or Z	
other	BDA	general photograph		
	BDB	general remark		
	BDC	inspection abandoned	A,B,C or Z	
	BDD	water level		1,2,3,4 or 5
	BDE	flow in incoming pipe	A or B	1 or 5
	BDF	atmosphere within the pipe	A,B,C or Z	
	BDG	loss of vision	A,B,C or Z	

pipeline (G), built into the structure (H) and other (Z).

3. Inspection course examination results

The Dutch centre of expertise in sewer management and urban drainage: 'RIONED'

certifies sewer inspectors. The candidate sewer inspectors have to follow a course which is followed up by an examination. Part of the examination is an assessment of photos according to the Dutch coding system. Each photo shows a sewer in which one or more aspects are present.

Between 1992 and 2012 most candidates assessed the same 10 photos. Because in this period the coding system was changed, it is possible to compare the responses of candidates that used different coding systems. The candidates that used the NEN3399:1992 were able to choose from all eighteen aspects mentioned in the NEN3399:1992 (table 1). For the NEN3399: 2004, a selection of 24 aspects was made by the examiners (table 2, codes printed in bold)

4. Materials and methods

In order to study the influence of a coding system on the quality of visual inspection data, the answers of graduated candidates using both standards are compared. The comparison is based on the ability of the candidates to recognize defects. In order to establish if a defect is present in a sewer, the 'correct' answers as decided by the examiners are used. In accordance with the method used by [Dirksen et al., 2013], two types of errors in the recognition of defects are defined:

- False Negative (FN): a defect is not observed although it is present.

- False Positive (FP): a defect is observed although it is not present.

To analyze the probability of each type of error for both coding systems, a list of eighteen defects is developed (table 3, defect id 1-18). Each defect on the list corresponds to one or more aspect(s) in the NEN3399:1992 and NEN3399:2004. A defect is considered unambiguously present on a photo if and only if the corresponding aspect from the old en new standard is present according to the answers defined by the examiners.

Dirksen et al. [2013] used the same database of examination results for candidates that assessed the photos using the NEN3399:1992. To compare the NEN3399:1992 and NEN3399:2004 exam responses, a couple of different choices are made with respect to the definition of defects. Starting point for this analysis was the conversion table included in the NEN3399:2004. For example, the defect 'fissure' is in this article linked to code B3 1-3 of the NEN3399:1992 instead of B3 1-4. B3 4 is in this article linked to 'break/collapse'.

For the old standard a database with responses of 314 graduated candidates is available. This database is analyzed by Korving [2004], Korving and Clemens [2004] and Dirksen et al. [2013].

For the candidate responses based on the new standard a new database has been constructed. This database contains responses for 178 graduated candidates to the photo assessment part.

For the eighteen defects the average probability of a FP and FN is calculated for both databases. For individual photos, either the probability of a FP or a FN is calculated depending on the presence of a defect. The ten defects only present

in the NEN3399:2004 are also considered (table 3, defect id 19-28). For these ten defects the probability of a FN and FP is calculated too (depending on the presence of a defect).

To assess whether the probabilities of a FN for the old standard (p_{old}) are significantly different from the probability of a FN in the new standard (p_{new}), the two-proportion z-test is used. The null hypothesis H_0: the change in coding system has no influence on the recognition of defects is tested against the alternative hypothesis H_a.

$$H_0 : p_{old} = p_{new} \tag{1}$$

$$H_1 : p_{old} \neq p_{new} \tag{2}$$

To calculate the test statistic z, first the combined probability p is calculated.

$$p = \frac{p_{new} * n_{new} + p_{old} * n_{old}}{n_{new} + n_{old}} \tag{3}$$

$$z = \frac{p_{new} - p_{old}}{\sqrt{p(1-p)(\frac{1}{n_{new}} + \frac{1}{n_{old}})}} \tag{4}$$

With n_{old} and n_{new}, the number of candidates that evaluated the photos according to the respectively the old and the new standard.

For this two-tailed test, the test statistic z is compared with the confidence limits. For the significance level 0.05 the confidence limits are $z = 1.96$ and $z = -1.96$.

Dirksen et al. [2013] analyzed both data gathered in practice and data from sewer inspection courses. By comparing the results for both data sources, it was possible to verify whether the results are consistent. Because the probability of a FP an a FN were in the same order of magnitude for both data sources, it was concluded that experienced sewer inspectors generally do not perform better compared to recently trained inspectors. Therefore it is expected that the findings in this paper apply to a large extent to 'real' inspections as well.

5. Results

Figure 1 presents the probability of a FN and FP for both the old and new standard for the defects listed in table 3. The results in figure 1 are based on the candidate responses to all 10 photos. The results of the two-sample z-test on the probability of a FN for both coding systems are added.

From the figure it can be seen that the probability of a FN is significantly larger than the probability of a FP for both coding systems. This observation corresponds with the results of Dirksen et al. [2013] where it was concluded that the probability of a FN is in the order of 0.25 while the probability of a FP is in the order of 0.04.

Comparing the results for both standards, several defects show a significant increase ($z > |1.96|$) in the probability of a FN. Therefore it can be concluded that

Table 3: List of compared codes.

id	defect name	NEN3399: 1992	photo id	NEN3399: 2004	photo id	photo id considered photos
1	infiltration	A1	1,6,8,9,10	BBF	1,6,8,9,10	1,6,8,9,10
2	ingress of soil	A2	4	BBD	4	4
3	longitudinal displaced joint	A3		BAJ A		
4	radial displaced joint	A4		BAJ B	1,8	
5	angular displaced joint	A5	2,4,5	BAJ C	2,4,5	2,4,5
6	intruding sealing ring	A6		BAI A		
7	intruding sealing material	A7	3,6,7,8	BAI Z	3,5,6,7,8	3,6,7,8
8	mechanical surface damage	B1	1,6	BAF A	1,6	1,6
9	chemical surface damage	B2	2,3,4,7,10	BAF B,C,D,E	2,3,4,7,10	2,3,4,7,10
10	fissure	B3 1-4	1	BAB	1,4	1
11	break/collapse	B3 5	4	BAC	4	
12	intruding connection	C1	1	BAG	1	1
13	roots	C2	9	BBA	9	9
14	attached deposits	C3,C4	3,5	BBB	3,5	3,5
15	settled deposits	C5	1,3,6,7,10	BBC	1,3,6,7,8,10	1,3,6,7,10
16	other obstacles	C6	8,10	BBE	8,10	8,10
17	water level	C7	2,3,4,5,6,7,9	BDD	2,3,4,5,6,7,9	2,3,4,5,6,7,9
18	deformation	B4		BAA		
19	defective brickwork or masonry			BAD		
20	missing mortar			BAE		
21	defective connection			BAH	1,4	1,4
22	lining defect			BAK		
23	defective repair			BAL		
24	weld failure			BAM		
25	porous pipe			BAN		
26	connection			BCA	1,4	1,4
27	local repair			BCB	4	4
28	pipe curvature			BCC		

the introduction of the new standard has an effect on the recognition of defects. To find the explanatory mechanisms behind this effect it is necessary to look in more detail to the responses to individual photos.

Three photos are selected for which the candidate responses to a specific, clearly present defect show a significant change before and after the introduction of a new coding system. With respect to the increased detail and extension of the coding system, several observations are made and discussed.

5.1 More detail, more confusion?

The confusion introduced by the increased detail in description by characterizations is illustrated by the candidate responses to the defect 'other obstacles' in photo 10 (figure 2). The defect 'other obstacles' is both included in the NEN3399:1992 (C6) and NEN3399:2004 (BBE). The probability of a FN for this defect increased from 0.04 to 0.33. Most of the 59 candidates that did not rec-
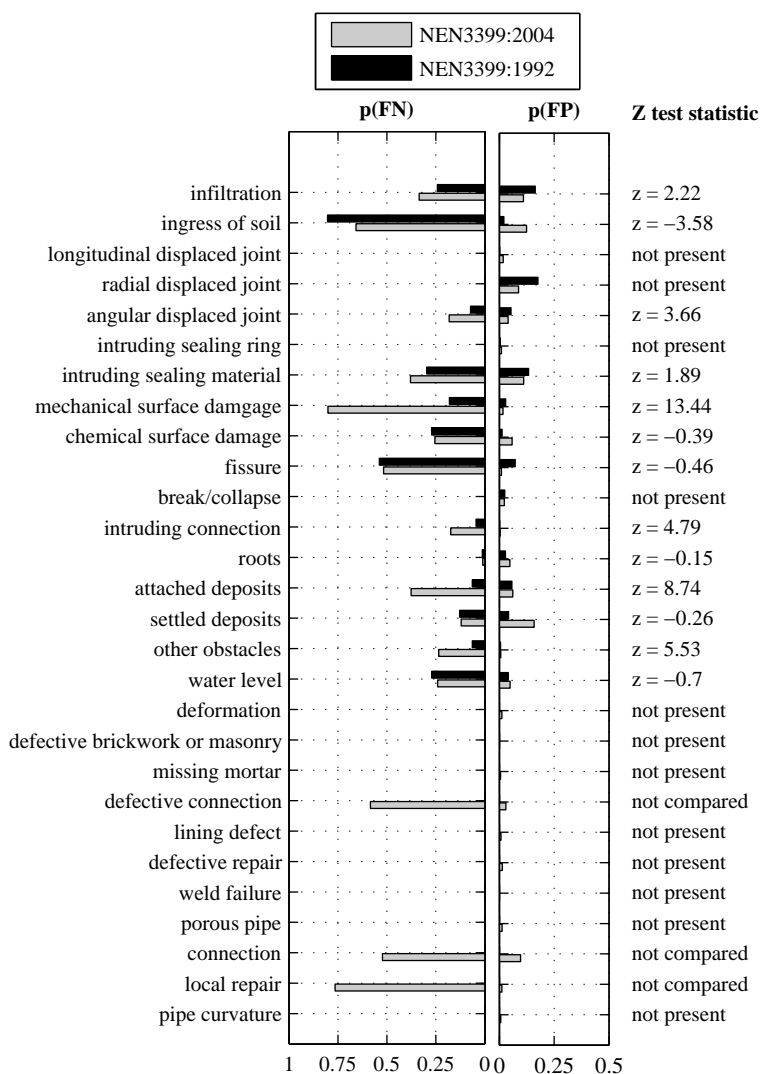
Figure 1: Probability of a False Positive recognition (FP) and a False Negative recognition (FN) derived from the inspector examination results from the visual inspection course using the NEN3399:1992 and the NEN3399:2004 coding system. Also the z-test statistic for the comparison of the p(FN) is indicated.

ognize the aspect 'other obstacles' (BBE) observed the aspect 'settled deposits' (BBC) instead. From these candidates, about half described the aspect 'settled

Intruding connection:
p(FN)old: 0.04
p(FN)new: 0.17
z:4.79

Mechanical surface damage:
p(FN)old: 0.28
p(FN)new: 0.88
z:12.76

Settled deposits:
p(FN)old: 0.01
p(FN)new: 0.06
z:3.04

Attached deposits:
p(FN)old: 0.06
p(FN)new: 0.38
z:8.74

Other obstacles:
p(FN)old: 0.04
p(FN)new: 0.33
z:8.78
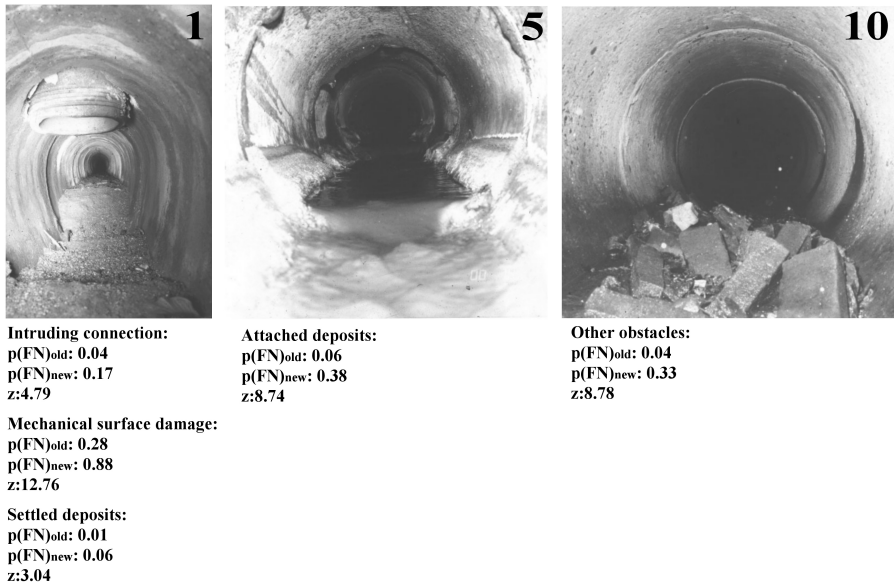
Figure 2: Discussed defects. From left to right, photo id: 1,5 and 10.

deposits' with a characterization 'coarse material' (B). The other half of the candidates described the aspect 'settled deposits' with a characterization 'hard or compacted material' (C). All of these candidates added a classification of 3 or higher (reduction of cross-sectional area by at least 10%) which indicates that these candidates where aiming at describing the defect 'other obstacles'.

This observation shows that probably the characterizations provided with the main defect 'other obstacles' in the new standard are too detailed. Because the characterizations do not perfectly fit with the actual situation, many candidates chose another main defect (BBC) with a more vague description. As described in paragraph 2, the old standard did not include characterizations, therefore the candidate is not mislead to choose a characterization that more or less fits the actual situation but does not belong to the correct aspect.

Another illustration of the confusion caused by the addition of characterizations are the responses to the defect 'attached deposits' present in photo 5 (figure 2). For this defect the probability of a FN increased significant from 0.06 to 0.38. As indicated in table 2, the defect 'attached deposits' refers to 'fouling' (C3) and 'encrustation of grease or other deposits' (C4) in the NEN3399:1992 and to 'attached deposits' (BBB) in the NEN3399:2004. Furthermore, there is a clear increase in the probability of a FP for the defect 'settled deposits'; from 0.06 to 0.43. The defect 'settled deposits' is included in both the NEN3399:1992 (C5) and the NEN3399:2004 (BBC). Analysis of the responses of the candidates revealed that the fast majority of candidates that did not recognize the aspect 'attached

deposits' (BBB) recognized the aspect 'settled deposits' (BBC) instead. Many candidates that chose the aspect 'settled deposits' assigned the characterization 'hard or compacted material' (C) or fine material (A), aiming at describing the visible crust.

Although more or less the same distinction between the defects 'attached' and 'settled deposits' is present in both coding systems, the candidates found it harder to make this distinction using the new coding system. This confusion is probably caused by the characterizations of the aspect 'settled deposits' in the new standard. The interpretation of these characterizations has for many candidates led to the conclusion that the main aspect 'settled deposits' (BBB) is appropriate to describe the visible crust.

5.2 More detail, more information?

In photo 1 the defect 'settled deposits' is clearly visible. Most candidates were able to recognize this defect: for the new standard only 11 candidates of the 178 did not recognize the defect. The candidates that recognized the defect however, did not unambiguously chose for the same characterization: 105 assigned the characterization 'fine' (A) and 54 assigned the characterization 'coarse' (B).

This example shows that for this defect the addition of characterizations did not lead to an increase in information content in sewer inspection reports. Because the distinction between all the different characterizations cannot be made, there is a risk that inspection reports only appear more detailed.

Also the introduction of more main codes to describe the same feature can lead to loss of information. In photo 1 (figure 2), an intruding connection is clearly visible. In the NEN3399:1992 only one aspect could be used to describe a connection (intruding connection: C1) in the NEN3399:2004, this increased to 3: the presence of a connection (BCA), intruding connection (BAG) and defective connection (BAH). For the candidates which evaluated the photo using the NEN3399:1992 the probability of a FN for the defect 'intruding connection' is 0.04 which increased significantly to 0.17 for the NEN3399:2004. Half of the candidates that did not recognize the intruding connection using the NEN3399:2004 described the feature as a defective connection (BAH). Three-quarter of the candidates described the feature as a connection (BAH). These observations show there is a risk that with the introduction of a more aspects describing the same feature, the probability that an aspect is not described correctly increases. Therefore relevant information of the feature is overlooked and not transmitted to the sewer manager.

5.3 Merged aspects, less attention?

In the new standard the aspect '(mechanical) damage' (B1) and 'surface damage' (B2) are merged into one aspect 'surface damage' (BAF). To make the distinction between 'mechanical damage' and 'surface damage' characterizations need to be used. To show the influence of this merge on the responses of the candidates, photo 1 (figure 2) is analyzed in more detail. In this photo the defect 'mechanical

surface damage' refers to the damage to the pipe caused by the installation of the connection. The probability of a FN for the defect 'surface damage' increased significant from 0.28 to 0.88. Furthermore, no increase in the probability of a FP is observed. It can therefore be concluded that the defect 'surface damage' is overlooked when it is merged with the defect 'chemical surface damage' to one main aspect (BAF). This observation shows that candidates have more attention to defects that are clearly distinguished by main codes than defects that are grouped under a main code, distinguished by characterization.

6. Conclusion and discussion

The question if, and in which manner the coding system has an influence on the quality of visual sewer inspection data is studied. Examination results of graduated sewer inspectors are used. The candidate responses to ten photos which are evaluated according to two different coding systems show that the introduction of a more extensive and detailed standard has a negative influence on the recognition of defects. Furthermore, the results show that the probability of a FN is significantly larger than the probability of a FP which corresponds with the results by Dirksen et al. [2013]. Explanatory mechanisms for the difference in recognition for both coding systems are found by studying significant changes in the percentage of candidates that failed to recognize clearly visible defects. According to the results the following causes are found:

- More detail in code description by characterization has led to an increase in candidates that describe a particular feature by an incorrect aspect and characterization.

- More detail in code description by characterization does not necessarily result in additional information about the observed aspect.

- More detail in code description by introducing more main codes to describe a specific feature has led to loss of information.

- Merging different distinct defects into one defect has led to an increase in the probability that an aspect is overlooked.

Although the graduated inspectors are not experienced and only photos of inspection recordings are assessed, the results clearly show that the implementation of a more detailed and extensive coding system influences the recognition of defects negatively. The results are therefore considered relevant for practice, especially in the considerations by developing, adjusting and implementing coding systems.

To improve the quality of visual sewer inspection data it is recommended to:

- avoid doubt: describe the defects very clear and make sure that a defect can only be described by one code. As shown by the results, a comprehensive description of a defect by a main code without any detailed characterization is for the inspector less confusing.

- only use defects, do not add characterizations: the added detail is nullified because the uncertainty of the sewer inspector makes that a characterization cannot be chosen unambiguously.

- use photographs: probably it is more informative to transfer information about the details of a defect by picture than by a pre-defined coding system.

- take into account the limitations of using a 'human sensor': in psychology it is common knowledge that there is a limit to the amount of information that can be transmitted by a human. Miller (1956) for example shows that the limit of our capacity for information processing is 7 plus or minus 2. Therefore, even assuming the best conditions, the number of defects to be recognized should not exceed 9.

The development of automatic evaluation of sewer inspection footage might help to limit the number of errors. However, these algorithms also need training and, as visual sewer inspection data is very unreliable, one should be very careful in selecting training data. Furthermore it is recommended to use other types of information as well to investigate the condition of a sewer.

References

Butler, D., Davies, J., 2011. Urban Drainage, 3rd Edition. Abingdon: Spon Press.

Dirksen, J., 2006. Probabilistic modelling of sewer deterioration. Master's thesis, Delft University of Technology.

Dirksen, J., Clemens, F., Korving, H., Cherqui, F., Le Gauffre, P., Ertl, T., Plihal, H., Müller, K., Snaterse, C., 2013. The consistency of visual sewer inspection data. Structure and Infrastructure Engineering 9 (3), 214–228, first published on: 07 February 2011 (iFirst).

EN13508-2, 2003. Conditions of drain and sewer systems outside buildings - part 2: Visual inspection coding system.

Korving, H., 2004. Probabilistic assessment of the performance of combined sewer systems. Ph.D. thesis, Delft University of Technology.

Korving, H., Clemens, F., 2004. Reliability of coding of visual inspections of sewers. In: Proceedings of the 4th international conference on Sewer Processes and Networks, Funchal, Madeira, Portugal.

Miller, G., 1956. The magical number seven, plus or minus two: some limits on our capacity for information processing. Psychological Review 63 (2), 81–97.

NEN 3399:1992, 1992. Buitenriolering, classificatie systeem bij visuele inspectie van riolen.

NEN 3399:2004, 2004. Buitenriolering, classificatie systeem bij visuele inspectie van riolen.

Appendix B: Analysis of settlement rates for the Amsterdam neighbourhoods.

Table 4: area average settlement rate

number	name	area average settlement rate $mm\,year^{-1}$ ± 95% CI	spatial variance $mm^2\,year^{-2}$ (95% CI)	number of measurements
1	Kantershof	0.4 ± 0.6	12.3 (8.6 - 17.0)	298
2	Den Texbuurt - K5	-0.3 ± 1	<0(<0 - 0)	96
2	Den Texbuurt - K4	-1.1 ± 0.8	7.2 (2.1 - 14.2)	38
3	Frederikspleinbuurt	-0.7 ± 0.6	17.6 (13.2 - 23.1)	157
4	Plantage	-8.8 ± 0.4	2.1 (0.1 - 4.6)	330
5	Kortvoort	-4. ± 0.6	<0 (<0 - 0.7)	92
6	Bijlmermuseum Zuid	-4.2 ± 0.7	4.8 (1.2 - 10.0)	269
7	Bijlmermuseum Noord	-3.7 ± 0.6	2.5 (<0 - 6.6)	48
8	Holendrecht Oost - S10	-2.4 ± 0.8	7.4 (2.9 - 13.7)	115
8	Holendrecht Oost - T10	-6.4 ± 0.6	6.4 (3.1 - 10.7)	180
9	Huntum	-3.5 ± 0.6	1.9 (<0 - 6.3)	69
10	Gaasperdam Noord	-3.2 ± 0.6	3.3 (0.1 - 7.5)	155
11	Gein Zuidoost	-0.7 ± 0.3	2.3 (0.5 - 4.4)	179
12	Leidsebuurt Zuidoost	-4.1 ± 1	<0 (<0 - 7.3)	35
13	Gein Noordwest	-4.2 ± 0.4	0.9 (<0 - 3.6)	33
14	Gein Noordoost - T11	-6.6 ± 0.7	3.0 (<0 - 7.6)	31
14	Gein Noordoost - T12	-2.7 ± 0.3	<0 (<0 - 0)	157
15	E-buurt - P10	-1.5 ± 0.9	7.6 (2.9 - 14.6)	291
15	E-buurt - P9	-3.1 ± 0.8	2.1 (<0 - 8.2)	167
16	Werengouw Zuid - E9	-7.7 ± 0.6	2.5 (<0 - 6.5)	57
16	Werengouw Zuid - F9	-7 ± 0.6	5.8 (2.5 - 10)	234
17	K-buurt Zuidoost	-5.4 ± 0.9	14.3 (8.1 - 23)	545
18	Gein Zuidwest	-1 ± 0.6	<0 (<0 - 4.0)	83
19	Weesperbuurt	-4.8 ± 0.9	6.8 (1.4 - 14.5)	78
20	L-buurt	-8 ± 0.7	13.2 (8.5 - 19.5)	38
21	Sarphatistrook	-5 ± 0.6	11.1 (7.9 - 15.5)	340
22	Reigersbos Zuid	-3.4 ± 0.4	2.4 (0.2 - 4.9)	166
23	Reigersbos Midden	-4.4 ± 0.8	8.6 (4.0 - 15.1)	654
24	Venserpolder West	-4 ± 0.6	8.0 (4.5 - 12.7)	117
25	Holendrecht West	-6.3 ± 0.5	6.7 (3.8 - 10.3)	101
26	Hakfort/Huigenbos	-7.2 ± 0.7	7.7 (3.6 - 13.2)	55
27	Reigersbos Noord - U10	-5 ± 0.7	1.2 (<0 - 5.6)	244
27	Reigersbos Noord - T9	-4.7 ± 0.7	10.1 (5.6 - 16.3)	300
28	D-buurt - P10	-2.7 ± 0.6	13.7 (9.6 - 19.0)	31
28	D-buurt - P9	-0.7 ± 0.9	8.0 (2.9 - 15.7)	138
29	Bijlmerpark Oost	-5.6 ± 0.7	<0 (<0 - <0)	140
30	G-buurt Oost - P11	-3.4 ± 0.4	1.3 (<0 - 4.0)	45
30	G-buurt Oost - P10	-1.9 ± 0.5	2.7 (0.1 - 6.1)	110
31	Leidsebuurt Noordoost	-3.7 ± 0.8	<0 (<0 - <0)	47
32	Waterloopleinbuurt	-1.9 ± 0.7	10.7 (5.9 - 17.0)	144
33	Gaasperdam Zuid	-6.2 ± 0.6	0.1 (<0 - 4.3)	62
34	Venserpolder Oost - Q8	-3.1 ± 0.8	<0 (<0 - 3.8)	42
34	Venserpolder Oost - P8	-3.5 ± 0.6	2.8 (<0 - 6.6)	232
35	Kelbergen	-0.3 ± 0.3	-9.3 (<0 - <0)	181
36	Markengouw Midden - D9	-5.3 ± 0.5	6.5 (3.4 - 10.4)	161
36	Markengouw Midden - E9	-5 ± 0.3	4.0 (2.3 - 5.9)	38
37	Lastage	-1.4 ± 0.8	<0 (<0 - 3.0)	403
38	Markengouw Noord	-8.1 ± 0.8	2.4 (<0 - 8.5)	140
39	Banne Noordoost - B6	-5.3 ± 0.6	<0 (<0 - <0)	226
39	Banne Noordoost - B7	-5.3 ± 0.6	<0 (<0 - 1.7)	50
39	Banne Noordoost - C7	-3.9 ± 0.7	11.7 (7.2 - 17.7)	378
40	Sloterdijk I	-5.1 ± 0.8	4.4 (0.7 - 9.8)	74
41	Kadijken	-4.7 ± 1	<0 (<0 - <0)	191
42	Marine-Etablissement	-7.7 ± 1	8.4 (2.0 - 17.7)	144
43	Oostenburg	-2.3 ± 1	-6.5 (<0 - 0.8)	31
44	Wittenburg	-10.3 ± 0.9	4.9 (<0 - 13.0)	191
45	Tuindorp Nieuwendam Oost - F8	-3.2 ± 0.5	2.0 (<0 - 5.0)	377
45	Tuindorp Nieuwendam Oost - E8	-4.4 ± 0.3	<0 (<0 - <0)	251
46	Buikslotermeerpleinbuurt - D8	-2.7 ± 0.8	10.6 (5.8 - 17.3)	97
46	Buikslotermeerpleinbuurt - E8	-1.1 ± 0.4	<0 (<0 - <0)	40
46	Buikslotermeerpleinbuurt - E7	-6.1 ± 0.6	<0 (<0 - 2.0)	304
47	Kattenburg	-6.9 ± 0.5	0.6 (<0 - 4.4)	258
48	Banne Noordwest - D8	-2.1 ± 1	3.4 (<0 - 10.9)	78
48	Banne Noordwest - C8	-6.4 ± 0.5	0.5 (<0 - 3.7)	60
49	Markengouw Zuid	-7.7 ± 0.6	12.1 (8.3 - 16.7)	74
50	Amerikahaven	-2.9 ± 0.7	0.6 (<0 - 5.5)	70
51	Rapenburg	-3.8 ± 0.8	13.1 (8.6 - 19.4)	255
52	Tuindorp Nieuwendam West	-3.5 ± 0.5	<0 (<0 - <0)	56
53	Burgwallen Oost	-4.5 ± 0.8	<0 (<0 - 2.0)	140
54	Schellingwoude Oost	-1.8 ± 0.8	1.9 (<0 - 7.9)	74
55	Kop Zeedijk	0.9 ± 0.9	<0 (<0 - 3.8)	229
56	Amsterdamse Poort - R8	-2.8 ± 0.8	0.8 (<0 - 5.9)	213
56	Amsterdamse Poort - R9	-3.4 ± 0.6	<0 (<0 - <0)	33

57	Hoptille	-5.5 ± 0.6	<0 (<0 - <0)	317
58	Nieuwendammerdijk West	-7.3 ± 1	<0 (<0 - <0)	1017
59	Van der Pekbuurt - F5	-4.8 ± 0.8	<0 (<0 - 4.3)	32
59	Van der Pekbuurt - E6	-2.6 ± 1	6.8 (0.1 - 16.4)	36
59	Van der Pekbuurt - F6	-4.9 ± 0.7	<0 (<0 - 0.7)	40
60	Rode Kruisbuurt	-4.2 ± 0.5	<0 (<0 - <0)	46
61	Werengouw Noord	-4 ± 0.6	<0 (<0 - 1.6)	37
62	Tuindorp Oostzaan West - B3	-4.3 ± 0.7	2.0 (<0 - 7.4)	66
62	Tuindorp Oostzaan West - A3/B4	-5 ± 0.8	17.4 (10.8 - 26.1)	107
63	Banne Zuidoos - C6t	-2.9 ± 0.4	2.4 (0.4 - 4.9)	107
63	Banne Zuidoost - D6	-5.6 ± 0.8	<0 (<0 - 5.9)	61
64	Terrasdorp	-5.3 ± 1	13.7 (7.8 - 22.6)	57
65	Groenmarktkadebuurt	-3.9 ± 0.6	0.3 (<0 - 3.3)	140
66	Anjeliersbuurt	-5.8 ± 0.8	<0 (<0 - 3.2)	226
67	Elandsgrachtbuurt	-5.7 ± 0.8	3.1 (0.1 - 8.3)	344
68	Tuindorp Oostzaan Oost	-1.2 ± 0.4	<0 (<0 - <0)	183
69	Blauwe Zand	-6.1 ± 0.5	<0 (<0 - <0)	65
70	Dorp Driemond	-0.4 ± 0.5	0.3 (<0 - 3.1)	56
71	Bloembuurt Zuid	-5.4 ± 0.8	16.6 (10.0 - 25.2)	31
72	Bloemenbuurt Noord	-4.3 ± 0.5	<0 (<0 - 0.1)	184
73	Nieuwendam Noordwest Noord - D8	-1.7 ± 0.6	1.6 (<0 - 5.2)	111
73	Nieuwendam Noordwest Noord - C8	-5 ± 0.8	1.2 (<0 - 7.1)	191
74	Loenermark	0.9 ± 0.6	11.1 (7.3 - 16.2)	123
75	IJplein e.o.	-3.6 ± 0.6	<0 (<0 - 4.0)	75
76	Papaverweg e.o.	-6.2 ± 1	<0 (<0 - 6.4)	83
76	Papaverweg e.o.	-4.7 ± 0.7	<0 (<0 - 4.9)	33
77	Amstel III deel C/D Noord - S7	-1.6 ± 0.8	1.2 (<0 - 6.2)	82
77	Amstel III deel C/D Noord - S8	-3.3 ± 0.5	4.5 (2.1 - 7.5)	127
78	Amstel III deel C/D Zuid	-3.2 ± 0.9	10.0 (4.8 - 17.7)	74
79	Amstel III deel A/B Zuid	-2.2 ± 0.8	11.7 (6.8 - 18.4)	51
80	Amstel III deel A/B Noord	-3.3 ± 0.5	6.7 (3.9 - 10.3)	133
81	Marnixbuurt Midden	-4.9 ± 0.8	<0 (<0 - 4.0)	92
82	Bloemgrachtbuurt	-5.3 ± 0.6	0.3 (<0 - 3.5)	137
83	Zaagpoortbuurt	-7.4 ± 0.8	1.8 (<0 - 6.7)	57
84	De Bongerd	-0.3 ± 0.6	<0 (<0 - <0)	98
85	Sloterdijk III West	-9.4 ± 0.4	12.9 (10.1 - 16.2)	66
86	Frederik Hendrikbuurt Noord	-5.1 ± 0.6	3.3 (1.1 - 6.4)	58
87	Kermisterrein	-9.5 ± 0.7	0.2 (<0 - 4.0)	334
88	Bedrijvencentrum Westerpark	-5.2 ± 1	0.3 (<0 - 6.7)	304
89	Buyskade e.o.	-4.9 ± 1	2.9 (<0 - 9.5)	178
90	Staatsliedenbuurt Noordoost	-4.9 ± 0.9	6.7 (1.8 - 14.1)	163
91	Spaarndammerbuurt Noordwest	-3.9 ± 0.6	2.1 (<0 - 6.4)	275
92	Spaarndammerbuurt Midden	-5.2 ± 0.6	<0 (<0 - 1.4)	238
93	Spaarndammerbuurt Zuidwest	-3.8 ± 1	1.4 (<0 - 8.5)	314
94	Kolenkitbuurt Zuid - G1	-4.4 ± 0.3	<0 (<0 - 0.3)	122
94	Kolenkitbuurt Zuid - H1	-4.6 ± 0.7	<0 (<0 - 1.2)	39
95	Erasmusparkbuurt West - G1	-2 ± 0.5	0.3 (<0 - 2.2)	831
95	Erasmusparkbuurt West - G2	-2.9 ± 0.6	0.4 (<0 - 2.7)	40
95	Erasmusparkbuurt West - H1	-3.3 ± 0.6	<0 (<0 - 2.4)	38
96	Poolbuurt Oost	-3.8 ± 0.4	0.7 (<0 - 2.2)	88
97	Landlust Zuid - H2	-5.3 ± 0.4	0.5 (<0 - 1.6)	358
97	Landlust Zuid - H2	-5.6 ± 0.5	0.2 (<0 - 2.4)	616
97	Landlust Zuid - G2	-5.3 ± 0.9	11.5 (6.2 - 19.1)	78
98	Bosleeuw - G2	-2.1 ± 0.6	<0 (<0 - 2.3)	253
98	Bosleeuw - F1	-6.2 ± 1	3 (<0 - 10.0)	65
99	Bedrijventerrein Landlust - G2	-2 ± 0.4	0.4 (<0 - 2.5)	176
99	Bedrijventerrein Landlust - F2	-5 ± 0.6	5.1 (2.2 - 9.0)	374
100	Landlust Noord - F2	-4 ± 0.8	5.4 (1.8 - 10.7)	67
100	Landlust Noord - F1	-3.9 ± 0.6	3.6 (1.0 - 7.1)	104
101	Sloterdijk	-3.3 ± 0.6	4.3 (1.4 - 8.4)	36
102	Bedrijvencentrum Osdorp	-1.3 ± 0.9	9.1 (3.8 - 16.7)	47
103	Osdorp Midden Noord - JJ4	-1.8 ± 0.6	1.9 (<0 - 6.2)	158
103	Osdorp Midden Noord - KK4	-3.8 ± 0.5	8.3 (5.2 - 12.2)	76
104	Osdorp Midden Zuid	-4.8 ± 0.4	5.4 (2.9 - 8.4)	397
105	Meer en Oever - JJ3	-1.6 ± 0.7	6.6 (3.0 - 11.6)	178
105	Meer en Oever - KK3	0.6 ± 0.6	3 (<0 - 6.9)	572
106	Osdorpplein e.o.	-2.3 ± 0.3	4.9 (3.0 - 7.1)	800
107	Osdorp Zuidoost - KK2	-0.3 ± 0.7	2.8 (<0 - 7.7)	49
107	Osdorp Zuidoost - LL2	-1.8 ± 0.6	8.4 (4.9 - 13.0)	98
108	Calandlaan/Lelylaan	-1.1 ± 0.8	4.8 (0.7 - 10.8)	93
109	Ookmeer	-3.3 ± 0.6	0.5 (<0 - 4.2)	115
110	Paramariboplein e.o. - J2	-5 ± 0.3	<0 (<0 0.1)	57
110	Paramariboplein e.o. - K2	-7.5 ± 0.5	3.2 (1.6 - 5.6)	95
111	Postjeskade e.o.- J2	-3.8 ± 0.6	1.1 (<0 - 3.3)	46
111	Postjeskade e.o. - K2	-6.4 ± 0.4	3.1 (0.7 - 6.0)	51
112	Columbusplein e.o.	-6 ± 0.1	<0 (<0 - 0.1)	46
113	Balboaplein e.o. - H2	-5.3 ± 0.5	0.6 (<0 - 2.1)	67
113	Balboaplein e.o. - J2	-7.2 ± 0.3	1 (0.3 - 2.0)	101
113	Balboaplein e.o. - H2	-5.7 ± 0.9	1.3 (<0 - 6.1)	108
114	Orteliusbuurt Midden	-8.4 ± 0.6	2.2 (0.8 - 4.8)	122
115	Orteliusbuurt Zuid	-5.6 ± 0.7	<0 (<0 - 3.3)	64
116	Orteliusbuurt Noord	-3.7 ± 0.6	1.7 (0.1 - 4.3)	77
117	John Franklinbuurt - H2	-5.3 ± 0.3	0 (<0 - 0.8)	132
117	John Franklinbuurt - H2	-4.6 ± 0.8	1.2 (<0 - 5.6)	132
118	Jan Maijenbuurt	-6 ± 0.4	1.2 (0.1 - 2.7)	32
119	Geuzenhofbuurt	-4.8 ± 0.2	0.1 (<0 - 0.6)	225
120	Trompbuurt - H2	-5 ± 0.2	<0 (<0 - 0.4)	281
120	Trompbuurt - H2	-5.3 ± 0.5	0.1 (<0 - 2.2)	147

153

121	Filips van Almondekwartier - H2	-5.4 ± 0.5	0.8 (<0 - 2.7)	83
121	Filips van Almondekwartier - J2	-6.5 ± 0.6	0.6 (<0 - 3.0)	553
122	Kortenaerkwartier	-6.6 ± 0.4	<0 (<0 - 0.8)	237
123	De Wester Quartier	-6.6 ± 0.3	0.6 (0 - 1.5)	242
124	Pieter van der Doesbuurt	-5.3 ± 0.4	0.6 (0.1 - 1.3)	470
125	Osdorper Binnenpolder	-2.8 ± 0.7	<0 (<0 - <0)	182
126	Buurt 10	-3.1 ± 0.8	<0 (<0 - 1.8)	44
127	Buurt 8	-0.9 ± 0.5	11.7 (8.9 - 15.1)	110
128	Buurt 7 - GG3	-2.3 ± 0.7	4.4 (0.8 - 9.7)	70
128	Buurt 7 - GG4	-0.9 ± 0.4	<0 (<0 - 2.3)	90
129	Buurt 6	-2.9 ± 0.7	11.2 (7.0 - 17.0)	39
130	Buurt 9 - GG3	-2.1 ± 0.3	4.5 (2.6 - 6.7)	36
130	Buurt 9 - GG4	1.6 ± 0.8	1 (<0 - 6.6)	37
130	Buurt 9 - FF3	-2.8 ± 0.5	<0 (<0 - 0.6)	62
130	Buurt 9 -FF4	0.1 ± 0.7	<0 (<0 - <0)	617
131	Slotermeer Zuid - GG1	-3.3 ± 0.9	15 (9.1 - 23.6)	46
131	Slotermeer Zuid - HH1	-1.2 ± 0.5	6.3 (3.6 - 9.6)	251
131	Slotermeer Zuid - HH2	-2.3 ± 0.8	<0 (<0 - 3.5)	271
132	Sloterpark - JJ3	-3.2 ± 1	<0 (<0 - 3.2)	49
132	Sloterpark - HH2	0.3 ± 0.9	2.9 (<0 - 9.7)	188
133	Buurt 5 Zuid	-3.6 ± 0.3	7.1 (5.1 - 9.4)	250
134	Buurt 4 Oost	-4.1 ± 0.8	2.7 (<0 - 8.6)	92
135	Noordoever Sloterplas - HH1	-2.1 ± 0.4	4.5 (2.1 - 7.3)	336
135	Noordoever Sloterplas - HH2	-1.7 ± 0.9	16.7 (10.3 - 25.9)	220
136	Buurt 3 - GG1	-4.1 ± 0.3	5.3 (3.5 - 7.5)	108
136	Buurt 3 - FF2	-3.7 ± 0.6	<0 (<0 - 2.2)	262
137	Buurt 2	-3.1 ± 0.4	<0 (<0 - 0.5)	238
138	Cremerbuurt West	0.1 ± 0.7	0.3 (<0 - 4.0)	98
139	Bellamybuurt Zuid - J2	-3.5 ± 0.9	2.3 (<0 - 8.2)	37
139	Bellamybuurt Zuid - J2	-2 ± 0.8	2.6 (<0 - 7.2)	46
140	Da Costabuurt Noord	-3.1 ± 0.6	4.0 (1.7 - 7.3)	33
141	WG-terrein	-2.4 ± 0.7	2.6 (<0 - 6.8)	103
141	WG-terrein	-3.5 ± 0.8	<0 (<0 - 3.9)	45
142	Helmersbuurt Oost	-3.6 ± 1	0.3 (<0 - 6.3)	237
143	Willemsparkbuurt Noord	-1.4 ± 0.5	1.4 (<0 - 4.0)	103
144	Valeriusbuurt West	-2.8 ± 0.7	5.8 (2.6 - 10.7)	356
145	Westlandgrachtbuurt	-4.4 ± 0.5	8 (4.6 - 12.0)	63
146	Legmeerpleinbuurt	-7.5 ± 0.7	1.5 (<0 - 7.1)	113
147	Aalsmeerwegbuurt West	-3.9 ± 0.6	6.1 (1.9 - 11.4)	159
148	Diepenbrockbuurt - M4	-2.6 ± 0.4	0.1 (<0 - 1.8)	185
148	Diepenbrockbuurt - M3	-1 ± 0.5	1.9 (0.4 - 4.2)	329
149	Minervabuurt Midden	-9.2 ± 0.5	<0 (<0 - 1.2)	45
150	Hiltonbuurt	-6.3 ± 0.7	7.7 (4.3 - 12.5)	43
151	Minervabuurt Noord - L3	-6 ± 0.7	6.8 (3.6 - 11.4)	81
151	Minervabuurt Noord - M3	-7.7 ± 0.9	<0 (<0 - 4.8)	54
152	IJsbaanpad e.o. - N2	-4.6 ± 0.4	0.6 (<0 - 2.5)	229
152	IJsbaanpad e.o. - N1	-4 ± 1	7 (3.2 - 13.8)	59
153	Marathonbuurt West	-6.3 ± 0.5	4 (1.5 - 7.3)	37
154	Marathonbuurt Oost - L2	-5.9 ± 1	1.7 (<0 - 8.0)	31
154	Marathonbuurt Oost - M2	-6 ± 0.7	6.6 (3.1 - 11.3)	48
155	Van Tuyllbuurt - M2	-1.8 ± 0.2	2.7(1.3 - 4)	74
155	Van Tuyllbuurt - M2	-1.8 ± 0.9	2.2 (<0 - 7.1)	48
156	Burgemeester Tellegenbuurt Oost	-2.8 ± 0.8	<0 (<0 - 4.0)	41
157	Diamantbuurt	-4.1 ± 0.6	<0 (<0 - 4.2)	51
158	Van der Helstpleinbuurt	-4.4 ± 0.7	4.8 (1.0 - 10.1)	84
159	Willibrordusbuurt	-6.4 ± 0.6	0.5 (<0 - 4.3)	33
160	Cornelis Troostbuurt	-0.5 ± 0.8	0.8 (<0 - 6.4)	84
161	Lizzy Ansinghbuurt	-1.6 ± 0.6	0.6 (<0 - 4.2)	53
162	Harmoniehofbuurt	-4.6 ± 0.9	5.4 (1.0 - 12.1)	727
163	Hondecoeterbuurt	-9.9 ± 0.6	0.4 (<0 - 3.8)	109
164	Banpleinbuurt	-8.6 ± 0.8	3.1 (<0 - 8.2)	46
165	P.C. Hooftbuurt	-1.3 ± 0.8	0.6 (<0 - 6.8)	117
166	Hemonybuurt	-7.3 ± 1	9.2 (3.7 - 17.8)	116
167	Hercules Seghersbuurt	-3.6 ± 0.9	4.9 (0.5 - 11.7)	147
168	Sarphatiparkbuurt	-3.4 ± 0.8	<0 (<0 - 4.7)	37
169	IJselbuurt West	-3.5 ± 0.5	2.3 (<0 - 5.4)	61
170	IJselbuurt Oost - M6	-6.6 ± 0.8	5.7 (1.5 - 11.9)	52
170	IJselbuurt Oost - M5	-4.2 ± 0.4	1.9 (<0 - 4.8)	44
171	Veluwebuurt - N4	-2.7 ± 0.4	1.7 (0.4 - 3.5)	39
171	Veluwebuurt - N5	-4 ± 0.5	2.0 (<0 - 5.4)	102
172	Rai	-3.3 ± 0.6	1.9 (0.1 - 4.6)	38
173	Scheldebuurt West - N4	-3.5 ± 0.5	1.3 (<0 - 3.4)	32
173	Scheldebuurt West - M4 zuid	-3.3 ± 0.4	0.7 (<0 - 2.1)	49
173	Scheldebuurt West - M4 noord	-4.4 ± 0.9	2.4 (<0 - 9.2)	161
174	Scheldebuurt Oost	-4 ± 0.5	4.8 (2.3 - 8.1)	126
175	Gelderlandpleinbuurt	0.1 ± 0.3	4.5 (2.2 - 7.1)	70
176	VU-kwartier	1.2 ± 0.9	6.8 (1.0 - 15.2)	58
177	Buitenveldert Midden Zuid	-0.6 ± 0.3	8.6 (6.3 - 11.0)	295
178	Buitenveldert West Midden - O2	0.7 ± 0.5	0.1 (<0 - 3.9)	181
178	Buitenveldert West Midden - O3	4 ± 0.9	<0 (<0 - <0)	32
179	Zuidas Noord	-2.2 ± 0.3	0.1 (<0 - 1.4)	520
180	Amstelpark - O4	-2.7 ± 0.7	10.7 (5.6 - 17.1)	82
180	Amstelpark - P4	-4.2 ± 0.8	15.7 (8.9 - 24.5)	62
181	Buitenveldert Zuidoost - P3	0.7 ± 0.7	6.0 (0.9 - 12.7)	44
181	Buitenveldert Zuidoost - P4	-3.3 ± 0.3	9.5 (6.6 - 12.7)	58
182	Buitenveldert Oost Midden	-4.2 ± 0.4	9.0 (5.9 - 12.4)	181
183	De Klenckebuurt	-3.2 ± 0.8	8.6 (3.0 - 16.1)	81
184	Rijnbuurt Midden	-4.9 ± 0.5	12.6 (9.3 - 16.8)	273

|			
185	Rijnbuurt Oost	-3.7 ± 0.7	0.5 (<0 - 4.1)	110
186	Rijnbuurt West	-5 ± 0.5	6.2 (3.5 - 9.5)	136
187	Kromme Mijdrechtbuurt	-5.7 ± 0.7	<0 (<0 - 3.0)	443
188	Dapperbuurt Noord	-5.6 ± 0.5	6.8 (3.2 - 11.3)	33
189	Oosterparkbuurt Noordwest	-5.7 ± 0.3	5.0 (3.7 - 6.7)	45
190	Oosterparkbuurt Zuidwest - K6	-3.7 ± 0.8	1.2 (<0 - 5.3)	60
190	Oosterparkbuurt Zuidwest - L6	-5.7 ± 0.4	<0 (<0 - 1.6)	40
191	Oosterparkbuurt Zuidoost	-4.2 ± 1	5.5 (2.1 - 11.8)	44
192	Parooldriehoek	-4 ± 0.5	1.7 (<0 - 4.2)	103
193	Swammerdambuurt	-5.2 ± 0.7	<0 (<0 - 0.8)	199
194	Transvaalbuurt Oost - L6	-4.3 ± 0.5	<0 (<0 - <0)	338
194	Transvaalbuurt Oost - L7	-6.1 ± 0.7	<0 (<0 - <0)	115
195	Transvaalbuurt West	-4.2 ± 0.3	0.1 (<0 - 1.5)	201
196	KNSM-eiland - H8	-3 ± 0.9	0.1 (<0 - 7.1)	78
196	KNSM-eiland - G8	-1.9 ± 0.6	7.9 (4.0 - 13.0)	116
197	Noordoostkwadrant Indische buurt	-6.5 ± 0.8	4.0 (<0 - 11.3)	168
198	Nwkwadrant Indische buurt Noord - J7	-5.7 ± 1	<0 (<0 - 7.3)	58
198	Nwkwadrant Indische buurt Noord - J8	-6.7 ± 1	1.6 (<0 - 10.5)	68
199	Schipluidenbuurt	-11.7 ± 0.9	14.9 (9.4 - 22.8)	136
200	Delflandpleinbuurt Oost	0.2 ± 0.7	1.6 (<0 - 7.3)	776
201	Delflandpleinbuurt West - LL1	-7.9 ± 0.6	6.5 (3.6 - 10.4)	184
201	Delflandpleinbuurt West - L1	-1.3 ± 1	7.7 (1.0 - 17.3)	421
201	Delflandpleinbuurt West - M1	-1.7 ± 0.9	<0 (<0 - 0.7)	525
202	Belgiplein e.o. - MM3	-2.2 ± 0.7	5.5 (2.9 - 9.6)	322
202	Belgiplein e.o. - MM2	-5.8 ± 0.6	4 (1.9 - 7.1)	48
203	Nieuw Sloten Noordwest	-2.7 ± 0.2	1 (0.5- 1.5)	587
204	Nieuw Sloten Noordoost - MM2	-6.8 ± 0.3	2.9 (1.9 - 4.0)	164
204	Nieuw Sloten Noordoost - LL2	-4.8 ± 0.4	0.9 (<0 - 2.3)	237
205	Overtoomse Veld Noord	-15.5 ± 0.7	42 (35.6 - 49.7)	803
206	Johan Jongkindbuurt	-8.4 ± 1	16.7 (10.5 - 25.8)	139
207	Louis Chrispijnbuurt	-0.2 ± 0.4	3.7 (1.7 - 6.1)	296
208	Jacob Geelbuurt - JJ1	-3.8 ± 0.5	2.2 (0 - 5.1)	119
208	Jacob Geelbuurt - KK1	-5.3 ± 0.3	0.9 (<0 - 2.3)	140
209	Staalmanpleinbuurt	-9.4 ± 0.5	8.7 (5.9 - 12.3)	80
210	Jacques Veldmanbuurt - LL1	-3.3 ± 0.4	5.3 (3.2 - 7.8)	79
210	Jacques Veldmanbuurt - KK1	-5 ± 0.6	4.2 (1.1 - 8.5)	84
211	Emanuel van Meterenbuurt - KK2	-4.3 ± 0.5	2.7 (0.4 - 5.7)	83
211	Emanuel van Meterenbuurt - KK1	-2.4 ± 0.3	5.1 (3.2 - 7.3)	39
212	Oostoever Sloterplas	-7.9 ± 0.7	31.9 (25.0 - 40.2)	459
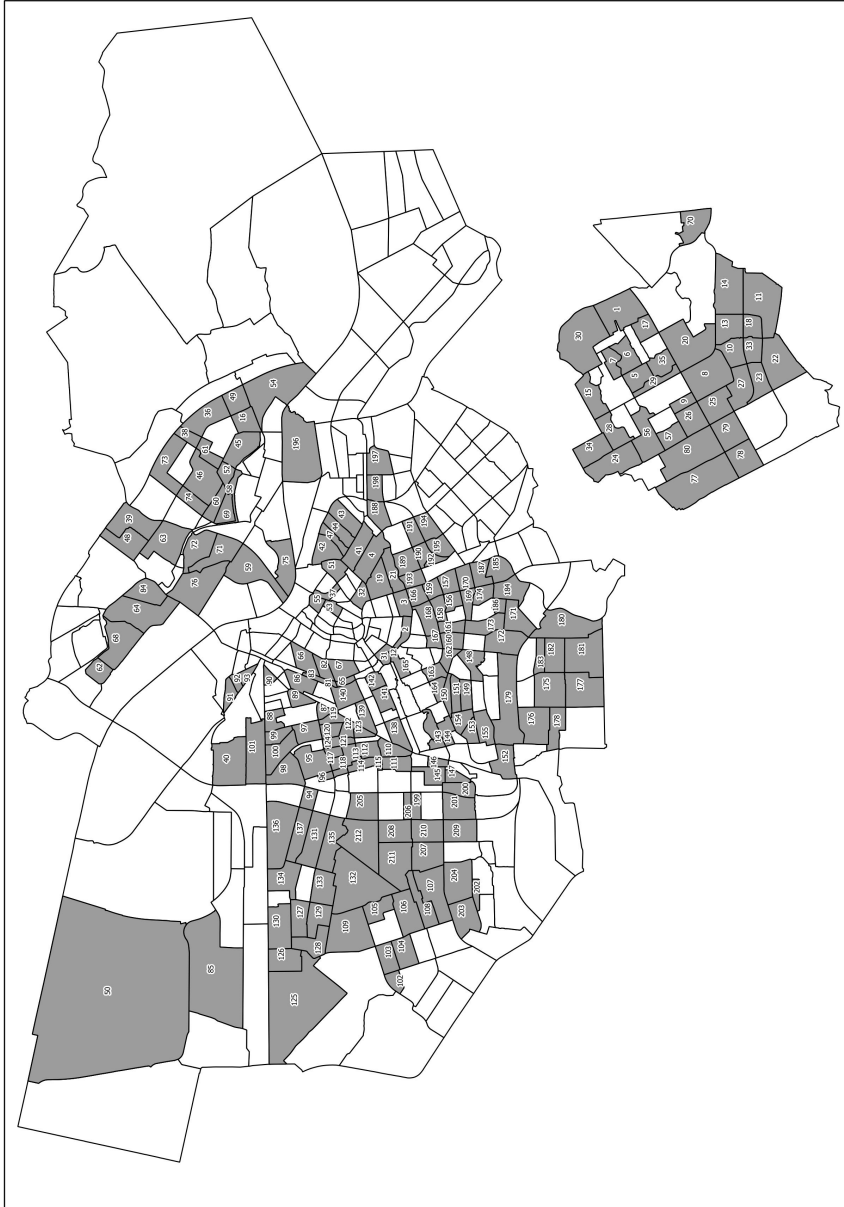
Figure 3: Neighbourhoods for which it was possible to calculate an area average settlement rate. Please note that the calculated area average settlement rates only refer to the part of the area where settlement measures were taken. The location of the measurements can be found in figure 4.13.

Notation and list of symbols

c	parameter
$\hat{c}$	estimation
$\bar{c}$	average
C	matrix
C'	transpose of a matrix

Table 2: List of symbols

z	vertical position ($mNAP$)
t	time (years) with $t = 0$ at year 0
a	(theoretical) vertical position at $t = 0$
b	settlement rate ($m/year$)
σ	standard deviation
s	sample standard deviation
x	horizontal position (m)
d	difference in horizontal position (m)
h	difference in vertical position (m)
l	total length of a sewer (m)
α	significance level
μ_b	area average settlement rate ($m/year$)
y	bias

Summary

Like many megacities (e.g. Jakarta, Bangkok, Tokyo, Shanghai), Amsterdam is situated in a delta area. As delta areas are characterized by soft soil conditions, it is likely that (differential) settlement is the most important cause for dysfunctioning. Therefore, studying the influence of settlement on sewer system functioning will probably give insight in the most relevant deterioration processes of sewer systems in these areas. Ultimately, knowledge of the ground settlement and the relation between settlement (differences) and sewer system dysfunctioning can help the sewer manager to predict and act upon these negative influences in an effective way.

Chapter 2: Visual inspection of sewers
Throughout Europe, decisions on sewer rehabilitation and replacement are often based on visual inspection reports according to the EN 13508-2. In practice the quality of the inspection data is generally not questioned although psychological research indicates that, as a consequence of the use of subjective analysis of the collected images, errors are inevitable.

Three types of capabilities to subjectively assess data are distinguished: the recognition of defects, the description of defects according to a prescribed coding system and the interpretation of sewer inspection reports. The introduced uncertainties are studied using three types of data: inspector examination results of sewer inspection courses, data gathered in day-to-day practice and the results of repetitive interpretation of the inspection results. After a thorough analysis of the data it is concluded that all three types of capabilities to subjectively assess data are poorly reproducible. For the recognition of defects it was found that the probability of a false positive is in the order of a few percent, the probability of a false negative is in the order of 25%; sewer inspection reports therefore provide a too optimistic view about the condition of a sewer. As the data is poorly reproducible, it is very likely that any decision or result of a deterioration model based on visual sewer inspection data is only tentatively linked to the actual (or future) condition of the inspected sewer pipe. Consequently, sewer management based on visual inspection data only will likely result in ineffective management.

Chapter 3 and 4: Monitoring Settlement and analysis of (sewer) settlement in the city of Amsterdam

As not managing sewer systems is no option, as deterioration will occur, there is an immediate need for an alternative source of reliable information to drive sewer rehabilitation. In many deltas, land settlement is one of the local characteristics that significantly influence the vertical position of sewer system elements and therefore the functioning of the system. Consequently it is to be expected that sewers might fail before the end of the expected service lifetime of 60 years.

As illustrated in figure 1, two types of settlement can occur: equal settlement (A) and differential settlement (B and C). Equal settlement of all elements of the sewer system, or connected to the system will not result in failure. For differential settlement two spatial scales are discriminated: differential settlement on network level (figure 1B) and differential settlement of sewer pipes (figure 1C). In order to study the influence of settlement on sewer system functioning, the potential and accuracy of methods to analyse settlement differences on both scales are assessed.

To analyse settlement on network level, sewer invert measurements are used. In order to determine the vertical position of the sewer invert, two properties are measured: the vertical position of the manhole cover and the distance between manhole cover and sewer invert. The former is measured relative to NAP (Normaal Amsterdams Peil or Amsterdam Ordnance Datum) using a levelling instrument. The latter is determined using a rod. The error of these measurements are respectively $\sigma_{manhole} = 0.007\,m$ and $\sigma_{distance} = 0.013\,m$, resulting in an error of $\sigma = 0.016\,m$ for the sewer invert. Although in the last decades several alternatives have been developed (e.g. GPS, aircraft based lidar), levelling is still the most suitable method to accurately determine vertical positions in an urban environment.

To assess the influence of settlement on the functioning of sewer systems, the sewer system of the city of Amsterdam is studied. As the subsoil of Amster-
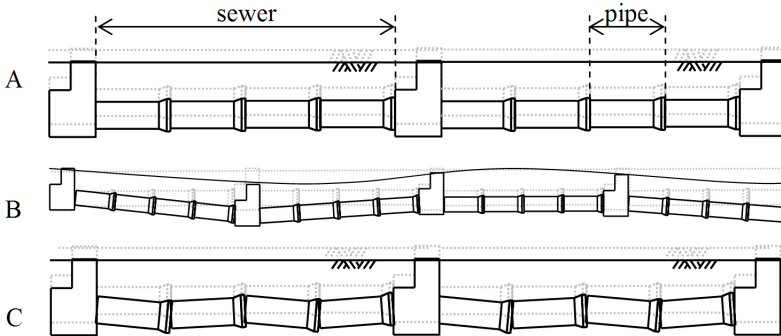

Figure 1: Differential settlement: a) no settlement difference, b) network level: settlement differences between manholes, c) pipe level: differential settlement of pipes.

dam consist of layers of peat, settlement is a known problem; the settlement rate, however, was unknown. Analysis of digital available sewer invert measurements showed that the settlement rate in the Amsterdam area is approximately $5\,mm\,year^{-1}$, ranging from a few mm per year up to $10\,mm\,year^{-1}$. As for each location the number of digital available sewer invert measurements is very limited (on average 2 measurements with a time interval of 5 years), settlement rate estimations for individual locations are unreliable. As a consequence additional measurements are necessary to assess settlement differences on network level. For one case study area in the north of Amsterdam, Waddendijk, historical maps were scrutinised to recover non-digital data. For most manholes in the area six sewer invert measurements were found, measured between 1980 and 2012 with an average interval of 5 years. Analysis of the time series showed that a linear model provides a good fit for the data (time invariant settlement rate).

As the error of the sewer invert measurements is known, the accuracy of the estimation of the settlement rate can be calculated. For the 6 measurements of the case study area this results in an accuracy of $\pm 1.4\,mm\,year^{-1}$ (95% confidence interval). The settlement rate of the case study area was on average $5\,mm\,year^{-1}$. The largest settlement differences in the area were found between manholes with and without a deep foundation. Because the sewers connecting these two types of manholes, hinge sewers, have to cope with the largest settlement differences, the settlement process of these sewers was further studied in chapter 5.

For the measurement of the sewer invert profile a sewer inspection camera equipped with an electronic tilt meter is used (figure 2). The accuracy of the results of this measurement technique is determined by the specifications of the
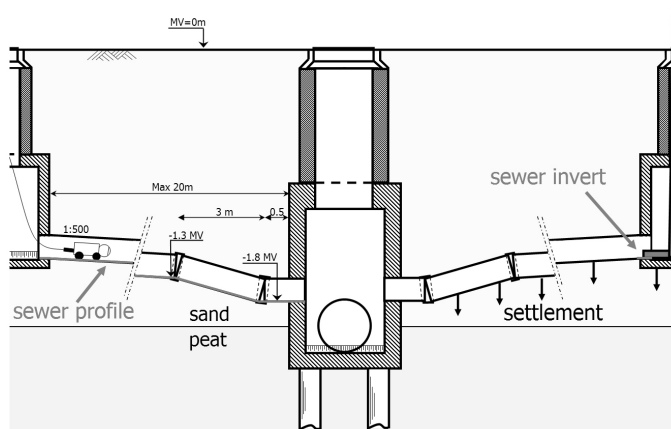

Figure 2: monitoring (differential) settlement: sewer profile and sewer invert measurements. The sewer in the middle of the figure is a pile founded manholes, the sewer connected to this manhole are hinge sewers. For the left hinge sewers some specifications of the design of a hinge sewer are indicated.

electronic tilt meter but also by the execution of the measurement and properties of the measured object. To assess the influence of the latter two, the sewer invert profile of one sewer was measured ten times. Analysis of the results showed that the random errors are small and cancel out. Therefore differences in the slope of individual sewer pipes can be measured fairly accurate. The determination of the difference in level between either end of the sewer is inaccurate because of the systematic error.

Chapter 5: Differential settlement of sewer pipes
In literature, differential settlement of sewer pipes is frequently mentioned as a cause for the development of cracks, open joints, deformation probably resulting in infiltration or collapse. If sewer pipes move relative to one another one would expect that the longitudinal profile of new sewers are less 'bumpy' compared to older sewers. To verify this assumption, the sewer invert profile of approximately 90 sewers of different ages, material and diameter in the case study area in Amsterdam North were measured. Surprisingly, analysis of the results revealed that new sewers are as 'bumpy' as older sewers. Also the few defects that were found could not be related to settlement (differences) of sewer pipes.

To study differential settlement of sewer pipes also some hinge sewers were selected. These hinge sewers connect a manhole with a deep foundation to a manhole without a deep foundation (figure 3). Most sewers in Amsterdam have a shallow foundation, but below the artificially applied sand layer (average thickness $2\,m$) the peaty subsoil does not provide enough support for a shallow foundation. Therefore pile foundations are used for all sewers from $1.8\,m$ below ground level. To mitigate the impact of the settlement differences, hinge sewers are specially designed in Amsterdam. Figure 3 shows the cross-section of this design. The idea is that the pipe closest to the manhole with a pile foundation would act as a rigid hinge. Analysis of the sewer invert profiles of the studied hinge sewers however
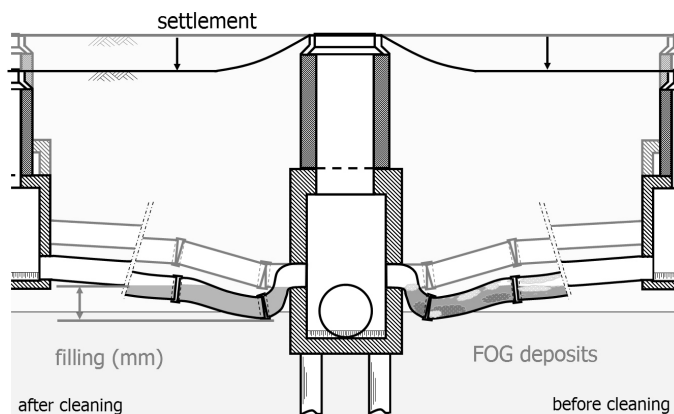

Figure 3: Differential settlement of a hinge sewer made of PVC.

showed a different trend: over time a sag will develop close to the manhole with a deep foundation (figure 3).

To analyse the differential settlement of hinge sewers in more detail, 60 hinge sewers were selected for further research. Is was chosen to study hinge sewers of sanitary sewers of separate systems because these are most sensitive to blockages. To be able to study relevant aspects of the settlement process the following measurements/action were (under)taken: assessment of the total settlement (settlement rate * age), visual inspection of the degree of fouling, cleaning of the sewer, visual inspection of the structural condition, the measurement of the sewer invert profile and analysis of the filling percentage. Analysis of the results showed that the depth of the sag is correlated to the total settlement. Visual inspection before cleaning revealed that fat oil and grease (FOG) deposits typically accumulate slightly above the low-flow water mark. Indications were found that bar-shaped pieces of FOG deposits occasionally detach. As these deposits are quite rigid, these lumps can easily get stuck initiating a blockage. Finally inspection of the structural condition of the sewers indicated that severe defects can develop at the connection with the deep founded manhole. The method of construction determines probably to a large extent if and when these defects will develop.

As FOG deposits might be an important cause for blockages in sanitary sewers of separate systems, the blockage frequency of the 60 hinge sewers is further looked into. For this assessment the depth of the sag (figure 3) was determined based on the sewer invert profiles. The number of blockages between November 2005 and October 2011 was estimated using the customer complaints database. Comparing both figures revealed that sewers with a filling percentage (depth of the sag as a percentage of the diameter) of less than 40% block rarely; sewers with a filling percentage of more than 40% are likely to block more often. As not all sewers with a high filling percentage were found to block frequently, it is concluded that the blockage frequency is also strongly dependent on other factors, e.g. the discharge behaviour of the customers.

Sewers of combined systems are unlikely to reach filling rates of 40% as diameters are much larger (during dry weather flow conditions). For this type of sewers the amount of pollution that can deposit in sagging sewers might be more relevant as sediments in the system have a negative influence on the pollution load in case of a combined sewer overflow (CSO) event. To analyse whether the pollution accumulated at locations with stagnant water is significant, the sewer system in the north of Amsterdam was used as a case study. For this system future sewer invert levels were estimated based on the previously calculated settlement rates. For this system it was found that the volume of stagnant water zones increases by $10\,m^3$ in a period of 20 years. As this volume of stagnant water will be filled with dry weather flow and/or sediment, it is concluded that the pollution potential of

the system increases significantly.

Chapter 6: Concluding remarks
A large part of this research is focussed on the assessment of the potential and accuracy of methods to study (differential) settlement. Based on the assessment it is concluded that suitable methods are available, however improvements are beneficial. Especially the necessity for long time series of sewer invert measurement to assess settlement differences on network level hampers further research. As the methods were only applied to a limited dataset in one area, it is difficult to draw any general conclusions. Nevertheless, the results show that even within an area with a limited settlement rate ($5\,mm\,year^{-1}$), the influence of settlement on sewer system functioning is significant and to a large extent predictable.

Nederlandse samenvatting

Net zoals megasteden zoals Jakarta, Bangkok, Tokyo en Sjanghai is Amsterdam gelegen in een deltagebied. Omdat bodemdaling kenmerkend is voor dit soort gebieden is het waarschijnlijk dat bodemdaling een belangrijke oorzaak is voor disfunctioneren. Onderzoek naar de invloed van zetting op het functioneren van de riolering kan uiteindelijk gebruikt worden om het riool beter te beheren.

Hoofdstuk 2: Visuele inspectie van riolen

Adequaat rioolbeheer vereist kennis over de toestand van het riool. In Europa wordt hiervoor meestal gebruik gemaakt van visuele inspectie gegevens. Ondanks deze belangrijke rol in het beheerproces wordt aan de betrouwbaarheid van de gegevens nauwelijks getwijfeld. Dit is opmerkelijk omdat uit psychologisch onderzoek bekend is dat bij subjectieve evaluatie van (visuele) informatie fouten onvermijdelijk zijn.

In het proces van visuele inspectie tot besluitvorming worden drie momenten van subjectieve evaluatie onderscheiden: de herkenning van toestandsaspecten, het beschrijven van toestandsaspecten en het interpreteren van inspectierapporten. De fouten die gemaakt worden in elk van deze stappen zijn onderzocht aan de hand van drie bronnen: examens van rioolinspecteurs, rioolinspectierapporten uit de praktijk en de resultaten van herhaalde interpretatie van rioolinspectierapporten door verschillende experts. Na een grondige analyse van de gegevens bleek dat elk van de drie stappen slecht reproduceerbaar is. Uit het onderzoek bleek dat er ongeveer 25% kans is op het over het hoofd zien van een toestandsaspect. Het foutief noteren van een toestandaspect komt minder vaak voor, de kans daarop is slechts een paar procent. Hieruit volgt dat rioolinspectierapporten een te rooskleurig beeld geven van de toestand van een riool. Omdat er in het proces van visuele inspectie tot besluitvorming zoveel onzekerheden insluipen, zal een besluit dat gebaseerd is op visuele inspectie gegevens nog maar nauwelijks gerelateerd aan de daadwerkelijke toestand van de riolering.

Hoofdstuk 3 en 4: Het meten van zetting en zettingsverschillen en de analyse van zetting van de Amsterdamse ondergrond

Omdat gegevens over de toestand van de riolering noodzakelijk zijn om het riool goed te kunnen beheren is dringend behoefte aan een alternatieve, betrouwbare

bron van informatie. Deltagebieden zoals Nederland worden vaak gekenmerkt door bodemdaling. De verticale positie van niet-onderheide riolering zal hierdoor in de tijd veranderen waardoor het stelsel op den duur niet meer goed zal functioneren. Daarom is in delta gebieden bodemdaling waarschijnlijk een maatgevend faalmechanisme. Als de invloed van bodemdaling op het functioneren van de riolering bekend is, kunnen gegevens over bodemdaling gebruikt worden om de riolering beter te beheren.

Zoals te zien is in figuur 1 zijn er verschillende soorten bodemdaling: gelijkmatige zetting (figuur 1A) en ongelijkmatige zetting (figuur 1B en C). Als alle elementen van het rioolstelsel (en verbonden met het rioolstelsel) even snel zetten zal dit geen problemen opleveren. Ongelijkmatige zetting kan voorkomen op verschillende schalen: op netwerk niveau (figuur 1B) en op lokaal, buis niveau (figuur 1C). Om de invloed van zetting op het functioneren van de riolering te kunnen bestuderen zullen eerst geschikte, betrouwbare onderzoekmethoden gevonden moeten worden.

Om zettingsverschillen op streng niveau te onderzoeken zijn BOB (Binnen Onderkant Buis) metingen gebruikt (zie figuur 2). De BOB maat wordt bepaald door de verticale positie ten opzichte van NAP (Normaal Amsterdams Peil) van een putdeksel in te meten met een waterpasinstrument. De afstand tussen een putdeksel en de binnenonderkant van een rioolbuis wordt gemeten met een baak. Uit onderzoek naar de betrouwbaarheid van de gegevens kwam naar voren dat de fout in deze metingen een standaarddeviatie heeft van $0.007\,m$ (putdeksel) en $0.013\,m$ (afstand putdeksel-binnenonderkant). Dit resulteert in een fout met $\sigma = 0.016\,m$ voor de BOB maat van een riool. Ondanks dat in de afgelopen tientallen jaren verschillende methodes ontwikkeld zijn om de verticale positie van het aardoppervlak te meten (bijvoorbeeld GPS, lidar en radar) is waterpassen nog steeds de meest geschikte en nauwkeurige methode om verticale posities te bepalen in een stedelijke omgeving.
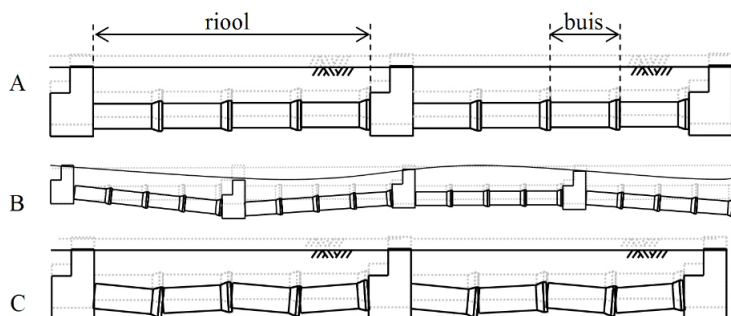
Figuur 1: Zettingsverschillen: a) geen zettingsverschillen, b) zettingsverschillen op streng niveau en c) ongelijke zetting van rioolbuizen.

Voor het onderzoek naar de invloed van zetting op het functioneren van een rioolstelsel is de riolering van Amsterdam bestudeerd. Omdat de ondergrond van Amsterdam onder andere uit veen bestaat is bodemdaling een bekend probleem; hoe hard de bodem daadwerkelijk zet was echter onbekend. Uit analyse van de digitaal beschikbare (historische) BOB metingen voor heel Amsterdam bleek dat de bodemdaling ongeveer $5\,mm\,jaar^{-1}$ is, variërend van bijna geen zetting met uitschieters tot $10\,mm\,jaar^{-1}$. Helaas zijn er voor de meeste locaties slechts 2 metingen met een interval van 5 jaar digitaal beschikbaar, wat te weinig is om iets te zeggen over zettingsverschillen op stelsel niveau (figuur 1B). Voor een wijk in Amsterdam Noord, Waddendijk zijn daarom ook de BOB metingen van oude stadskaarten verzameld. Een tijdrovende analyse leverde 6 metingen per punt op die uitgevoerd waren tussen 1980 tot 2012 met een interval van ongeveer 5 jaar. Op basis van deze gegevens kon vastgesteld worden dat bodemdaling (op deze tijdsschaal) een lineair proces is, wat betekent dat de zettingssnelheid niet verandert in de tijd.

Omdat de standaarddeviatie van de fout van een BOB meting bekend is kan ook de fout in de schatting van de zetting van een individuele locatie berekend worden. Voor deze 6 metingen is dat $\pm 1.4\,mm\,jaar^{-1}$ (95% betrouwbaarheids-interval). Voor het gebied in Amsterdam Noord bleek dat de zetting gemiddeld $5\,mm\,jaar^{-1}$ is. De grootste verschillen in zetting op stelsel niveau vinden plaats waar een onderheide put aangesloten is op een niet-onderheide put. Omdat de niet-onderheide riolen die deze twee type putten verbinden de grootste zettingsver-schillen moeten opvangen, zijn deze riolen (pendel riolen) verder onderzocht.
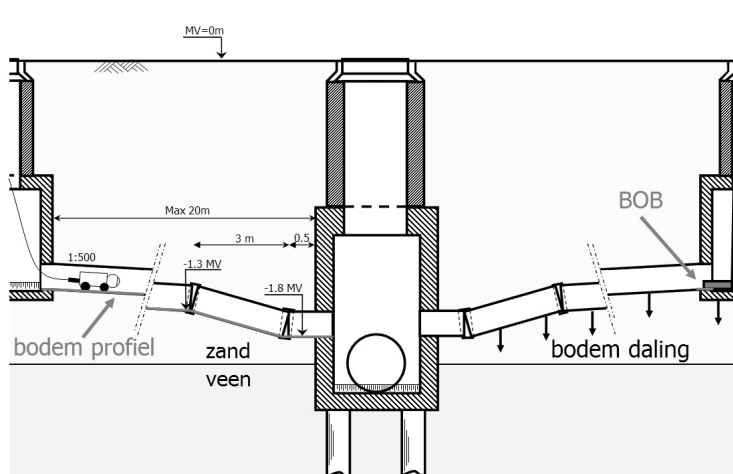
Figuur 2: Meten van het bodemprofiel van een riool en de verticale positie van een BOB. De put in het midden van het figuur is onderheid. De niet onderheide riolen die hierop aansluiten zijn pendel riolen. De ontwerp waarden voor het linker pendelriool zijn aangegeven in de figuur.

Om zettingsverschillen op buis niveau te onderzoeken is gebruik gemaakt van een rioolinspectiecamera met een geïntegreerde elektronische waterpas (IBAK KRA65). Door de helling van het riool over de lengte van het riool te meten kan het bodemprofiel van een riool bepaald worden (figuur 2). De nauwkeurigheid van het gemeten bodemprofiel is afhankelijk van zowel de specificaties van de elektronische waterpas maar ook van het te meten object. Om te kunnen bepalen in hoeverre het te meten object de kwaliteit van de meting beïnvloed is eenzelfde riool tien keer gemeten: vijf keer vanaf elke kant. Door de tien meetresultaten met elkaar te vergelijken werd duidelijk dat de willekeurige (random) fouten klein zijn en elkaar opheffen. Hierdoor zijn verschillen in helling tussen met elkaar verbonden buizen vrij nauwkeurig te bepalen. Het meten van het verschil in verticale positie van het begin en eind van een riool is daarentegen wel onnauwkeurig omdat de systematische fout hiervoor te groot is.

Hoofdstuk 5: Ongelijke zetting van rioolbuizen

In de literatuur wordt ongelijke zetting van riool buizen (figuur 1C) vaak genoemd als oorzaak voor het ontstaan van scheuren, openstaande voegen en deformatie en de daaruit volgende infiltratie of instorting. Als buizen door zettingsverschillen ten opzichte van elkaar bewegen zou je verwachten dat riolen in de loop van de tijd steeds 'hobbeliger' worden. Deze verwachting is getoetst door ongeveer 90 riolen van verschillende leeftijden, materialen en diameters in het onderzoeksgebied in Amsterdam Noord te onderzoeken. Dit onderzoek bestond uit zowel een bodemprofiel meting als visuele inspectie. Verrassend genoeg bleek na analyse dat nieuwe riolen net zo 'hobbelig' zijn als oudere riolen. Ook de enkele toestandsaspecten die gevonden werden konden niet gerelateerd worden aan verschillen in helling tussen naast elkaar gelegen rioolbuizen.

Voor het onderzoek naar zettingsverschillen op buis niveau waren ook een aantal pendel riolen geselecteerd. Dit zijn niet-onderheide riolen die verbonden zijn met een onderheide put (figuur 2). De meeste riolen in Amsterdam zijn niet onderheid, maar omdat vanaf ongeveer 2 meter diepte de bodem niet draagkrachtig genoeg is, zijn alle riolen dieper dan 1.8m onderheid. De riolen die het niet onderheide stelsel met het onderheide stelsel verbinden zijn pendel riolen. Deze riolen worden pendel riolen genoemd omdat de laatste rioolbuis voor de onderheide put aangelegd wordt met een steilere helling. Het idee achter dit ontwerp is deze buis als een starre pendel het zettingsverschil opvangt (figuur 2). De meetresultaten van het bodemprofiel van een aantal van dit type riool in het onderzoeksgebied in Amsterdam Noord wees echter uit dat de praktijk anders is dan de theorie: door zettingsverschillen zal in verloop van tijd een zak (locatie waar permanent water blijft staan) ontstaan net voor de onderheide put (figuur 3).

Om de problemen met de pendel riolen verder te onderzoeken zijn verspreid over Amsterdam 60 pendel riolen geselecteerd. Er is er voor gekozen om pendel riolen van vuilwaterriolen van gescheiden stelsels te onderzoeken omdat deze het meest gevoelig zijn voor verstoppingen. Het onderzoek van deze riolen bestond uit het bepalen van totale zetting (zettingssnelheid x leeftijd), het visueel inspecteren

van de vervuilingsgraad, het reinigen van het riool, het visueel inspecteren van
de structurele toestand en het meten van het bodemprofiel. Uit dit onderzoek
bleek dat de diepte van de zak sterk gerelateerd is (en dus voorspeld kan worden)
aan de totale zetting. Bij het visueel inspecteren van de vervuilingsgraad kon
vastgesteld worden dat op locaties waar permanent water blijft staan vet zich
afzet tegen de buiswand net boven de waterrand (figuur 3). Deze afzettingen zijn
door een chemische reactie (verzeping) zeer hard. Er zijn aanwijzingen gevon-
den dat deze randen zo nu en dan los raken. Omdat deze langwerpige, harde
korsten benedenstrooms gemakkelijk vast kunnen gaan zitten zou dit een belang-
rijke oorzaak kunnen zijn voor verstoppingen in vuilwaterriolen. Inspectie van de
structurele toestand van de pendel riolen gaf tot slot aan dat de verbinding van
dit riool met de onderheide put gevoelig is voor het ontstaan van scheuren, open-
staande verbinding en deformatie. Wanneer en waarom deze defecten ontstaan is
waarschijnlijk sterk afhankelijk van hoe het riool aangelegd was.

Hoofdstuk 6: Invloed van zetting op het functioneren van het rioolstelsel

Omdat uit de visuele inspectie van de vervuilingsgraad van pendel riolen bleek dat
vet zich in deze riolen afzet, wat kan leiden tot verstoppingen, is verder onderzoek
gedaan naar de verstoppingsgevoeligheid van deze riolen. Hiervoor is de diepte
van de zak (figuur 3) bepaald aan de hand van de meting van het bodemprofiel.
Het aantal verstoppingen tussen november 2005 en oktober 2011 is afgeleid uit de
klachten/meldingen database. Uit deze analyse bleek dat vuilwaterriolen met een
vullingsgraad (diepte van de zak als percentage van de buisdiameter) groter dan
40% een grotere kans hebben om regelmatig te verstoppen (meer dan 1 keer per
jaar bij een preventieve reinigingsfrequentie van eens per 5 jaar). Hoe vaak een
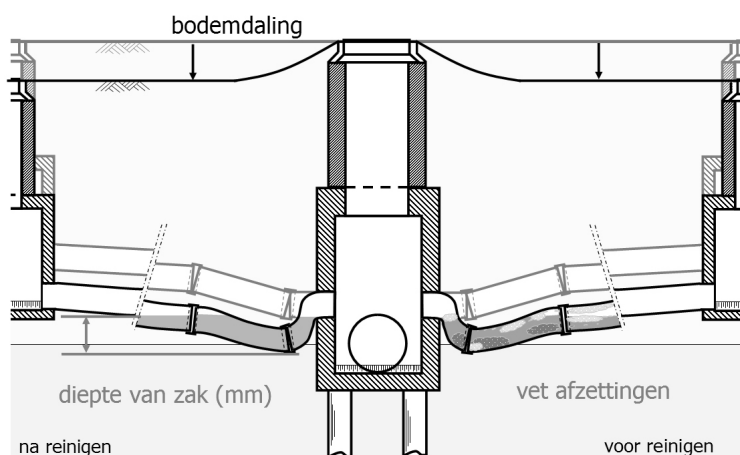
Figuur 3: Ongelijke zetting van een pendel riool gemaakt van PVC.

riool daadwerkelijk verstopt, is in grote mate afhankelijk van het lozingsgedrag van de gebruikers.

In gemengde stelsels zullen zettingsverschillen niet zo snel resulteren in een vullingsgraad van 40% of meer, omdat de diameters veel groter zijn. In dit type riolen is het sediment dat kan bezinken op locaties waar permanent water blijft staan (dode berging) mogelijk een groter probleem. Omdat de omstandigheden op deze locaties gunstig zijn is het zeer waarschijnlijk dat gedurende droog weer (langere verblijftijd, hogere concentraties aan vervuiling) sediment bezinkt. Het opwoelen van dit sediment tijdens een regenbui kan in het geval van een over-stortingsgebeurtenis leiden tot vervuiling van het oppervlaktewater. De locaties waar water blijft staan en het volume water dat niet meer afstroomt onder vrij verval kan voorspeld worden aan de hand van de BOB metingen en de geschatte zetting. Voor het onderzoeksgebied in Amsterdam Noord bleek dat in een periode van 20 jaar het volume dode berging toeneemt met ongeveer $10\,m^3$. Door een ruwe schatting van de hoeveelheid vervuiling op deze locaties te vergelijken met de toegestane hoeveelheid vuilvracht dat per jaar door dit stelsel overgestort mag worden bleek dat de vervuilingspotentie van dit stelsel significant toeneemt.

Hoofdstuk 7: Afrondende beschouwingen

Een groot gedeelte van dit onderzoek is besteed aan het bestuderen van geschikte, betrouwbare methoden om (ongelijke) zetting van riolen te kunnen onderzoeken. Uiteindelijk is geconcludeerd dat deze methoden beschikbaar zijn, maar dat er nog wel verbeterpunten zijn. Vooral de lange tijdreeksen (> 30 jaar) die nodig zijn voor het betrouwbaar inschatten van zetting en zettingsverschillen op stelsel niveau met een waterpasinstrument vormen een belemmering. Dit betekent dat op een andere manier moet worden voorzien in de informatiebehoefte. Desalniettemin laat het onderzoek zien dat zetting van slechts $5\,mm\,jaar^{-1}$ significante en voor een groot deel voorspelbare gevolgen heeft voor het functioneren van de riolering met betrekking tot verstopping, vuiluitworp en vetophoping.

List of publications

International peer-revieuwed journals

Dirksen, J., Baars, E., Langeveld, J., Clemens, F., 2012. Settlement as a driver for sewer rehabilitation. Water Science and Technology 66 (7), 1534–1539.

Dirksen, J., Baars, E., Langeveld, J., Clemens, F., 2013a. Quality and use of sewer invert measurements. Structure and Infrastructure Engineering.First published on: 07 January 2013 (iFirst).

Dirksen, J., Clemens, F., 2008. Probabilistic modeling of sewer deterioration using inspection data. Water Science and Technology 57, 1635–1641.

Dirksen, J., Clemens, F., Korving, H., Cherqui, F., Le Gauffre, P., Ertl, T., Plihal, H., Müller, K., Snaterse, C., 2013b. The consistency of visual sewer inspection data. Structure and Infrastructure Engineering 9 (3), 214–228, first published on: 07 February 2011 (iFirst).

Dirksen, J., Pothof, I., Langeveld, J., Clemens, F., under review. Slope profile measurement of sewer inverts. Journal of Infrastructure Systems.

Dirksen, J., ten Veldhuis, J., Schilperoort, R., 2009. Fault tree analysis for data-loss in long-term monitoring networks. Water Science and Technology 60 (4), 909–915.

Schilperoort, R., Dirksen, J., Langeveld, J., Clemens, F., 2012. Assessing characteristic time and space scales of in-sewer processes by analysis of one year of continuous in-sewer monitoring data. Water Science and Technology 66 (8), 1614–1620.

van der Steen, A., Dirksen, J., Clemens, F., accepted, 9 May 2013. Visual sewer inspection: detail of coding system versus data quality? Structure and Infrastructure Engineering.

Conference proceedings

Dirksen, J., Baars, E., Clemens, F., 2010a. Settlement analysis for the sewer system of amsterdam. In: proceedings of the 6th international conference on Sewer Processes and Networks, Gold Coast, Australia.

Dirksen, J., Baars, E., Langeveld, J., Clemens, F., 2011a. Settlement as a driver for sewer rehabilitation. In: proceedings of the 12th International Conference on Urban Drainge, Porto Alegre, Brazil.

Dirksen, J., Baars, E., Langeveld, J., Clemens, F., 2011b. Settlement as a driver for sewer rehabilitation: Amsterdam case study. In: proceedings of the 4th Leading Edge conference on Strategic Asset Management, Mülheim an der Ruhr, Germany.

Dirksen, J., Baars, E., Langeveld, J., Clemens, F., 2012. Analysis of fat, oil, and grease deposits in sagging sanitary sewers. In: proceedings of the 9th international conference on Urban Drainage Modelling, Belgrade, Serbia.

Dirksen, J., Baars, E., Langeveld, J., Clemens, F., submitted. The impact of fat, oil, and grease deposits on the performance of sanitary sewers. In: 7th international conference on Sewer Processes and Networks.

Dirksen, J., Clemens, F., 2007. Probabilistic modeling of sewer deterioration using inspection data. In: proceedings of the 5th international conference on Sewer Process and Networks, Delft, the Netherlands.

Dirksen, J., Glodina, A., ten Veldhuis, J., Clemens, F., 2007. The role of uncertainty in urban drainage decisions: uncertainty in inspection data and their impact on rehabilitation decisions. In: proceedings of the 2nd Leading Edge conference on Strategic Asset Management, Lisbon, Portugal.

Dirksen, J., Glodina, A., ten Veldhuis, J., Clemens, F., 2009a. Strategic Asset Management of Water Supply and Wastewater Infrastructures. IWA Publishing, Ch. Chapter 6. Target definition and assessment of risks., pp. 273–286, iSBN-13: 978-1843391869.

Dirksen, J., ten Veldhuis, J., Clemens, F., Baars, E., 2010b. Sensible sewer system rehabilitation using information on sewer system settlement. In: proceedings of the 7th International Conference on Sustainable Techniques and Strategies for Urban Water Management (NOVATECH), Lyon, France.

Dirksen, J., ten Veldhuis, J., Schilperoort, R., 2009b. Fault tree analysis for dataloss in long-term monitoring networks. In: proceedings of the10th international conference on Instrumentation, Control and Automation, Cairns, Australia.

Schilperoort, R., Dirksen, J., Clemens, F., 2008. Practical aspects for long-term monitoring campaign pitfalls to avoid to maximize data yield. In: proceeding of the 11th International Conference on Urban Drainage, Edinburgh, Scotland.

Schilperoort, R., Dirksen, J., Langeveld, J., Clemens, F., 2009. Assessing characteristic time and space scales of in-sewer processes by analysis of one year of continuous in-sewer monitoring data. In: proceedings of the 8th international conference on Urban Drainage Modeling, Tokyo, Japan.

ten Veldhuis, J., Dirksen, J., Clemens, F., 2009. Evaluation of operational strategies for sewer flooding based on failure data. In: proceedings of the 3rd Leading Edge conference on Strategic Asset Management, Miami, USA.

National publications

Dirksen, J., Baars, E., Kaptijn, R., 2013. Schuif, pendel of toch iets anders: hoe sluit je een niet-onderheide buis aan op een onderheide put? Vakblad riolering.

Dirksen, J., Goldina, A., Korving, J., 2007. (on)betrouwbaarheid kwaliteitsbeeld rioolstelsel bij nederlandse gemeenten. Rioleringswetenschap 7 (26), 68–75.

Dirksen, J., Langeveld, J., 2010. Novatech 2010. WT afvalwater 10 (4), 271–275.

Dirksen, J., ten Veldhuis, J., Clemens, F., Baars, E., 2009. Rationeel vervangen van riolering op basis van zetting. Rioleringswetenschap 36 (9), 40 – 49.

Langeveld, J., ten Veldhuis, J., Dirksen, J., 2011. International conference of urban drainage 2011, porto allegrebrazil. WT afvalwater 11 (5), 230–234.

Schilperoort, R., Dirksen, J., Langeveld, J., Clemens, F., 2009a. De dynamiek in het aanvoerpatroon van de rwz eindhoven in beeld: een studie naar karakteristieke tijd- en ruimteschalen van rwzi influent op basis van 1,5 jaar hoogfrequente kwantiteits- en kwaliteitsgegevens. Rioleringswetenschap 34 (9), 58–66.

Schilperoort, R., Dirksen, J., Langeveld, J., Clemens, F., 2009b. Piekvrachten naar rioolwaterzuivering eindhoven in beeld. Land+Water 49 (12), 26–27.

Curriculum vitae

Jojanneke Dirksen werd op 12 november 1982 geboren in Fijnaart en Heijningen. Haar VWO-opleiding volgde ze aan de Christelijke Scholengemeenschap Comenius in Leeuwarden, waar ze in 2000 haar diploma behaalde. Aansluitend is ze Civiele Techniek gaan studeren aan de Technische Universiteit Delft. In 2006 afgestudeerd aan de sectie gezondheidstechniek op het modelleren van rioolveroudering op basis van visuele inspectie data. Belangrijkste conclusie van dit onderzoek was dat de kwaliteit van visuele inspectiedata niet betrouwbaar genoeg is.

Na haar afstuderen in 2006 heeft ze een jaar als onderzoeker op de Technische Universiteit Delft samengewerkt met Remy Schilperoort waar ze zich voornamelijk bezig heeft gehouden met data analyse van water kwaliteits- en kwantiteits-sensoren. In 2007 is ze geselecteerd voor het Japanese Prizewinners Programme; een programma van de Nederlandse overheid om de samenwerking met Japan te bevorderen. Aansluitend op een intensieve cursus Japans in samenwerking met de Universiteit Leiden en het Japans-Nederlands instituut in Tokyo volgde een stage van 4 maanden bij Taisei, Tokyo, Japan.

Na terugkeer in Nederland in 2008 is ze in dienst getreden bij Waternet om, in samenwerking met de Technische Universiteit Delft verder onderzoek uit te voeren op het gebied van rioolbeheer. Hiervan is dit proefschrift het resultaat.